POLITECNICO DI MILANO

Scuola di Ingegneria Industriale e dell'Informazione

Corso di Laurea Magistrale in
Ingegneria Energetica

Temperature Swing Adsorption processes for CO_2 capture from power plants in integrated steel mills

Supervisor: Dr. Matteo Carmelo ROMANO

Co-supervisors at ETH Zurich: Dr. Matteo GAZZANI
Prof. Dr. Marco MAZZOTTI
Lisa JOSS

Co-supervisor at Politecnico di Milano: Dr. Isabel MARTINEZ

Master thesis of:
Stefano Edoardo ZANCO
matr. 801055

Academic Year 2013/2014

Acknowledgments

I am grateful to Dr. Matteo Romano for offering me the opportunity of this thesis and for constantly supervising its elaboration. I also want to thank Dr. Matteo Gazzani and Prof. Marco Mazzotti for allowing me to join the group of Separation Processes Laboratory and to work at my thesis under their direct supervision: during my stay in Zurich I have learnt much, not only about the topics discussed here. Moreover, I would like to thank Lisa Joss and Dr. Isabel Martinez, who have both significantly contributed to this work giving always precious advice.

My special, sincerest thanks go to my parents and my brother, for supporting me in so many ways, and to all my close friends, with whom I have lived these years to the fullest.

Extensive summary

This thesis work has been carried out in the context of a collaboration between the GECOS group (Group of Energy Conversion Systems) at the Department of Energy of Politecnico di Milano and the Separation Process Laboratory of the Institute for Process Engineering at ETH (Eidgenössische Technische Hochschule, Zurich).

The aim of this dissertation is the investigation of the potential of the temperature swing adsorption processes as an innovative system for the capture of carbon dioxide. In particular, a specific post-combustion carbon capture application is analyzed, namely the treatment of the flue gas released by power plants within integrated steel mills. In fact, steel industry plays a prominent role in the global emissions of CO_2, accounting for roughly 6% of the total amount yearly produced worldwide, the highest share held by an industrial sector.

Most big size steel factories include within their boundaries a power plant dedicated to their internal electric power demand; the power plant is mainly fed with the off-gases produced by the units forming the steel production chain, while possibly an additional stream of gaseous fuel is employed, usually natural gas. The resulting flue gas has a high content of CO_2, due to the extensive use of coal as processing material in the steel mill. In this study two different reference integrated power plants are considered: on the one hand a more traditional subcritical steam cycle, whose boiler is fired with the off-gas coming from the steel production units; on the other hand a more innovative combined cycle, which represents a common solution adopted in case of new construction. Both the power production units are described in literature, for they have been previously adopted in some research work as reference case for the implementation of a tail end post-combustion CCS system.

A suitable carbon capture process must be adequate to treat a gas flow with this specific CO_2-rich composition in order to be implemented into a steel mill. Moreover, according to the efficiency targets that drive the design of this industrial process, it should require the minimum amount of energy possible to operate. Since the most established technologies for this kind of application feature an approximate 3.5 MJ consumption for each kilogram of CO_2 removed, this value can be employed as reference to identify a range of competitiveness for any alternative system.

In this sense the limited amount of energy required by the regeneration of a physisorbent in the context of an adsorption-regeneration loop puts TSA processes forward as a promising alternative for CCS applications. Adsorption of CO_2 out of a flue gas is still a current research subject, but a certain quantity of data has already been collected by means of experimental measurments. All the data employed in this study for the computation of thermodynamics

and kinetics of adsorption have been made available on purpose by the Separation Process Laboratory.

In order to study the implementation of a temperature swing adsorption process as a tail end unit for post-combustion CO_2 capture, two different types of gas-solid systems are investigated and compared, namely a fixed bed solution and a circulating fluidized bed one.

Fluidized bed reactors are extensively employed in various industrial activities thanks to the high degree compactness that characterize them, an extremely valuable quality in all those applications where a gas-solid process has to be conducted dealing with enormous flow rates. Their implementation as adsorption reactors is though not widely reported in literature and is a quite innovative concept. For this reason, a completely new modeling is developed for adsorption and desorption processes inside CFB reactors and is implemented into a computational code to simulate the operational conditions investigated in this study. The model consists of two sections: In the first one the fluid dynamics of the system are calculated, while in the second one heat exchange is modeled. Both the model and the computational code are original contributions of the author; for the development of the simulation tool, the Matlab® programming language has been opted for.

A few essential assumptions form the basis of the CFB modeling for adsorption. First of all, the reactor is assumed to be operated at steady state, isothermally and at constant pressure; the pressure variation disappears from the momentum equations, while the mass balances may be consequently decoupled from the energy ones. Moreover, a perfect mixing of solids is hypothesized inside the reactor, so that all sorbent particles are characterized by the same temperature and degree of conversion; their behavior may be described by means of the continuous flow stirred tank reactor theory, whereas the gas stream is modeled as a plug flow. A single dimension spatial discretization is therefore employed to characterize the system. Furthermore, entrainment is considered as the only mechanism providing displacement of the solid matter out of the reactor.

Given the fact that adsorption and desorption are to be modeled by means of the same kinetics equations, the simulation tool is in principle developed to perform the calculations of both processes. It is capable of returning results for a wide range of conditions, which extends significantly beyond the constraints posed by standard TSA application. Regarding the goal of this study, it can be profitably used to simulate both the adsorption and the regeneration phase without requiring any substantial modification.

As regards fixed beds, more research has been already conducted on their application in the context of CO_2 capture. For the purposes of this study, simulations of the fixed bed operation is performed with a tool made available at Separation Processes Laboratory. This tool, which is implemented using a FORTRAN code, has been validated by means of series of experimental measurements performed on a scaled laboratory column. The model employed is featured with a one dimension spatial discretization as well as a time discretization, as required by the cyclic operation the single units for TSA processes; it allows to compute the fluid dynamics and thermodynamics of a single fixed bed column which undergoes a sequence of adsorption and desorption steps exchanging heat with an external fluid.

For this technology, the first original contribution of the author consists in the investi-

gation of various possible cycle designs and in the definition of an optimal configuration of the process cycle. Such a configuration is meant to fulfill the requirements in terms of separation performances and at the same time, if possible, to limit the total consumption of the system below the threshold set by the competing technologies. The second major effort of the author is to simulate the implementation of the best configuration found into a real size plant, starting from the results obtained on a single reactor scale and applying them to the scheduling of the operation of the single vessels.

Both the CFB and the fixed bed technology are tested performing numerous simulations for each of the two steel mill adopted reference cases, namely the steam cycle and the combined cycle. The results obtained confirm the expected qualities of the circulating fluidized beds in terms of enhanced contacting between solid and gas phase, high heat exchange coefficients and global compactness of the system. Nevertheless, a series of issues hinders the achievements of satisfying performances, as far as carbon capture is concerned. In particular, the necessity to operate the system in a range of relatively low temperatures, as suggested by the nature of the adsorption process, limits the capability of the system to exchange heat with an external fluid. At the same time, the limited residence time of solids and the combination of ambient pressure and high CO_2 concentrations during the regeneration stage place restrictive constraints on the maximum achievable cyclic capacities of the adsorbent. Furthermore, the amount of solids displaced by the gas flow results to be insufficient to remove the target amount of carbon from the flue gas. The recovery of the sensible heat stored in the adsorbent material represents a significant possibility to reduce the total energy consumption of the system under interesting threshold, but its implementation in a real size plant is found to cause inevitably some additional technical problems.

As far as fixed bed are concerned, on the contrary, their cyclic operation seems to suit better the schedule of a temperature swing adsorption process. The simulation conducted over the optimal cycle defined in this study returns promising values in terms of separation performances. The corresponding energy consumption levels are found to be almost still slightly higher than those of the most established technologies, but at the same time the results suggest there should be some room for improvement in this direction. Nevertheless, the scheduling of a full size plant application outlines the main limitation of this technology: a vast number of vessels, and consequently a copious inventory of solids, are required to process flow rates as high as that of a flue gas coming out of a power plant.

In conclusion, TSA process appeal as efficient alternatives for post-combustion CCS applications, thanks to the reduced amount of energy required for the regeneration of the sorbent. Nevertheless, as far as their implementation by means of both circulating fluidized beds and fixed beds are concerned, a series of remarkable issues prevent from achieving the expected and desired outcome, either in terms of separation performances, efficiency of the system, cost-effectiveness or real feasibility of the realization of the plant.

Riassunto esteso

Il presente lavoro di tesi è stato sviluppato nel contesto di una collaborazione tra il gruppo GECOS (Group of Energy Conversion System) del Dipartimento di Energia del Politecnico di Milano e il Separation Process Laboratory dell'Institute for Process Engineering presso l'ETH (Eidgenössische Technische Hochschule, Zurigo).

Lo scopo primo di questa trattazione è lo studio delle potenzialità dei processi Temperature Swing Adsorption come sistemi innovativi per la cattura di anidride carbonica. In particolare in questo lavoro viene analizzata una specifica applicazione post-combustione di cattura di CO_2, ossia il trattamento dei fumi di un impianto di produzione di potenza asservito ad un'acciaieria integrata. Di fatto, l'industria siderurgica svolge un ruolo di primo piano nel contesto delle emissioni globali di CO_2, dal momento che le può essere accreditato all'incirca il 6% della quantità emessa ogni anno su scala mondiale, la quota più alta detenuta da un singolo settore industriale.

La maggioranza degli impianti di grande taglia include entro i limiti del proprio stabilimento una centrale di produzione di potenza dedicata al soddisfacimento del fabbisogno interno di potenza elettrica. L'impianto è alimentato principalmente con i gas residui rilasciati dalle sezioni dello stabilimento che compongono la catena di produzione dell'acciaio; in casi specifici si ricorre anche ad un ulteriore flusso di combustibile gassoso, di norma gas naturale. Ne consegue che i fumi emessi dalla centrale siano caratterizzati da un alto contenuto di CO_2, dovuto al largo uso di carbone nei processi siderurgici. In questo studio vengono presi in considerazione come termini di riferimento due diversi impianti integrati per la produzione di potenza: nel primo caso un ciclo a vapore subcritico, nella cui caldaia sono combusti i gas residui dei processi di lavorazione del metallo; nel secondo caso, invece, un più innovativo ciclo combinato, che rappresenta una soluzione comunemente adottata in sede di nuova costruzione. Entrambe le unità di produzione di potenza sono descritte in letteratura, poiché sono state precedentemente adottate come impianti di riferimento nel contesto di studi per l'analisi di sistemi CCS post-combustione. Per essere idoneo ad essere integrato all'interno di un'acciaieria, un sistema di cattura deve essere in grado di trattare un flusso di fumi con una composizione altrettanto ricca di CO_2. Inoltre, per assecondare gli sforzi di efficientamento che forniscono le linee guida per la progettazione di questo processo industriale, il funzionamento del sistema deve richiedere la minor quantità possibile di energia. Dal momento che le tecnologie più consolidate per questo tipo di applicazione sono caratterizzate da un consumo energetico di circa 3.5 MJ per chilogrammo di CO_2 rimossa, questo valore può essere convenientemente impiegato come termine di paragone per identificare un

intervallo di competitività per possibili sistemi alternativi.

In questo senso, la limitata quantità di energia richiesta per la rigenerazione di un sorbente fisico all'interno di un ciclo di adsorbimento e rigenerazione candida i processi TSA come possibili alternative per un'applicazione CCS. La separazione della CO_2 da una miscela di fumi per mezzo di un processo di adsorbimento è un tema attualmente oggetto di ricerca, ma già in passato un cospicuo numero di dati è stato raccolto effettuando misurazioni in sede sperimentale. Tutti i dati relativi alla termodinamica e alla cinetica dei processi di adsorbimento impiegati in questo lavoro sono stati resi disponibili dal Separation Process Laboratory.

Per poter studiare l'applicazione dei processi Temperature Swing Adsorption come unità di trattamento fumi per la cattura post-combustione di CO_2, si ricorre all'analisi di due diversi sistemi finalizzati all'interazione gas-solido, ovverosia una soluzione a letti fissi e una a letti fluidi circolanti. È stato inoltre condotto un confronto tra le due tecnologie.

I reattori a letto fluido sono ampiamente impiegati per diverse funzioni in campo industriale per via dell'alto grado di compattezza che li contraddistingue, una caratteristica estremamente desiderabile in tutte quelle applicazioni in cui sia necessario implementare un processo gas-solido in cui sono coinvolte portate ingenti. Il loro utilizzo come reattori di adsorbimento non è tuttavia largamente trattato in letteratura ed è un'introduzione tecnica piuttosto recente. Per questa ragione, per gli scopi di questo studio viene sviluppato un metodo completamente nuovo di modellizzazione dei processi di adsorbimento e desorbimento all'interno di reattori CFB; il modello che ne deriva è succesivamente tradotto in un codice di calcolo per simulare le condizioni operative oggetto d'analisi. Questo modello consta di due parti: nella prima viene risolta la fluidodinamica del sistema, mentre nella seconda ne viene modellizzato lo scambio termico. Il modello e il codice di calcolo sono contributi originali dell'autore; per lo sviluppo del codice di simulazione, si è optato per il linguaggio di programmazione Matlab®.

Alla base della suddetta modellizzazione di un reattore CFB per un processo di adsorbimento vi sono alcune ipotesi fondamentali. Innanzitutto si immagina che il reattore operi in regime stazionario, isotermicamente e a pressione costante; di conseguenza non compare alcuna variazione di pressione nell'equazione della quantità di moto, mentre i bilanci di massa e i bilanci di energia possono essere risolti separatamente. Inoltre, si ipotizza una perfetta miscelazione dei solidi all'interno del reattore; di conseguenza tutte le particelle di sorbente si trovano ad avere la stessa temperatura e lo stesso grado di conversione. Il loro comportamento può perciò essere descritto per mezzo della teoria dei reattori perfettamente miscelati, mentre il flusso di gas è modellizzato come plug flow. Di conseguenza per descrivere il sistema viene impiegata una discretizzazione spaziale monodimensionale. Infine, si ipotizza che il trascinamento da parte dei gas sia l'unico meccanismo di trasporto dei solidi verso l'esterno del reattore.

Dal momento che la cinetica può essere rappresentata per mezzo delle stesse equazioni per i processi di adsorbimento e desorbimento, il codice di calcolo è in principio sviluppato per poter simulare entrambi i processi. Il codice è peraltro in grado di produrre risultati per un intervallo di condizioni operative più vasto di quello delineato dalle limitazioni normalmente

imposte per i comuni processi TSA. In merito agli scopi di questo studio, il codice può essere usato con successo per simulare sia la fase di adsorbimento sia quella di rigenerazione senza richiedere adattamenti rilevanti.

La ricerca sui sistemi a letto fisso nell'ambito della loro applicazione per la cattura di CO_2 ha ad oggi conosciuto un maggiore sviluppo. Per simulare il comportamento dei reattori a letto fisso è impiegato un codice di simulazione reso disponibile dal Separation Processes Laboratory ai fini del compimento di questo lavoro di tesi. Questo codice è stato sviluppato attraverso uno script in linguaggio FORTRAN e validato attraverso campagne sperimentali condotte in laboratorio su una colonna in scala ridotta. Il modello fisico impiegato è caratterizzato da una discretizzazione spaziale monodimensionale e da una discretizzazione temporale, resa necessaria dalla natura ciclica dell'attività dei singoli reattori; questo modello permette di ricostruire la fluidodinamica e la termodinamica di una singola colonna a letto fisso che sia sottoposta ad una sequenza di fasi di adsorbimento e desorbimento, durante le quali scambia calore con un fluido termovettore esterno.

Per quanto riguarda questa tecnologia, il contributo originale dell'autore consiste in primo luogo nello studio delle varie possibili sequenze di ciclo e nella definizione di una configurazione ottimale, finalizzata al soddisfacimento dei requisiti in termini di efficacia del processo di separazione e al tempo stesso, se possibile, al contenimento dei consumi energetici del sistema al di sotto della soglia delineata dalle tecnologie più competitive. In secondo luogo, gli sforzi dell'autore si concentrano sull'adattamento della migliore configurazione trovata ad un'applicazione in un impianto a grandezza reale, inteso come trasposizione dei risultati ottenuti per una singola colonna in un contesto operativo di sistema mediante la pianificazione dell'attività dei diversi reattori che compongono l'impianto.

Sia i sistemi CFB sia quelli a letto fisso vengono testati conducendo numerose simulazioni per ciascuno dei due scenari di riferimento adottati per ricreare il contesto dell'acciaieria, ossia il ciclo a vapore in un caso e il ciclo combinato nell'altro. I risultati ottenuti confermano le aspettative per quel che riguarda le qualità peculiari dei reattori a letto fluido circolante: essi assicurano un elevato grado di interazione tra la fase solida e quella gassosa, alti valori dei coefficienti di scambio termico e ridotte dimensioni totali del sistema. Tuttavia, ai fini della cattura di anidride carbonica, una serie di inconvenienti ostacolano il raggiungimento di prestazioni soddisfacenti. In particolare la necessità di condurre i processi entro un intervallo di temperature confinato al di sotto di soglie relativamente ridotte, come suggerito dalle dinamiche dell'adsorbimento, limita la capacità del sistema di scambiare calore con un fluido esterno. Allo stesso tempo, tempi di permanenza dei solidi non particolarmente lunghi e condizioni di rigenerazione sfavorevoli, caratterizzate dalla combinazione di pressione ambientale e alta concentrazione di CO_2, impediscono di raggiungere alti valori di capacità ciclica del sorbente. Oltre a ciò, la quantità di solidi effettivamente trascinata dal flusso di gas risulta in molti casi essere del tutto insufficiente per rimuovere dai fumi la quantità desiderata di anidride carbonica. Una significativa possibilità di ridurre i consumi energetici complessivi del sistema entro valori interessanti consisterebbe nel recupero del calore sensibile associato alla massa di sorbente; tuttavia la realizzazione tecnica di questo recupero termico si scontra inevitabilmente con una serie di ulteriori problematiche impiantistiche.

Nel caso dei letti fissi, al contrario, si nota una migliore corrispondenza tra le dinamiche operative del sistema e lo svolgimento dei cicli dei processi TSA. Le simulazioni condotte per la configurazione ottimale definita in questo studio restituiscono esiti promettenti in termini di efficacia del processo di separazione. È possibile riscontrare che i consumi energetici associati si collocano leggermente sopra quelli delle tecnologie più consolidate, ma allo stesso tempo i risultati evidenziano la presenza di un discreto margine di miglioramento. Ciononostante la pianificazione del processo su scala d'impianto reale mette in luce la maggiore controindicazione di questa tecnologia: per processare portate di gas, ingenti come quelle dei fumi rilasciati da un impianto di produzione di potenza è necessario un numero irrealisticamente elevato di reattori e, conseguentemente, un oneroso inventario di solidi.

In conclusione, i processi TSA si presentano come un'alternativa allettante per le applicazioni CCS postcombustione, grazie alla ridotta quantità di energia richiesta per la rigenerazione del sorbente. Tuttavia sia nel caso dei sistemi a letto fluido circolante, sia nel caso dei sistemi a letto fisso, una serie di problematiche di una certa rilevanza impedisce di raggiungere le prestazioni attese, talvolta in termini di efficacia del processo di separazione in sé, talaltra in termini di efficienza del sistema, convenienza economica o praticabilità della realizzazione dell'impianto.

Abstract

This dissertation aims at assessing the potential of employing temperature swing adsorption processes to perform carbon capture from the flue gas of the power plants integrated into steel mills. In order to provide a more comprehensive overview of the application, two different types of power production plants are considered, namely a subcritical steam cycle and a combined cycle. Two gas-solid reactor technologies are investigated and compared for the operation of adsorption-regeneration cycles: circulating fluidized beds and fixed beds. As regards the former, a completely original model is developed and implemented into a new simulation tool, whereas for the latter an already validated model made available at Separation Processes Laboratory (ETH, Zurich) is employed. The results highlight appealing features and remarkable technical issues for both technologies: on the one hand circulating fluidized beds could be synonym of low energy consumptions and compact plant layouts, but major issues concerning heat exchange from the vessel to an external fluid and the handling of the solid sorbent place restrictive constraints on the achievement of notable performances; on the other hand fixed beds seem to suit better the course of a TSA process, though the implementation of a real size carbon capture plant appears unrealistic, owing to the enormous number of vessel required to process sizable flow rates.

Key words

Temperature swing adsorption

Integrated steel mill

Fixed bed

Circulating fluidized bed

CO_2 post-combustion capture

Sommario

Il presente lavoro di tesi è finalizzato alla valutazione della possibilità di impiegare processi Temperature Swing Adsorption per effettuare il sequestro di CO_2 dai fumi di centrali per produzione di potenza asservite ad acciaierie integrate. Al fine di offrire una panoramica più ampia su questa applicazione, vengono analizzate due diverse tipologie di impianti di produzione di potenza: un ciclo a vapore subcritico e un ciclo combinato. Lo studio si incentra sull'analisi e il paragone tra due tecnologie di reattore per processi gas-solido: sistemi a letti fluidi circolanti e sistemi a letti fissi. Per i primi, un nuovo metodo di modellizzazione è sviluppato e tradotto in un codice di calcolo, mentre per i secondi viene utilizzato un modello già convalidato reso disponibile dal Separation Process Laboratory (ETH, Zurigo). I risultati evidenziano per entrambe le tecnologie la presenza di caratteristiche interessanti così come di problematiche rilevanti: da un lato i letti fluidi circolanti sono potenzialmente sinonimo di bassi consumi energetici e ridotte dimensioni di impianto, ma il raggiungimento di prestazioni di rilievo è pregiudicato dai limiti riscontrati nello scambio termico tra il reattore e un fluido termovettore esterno e da complicazioni legate alla movimentazione dei solidi; d'altra parte, i letti fissi sembrano essere una soluzione più conforme alle dinamiche dei cicli TSA, ma la realizzazione di un impianto in scala reale per la cattura di anidride carbonica appare del tutto irrealistica, per via dell'enorme numero di reattori necessari per processare ingenti portate di gas.

Parole chiave

Temperature swing adsorption

Acciaieria integrata

Letto fisso

Letto fluido circolante

Sequestro di CO_2 post-combustione

Contents

Introduction

A significant share of the global anthropogenic CO_2 emissions derives from industrial processes. The steel industry represent one of the largest sources of emission, as it accounts for roughly 6% of all the carbon dioxide yearly produced worldwide. Recent estimates suggest that this percentage corresponds to approximately 1.5 Gt of CO_2 released in the atmosphere every year, a value which, translated into average specific amounts, would range from 0.6 to 2.2 ton of CO_2 per ton of steel produced, depending on the process technology adopted for the production [1]. In the last decades a very steep growth trend has been registered in steel demand on a global-scale, already entailing the yearly amount of produced steel to almost double in the last ten years, thanks to the remarkable recent contribution of the developing countries. Moreover, the most current predictions forecast that the steel industry will continue growing further in the near future.

The premise of such an important role in global CO_2 emissions is the impressive fraction of the global energy consumption which can be ascribed to this manufacturing sector. Considering the fact that each ton of crude cast steel correspond to an average energy consumption of 20.8 GJ [1], it might not be hard to believe that steel production is one of the most energy-intensive industrial processes. Its energy demand is commonly fulfilled by means of both direct combustion of fossil fuels and electricity utilization, the latter being in the vast majority of cases anyway linked to a traditional fossil source.

Aiming at reducing these CO_2 emissions, a first attempt may be sensibly done by improving the efficiency of the process, in order to limit its energy requirements and thus the consumption of C-based fuels. In the last decades many efforts have been dedicated to this goal, achieving remarkable improvements in terms of efficiency of the processes performed in the factories. Nevertheless, to cut down CO_2 emissions under a threshold as low as 50% of today's value, carbon capture and storage systems (CCS) appear to be the only feasible solution. The development of suitable technologies to accomplish this target is an on-going issue on which numerous research projects are currently focused.

The CO_2 emitted by a steelwork derives from both a variety of processes related to steel production chain and the power plant that provides the amount of energy required in the steel mill. Given the huge energy consumption caused by the operation of the manufacturing activity, often a power plant is directly included within the factory boundaries. This solution appeals thanks to a wide availability of off-gases from the iron and steel making units. These gases feature a significant content of both CO and H_2 and therefore still own a notable calorific value; consequently, they can be used as fuels in a power production plant.

The overall CO_2 emissions that can be ascribed to the steel production activity can be reduced following different routes. A first solution would be that of directly treating the off-gases released by the most important iron and steel making processes, gases which have both high CO and CO_2 contents; such a solution involves the installation of carbon capture systems specifically adapted to be integrated with those processes. If a power plant is integrated in the steel mill to exploit the calorific value of the off-gases reusing them as fuel, a better option might be that of combining the capture system with the power production, adopting either a pre-combustion (applied on C-based fuels before being burnt) or a post-combustion capture technology (which treat the flue gas released by the power production unit). While the former necessarily implies a higher degree of integration between the capture system and the power plant, the latter allows an easier implementation, as the CCS unit can be simply added as tail end process to a plant layout originally design without it.

A wide variety of different methods have been proposed in literature to perform both pre- and post-combustion capture from power plants within integrated steel mills. Nowadays the most established technology is represented by post-combustion systems based on absorption processes, where aqueous solutions of amines are employed to separate CO_2 from the flue gas mixture. Although the effectiveness of this technology makes it perfectly suitable for the purpose of carbon capture, it has a burdensome impact on the overall energy consumption of the manufacturing plant. As a consequence, the search for less energy-demanding options is undoubtedly a current topic.

Since various mutual characteristics make adsorption and absorption processes suitable for the same types of applications, the possibility of following an adsorption-based route instead of an absorption-based one has been recently contemplated as well. The regeneration of solid sorbents, compared to liquid ones, requires on average a lower amount of energy, although the effectiveness of the two processes is in general terms comparable in regard to their separation performance. For this reason adsorption-based technologies appear to be promising alternatives for the same post- and pre-combustion applications where the suitability of the absorption processes has already been proven.

In analogy to what occurs for absorption, the only convenient route to perform large scale separation of CO_2 through adsorption is resorting to the regeneration of the sorbent material, so that it can be reused several times in a cost-effective way. Regeneration implies that a desorption stage should follow the adsorption phase, bringing the conversion degree of the sorbent back to a favorable condition to perform separation. As far as solid adsorbents are concerned, this step sequence is commonly performed by means of either pressure swing adsorption (PSA) or temperature swing adsorption (TSA) cycles, in which the evolution of the conversion degree of the solids is driven by a variation of the pressure or temperature levels of the system, respectively. However, the conceptual boundary between the two different routes can be easily trespassed when designing a cycle, so that many applications could be actually considered as halfway technologies that combine both methods. When compared to TSA, PSA processes represent for the time being a better-known technology, as more research has so far been conducted about their implementation. TSA cycles, though, offer a notable advantage for post-combustion CCS applications: since they do not need any partic-

ular pressure level to be maintained inside the process reactors, neither in the adsorption nor in the regeneration phase, there is no need to compress the flue gas as it comes out of the power plant at almost ambient pressure.

Theoretically speaking, excellent results are expected employing temperature swing adsorption processes for a post-combustion application, in terms of both separation performances and overall efficiency; however, reliable models must be developed in order to test the technical feasibility of these systems and provide tangible results of their performance. Thus, the main aim of this dissertation is to investigate the actual potential of this option, with respect to the particular case of the power plants within integrated still mills.

The first premise to accomplish this goal consists in defining a realistic implementation context for the processes at issue. Two different reference cases are referred to in this study: On the one hand a steelwork integrated with a steam cycle power plant, representing the most common type of power production system historically adopted within steel mills; on the other hand a steel factory where electrical energy is supplied by a combined cycle, that is a more efficient, up-to-date technology. The parallelism between these two scenarios is meant to provide a more comprehensive overview of the distinctive features that distinguish the actualization of carbon capture in the specific context of steel production.

A detailed discussions of the operational aspects and of the modeling of the temperature swing adsorption processes, starting from the understanding of the chemical and physical phenomena involved and broadening out to their adaptation for CO_2 capture processes, provides the proper knowledge to understand why some operational procedures are credited to fit these processes better than others. Two possible routes are contemplated in this study for the operation of the adsorption and desorption processes, each of them resorting to a different type of gas-solid reactors. Alongside the investigation of the more traditional solution for all PSA and TSA processes, which consist in using fixed bed reactors, a more unusual option is contemplated, which involves the operation of circulating fluidized bed (CFB) reactors.

Although fluidized beds do not represent an innovative technology, given the fact they are extensively employed in a wide variety of industrial processes since the first decades of the last century, combining adsorption for CO_2 separation with the fluidization of the sorbent bed is a quite recent proposal, which has not been extensively investigated in literature yet. For this reason, this study includes the development of a completely new model aimed at simulating the operation of adsorption processes inside CFB reactors, whereas for the computation of the fixed beds behavior validated tools are already available and can be profitably used for the purposes of this thesis.

In order to conduct a comprehensive analyses of the application at issue, both technologies have to be tested with reference to both steel mill scenarios. The results obtained from the simulation of the four resulting cases should allow to observe the most significant trends that characterize the implementation of TSA processes for CO_2 capture, so that some conclusions could be drawn about their actual potential and a few directions could be indicated for possible further research about the topic.

Chapter 1

Integrated steel mills

A steel mill plant consist of several units, each of those executing some of the necessary functions needed to transform iron ore or scrap steel into a new final steel product. Among all the processes involved in the production chain, the core ones can be summarized by means of the following short list:

- preparation of the raw materials, which involves the addition limestone and other additives to the sinter that is later turned into iron and the handling of the coke and lime needed by the steel making processes;
- iron making process, where the hot metal is produced; its sulphur content is also adjusted in a dedicated unit;
- steel making process, where the metal is converted into steel with the desired specifications;
- casting, where the steel is shaped accordingly to its end use;
- product finishing, where the production is accomplished yielding the final product.

Depending on the technology adopted, two main categories of processes can be identified [1]:

- about 65-69% of the steel production worldwide (58% within the European Union) is operated reducing iron ore in a blast furnace and then processing it into a basic oxygen furnace steel making plant;
- another significant fraction, around 29%, derives from melting recycled metal scraps in an electric arc furnace;
- the rest of it is produced following a few other steel making routes.

The blast furnace–basic oxygen furnace systems are not only the most extensively employed, but also the one traditionally opted for in the largest plants. Whenever the plant size oversteps a certain threshold, a power plant is more likely to be directly integrated within the steel mill. For these reasons, accordingly to the purposes of this study, the former of the listed categories is focused on in these pages.

In a blast furnace–basic oxygen furnace steel mill, many of the units which form the steel production chain are responsible for emitting flue gases which contain CO_2. Three of them can be identified as the main carbon dioxide producers:

- the blast furnace and the hot stoves, the core units of the iron making process, out of which the hot metal is produced before being sent to the desulphurization unit; the gas that flows out of them is indicated as 'BFG';
- the basic oxygen furnace, where the steel making process is conducted; its flue gas is called 'BOFG';
- the coke oven, where coke is peparated; its corresponding gas is usually labeled as 'COG'.

All these off-gas streams have a significant CO_2 content, but at the same time their heating value is high enough to make them suitable for further exploitation as fuel, in order to produce the electricity or the steam required by the plant units.

1.1 Integration of a power plant

Since a huge amount of energy is required by the steel production in the form of electricity and some process off-gases can be effectively employed as fuels, directly integrating a power plant within the boundaries of the steel mill appeals as a sensible alternative to outer provision. Figure 1.1 shows a schematic example of how a power plant integration is implemented, displaying the most important units connected to the power production system and the gas flows involved.

Historically, the most common way to implement this integration has consisted in adopting a steam power cycle. The boiler of a steam cycle can be easily fired with off-gases characterized by a low calorific value, which means indeed an operative advantage; however, other fuels (mainly natural gas) are usually fed to the boiler. The steam produced can be either completely expanded in a steam turbine to yield electrical power or can be partially utilized in the processes which require some. Its technical simplicity has promoted this solution in the last century, so that steam cycle represents at present time the most common power plant type within operating integrated steel mills.

More recently, though, combined cycles have gained a major role in the context of steel production, thanks to the higher efficiency they achieve. They represent the modern technology for integrated steel mill applications and are already nowadays opted for in most cases of new construction or renovation.

Given the interest both power plant technologies arouse with respect to integration inside steel mills, for the purposes of this study two different reference plants are identified: In one case a traditional integrated steel mill featured with a steam power cycle is considered, in the other case a more modern plant characterized by a combined cycle. For the sake of clarity, throughout the whole work the first will be generally denoted as 'boiler case', while the latter will be labeled as 'combined cycle case'.

The choice of these references is made taking into account only currently available technologies; both plants have been previously identified in literature as proper references case to investigate the implementation of post-combustion CCS systems in power plants within integrated steel mills.

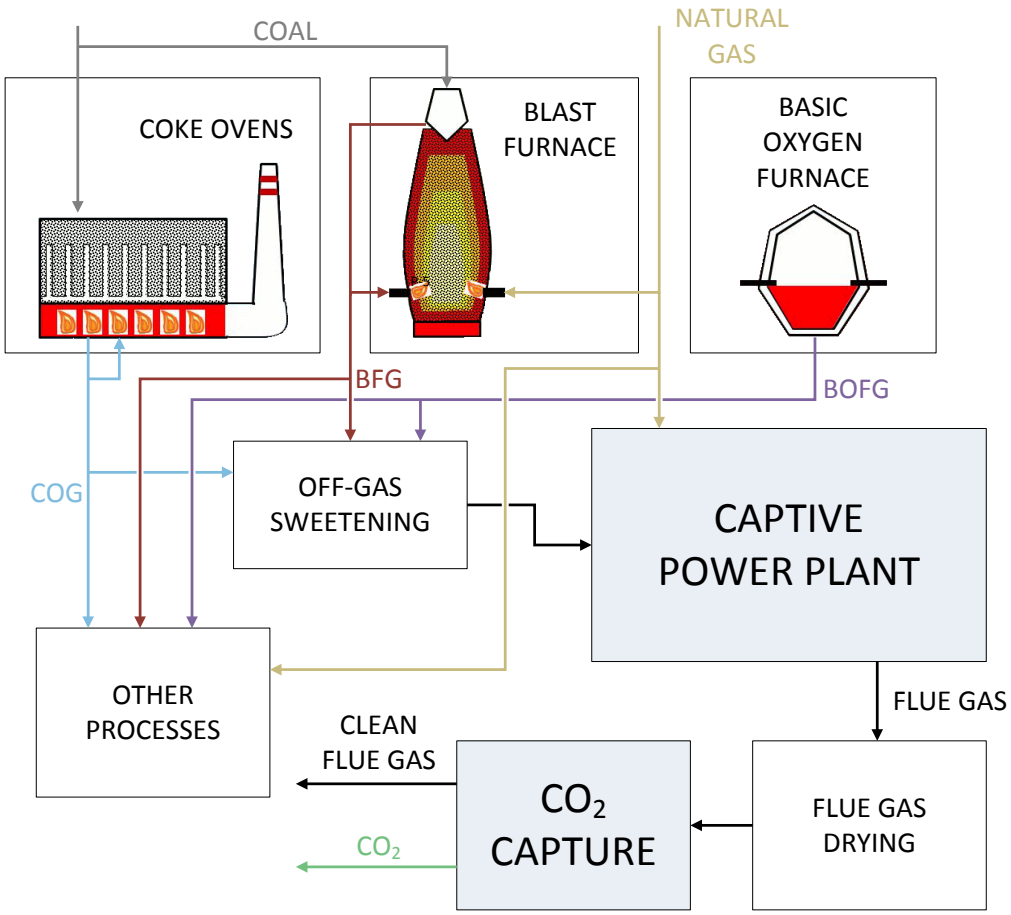

Figure 1.1: Schematic example of integration of a power plant into a steel mill [2]

Being each of them related to a specific steel production plant, there is an obvious discrepancy between the power outputs and the flue gas flow rates of the two plants, but the orders of magnitude are consistent, so that it seems legitimate to carry out a parallel analyses on the two scenarios.

1.2 Boiler case

A report published in 2013 by the International Energy Agency in the context of its Greenhouse Gas Protocol [1] gives a detailed description of an example blast furnace steel mill – which is stated to be representative of several plants located on the Atlantic Cost of Europe– and it adopts it as reference plant for the purposes of the investigations conducted in the paper.

The steel mill at issue integrates a steam cycle power plant whose boiler is fed not only with the off-gases coming out of some steel production units, but also with an additional share of externally provided fuel. The following assumptions define the power plant in details:

- all the flue gas is produced from three units, namely the coke ovens, the blast furnaces and the basic oxygen furnaces; it is completely recovered to be used within the steel mill, as fuel in the power section as well as process gas in other units;
- the power plant produces an amount of electric power exactly correspondent to the need of the steel mill, so that no external provision of electricity is required and no power can be exported out of the factory;
- an additional stream of natural gas is fired together with the off-gases inside the boiler of the steam cycle, in order to supply the demanded power at the generator of the steam turbine.

This power plant produces electrical power by means of a subcritical steam cycle, operated without steam reheat. The steam produced in the boiler is entirely sent to the steam turbine, whereas the amount required by the steel mill processes is extract during the expansion in the form of steam bleedings.

Table 1.1: Boiler case: power plant flue gas data

	volumetric fraction
CO_2	26.43%
O_2	0.71%
N_2	65.88%
H_2O	6.98%
Pressure	1.03 bar
Temperature	150°C
Mass flow rate	338.13 kg/s

The flue gas fed into the boiler together with natural gas is a mixture of BFG and BOFG only, while COG is not conveyed directly into the power plant, but it is partially used in the blast furnace instead, affecting the final composition of the off-gas used as fuel in the boiler.

In the end, the power unit yields a flue gas stream with the specifications reported in Table 1.1. It is interesting to notice how the concentration of CO_2 is eventually much higher than those usually encountered in stand-alone power plants which operate burning standard fossil fuels. This is of course caused by the high initial carbon content of BFG and BOFG.

More data about the gas streams involved in the power production, the plant schematic layout and other information as provided in the report by International Energy Agency [1] can be found in Appendix 1.

1.3 Combined cycle case

For the combined cycle scenario, the reference case adopted in this work is the one outlined by Gazzani et al. [2] in their study about sorption enhanced water gas shift as pre-combustion technology in steelworks power plants. The combined cycle at issue is presented in their paper both as reference case without carbon capture and as base plant to implement a MEA post-combustion capture system; therefore it appears to be perfectly suitable for the application of a any other post-combustion capture technology as well.

The described plant is a state-of-the-art integrated blast furnace steel mill factory, within whose boundaries a combined cycle is installed. The two following main assumptions are

made:

- off-gases are produced by the steel mill processes at constant flow rate; in particular, a fraction of the gas flowing out of coke ovens (COG) and blast furnace (BFG) forms the fuel used in the gas turbine of the combined cycle;
- neither natural gas nor any other fuel is blended with the off-gases before they are fed into the power plant.

The combined cycle is derived from a standard NGCC featured with a generic F class gas turbine; no derating is needed for the turbine inlet temperature because of the low calorific value of the burnt fuel. In these configuration, steam bleedings can be employed to meet the internal demand of the steelwork plant. Compared to a standard application, where natural gas is already under pressure when it enters the plant, if low pressure off-gases are to be fed at the turbine burners, a significant amount of power must be spent to compress them. Therefore the total efficiency of the system is presumably lower than what could be expected by an analogous system burning natural gas.

Table 1.2: Combined cycle case: power plant flue gas data

	volumetric fraction
CO_2	9.59%
O_2	10.06%
N_2	72.90%
H_2O	6.68%
Ar	0.77%
Pressure	1.01 bar
Temperature	80°C
Mass flow rate	525.80 kg/s

The overall size of the power plant in this scenario is remarkably larger than in the previous reference case, being the total electric power released by the system almost 75% higher and the total flue gas mass flow rate around 55% greater. Despite this discrepancy, the two application still have common order of magnitude for all the parameters enquired in this study; however, no direct comparison is ever conducted between the two scenarios in terms of absolute quantities.

This power plant yields a flue gas whose specifications are listed in Table 1.2. It can be observed how the concentration of CO_2 in the flue gas is significantly lower of that of the boiler case. It is comparable to the values found in traditional coal firing power plants, which means anyway higher than what could be expected from a standard NGCC plant. Moreover, also the content of O_2 is very different from the one of the previous case, due to the typical high air-to-fuel ratios of combined cycles.

More data about the off-gases burnt in gas turbine, the plant schematic layout and other information as provided in the paper by Gazzani et al. [2] can be found in Appendix A.

1.4 Carbon capture

As already mentioned, within a steelwork both the processes related to steel production and the power production are responsible for the emission of sizable amounts of CO_2. Depend-

ing on which CO_2 source is to be handled to reduce the emissions, a variety of different CCS systems can be taken into account. If the goal is to directly reduce the emissions yielded by the steel making sections, a well-known possibility consists in applying an oxy-combustion system to the blast furnace, the unit which accounts for the largest share of CO_2 emissions among the different steel production steps (representing up to 70% of the total emissions). This option is based on the replacement of a traditional blast furnace with an oxy-blast furnace. An OBF (also known as 'nitrogen free blast furnace (NFBF)' or 'top gas recycle blast furnace (TPR-BF)' is a furnace which employs an oxygen-rich stream instead of the air for the production of the hot metal; furthermore, it partially recirculates the CO- and CO_2-rich top gas back into the furnace feed, reducing the total amount of coke required for oxygen removal from the iron ore used as feedstock. A CO_2 capture system can be inserted directly into the the recycle loop, taking advantage of the absence of nitrogen in the treated gas and of the high CO_2 partial pressure in the flow. A scrubbing of the top gas by means of aqueous solutions of amines, like in MEA or MDEA processes, is an advisable solution to perform carbon capture under this conditions and appears to be nowadays the most credible system for this specific implementation, but also PSA processes might be suitable for the purpose [1]. If no OBF is used, a standard carbon capture technology could be adopted to process the off-gas exiting from the top of the blast furnace, but lower CO_2 contents and the presence of N_2 would inevitably hinder the capture process.

A different approach would be that of reducing the emissions caused by the operation of the integrated power plant. Since most of the off-gases released by the steel making units are used as fuel in the power section, most of the total CO_2 produced in the factory could be then separated integrating a CCS system. With respect to the power plant, the capture procedure can be performed by means of either pre-combustion or post-combustion solutions. In this sense, various approaches have been suggested to implement these technologies inside steel mills, with the post-combustion solutions being today accredited as the most established ones. The pre-combustion systems require on average a higher degree of integration between the CCS process and the plant, because their implementation usually entails –beside the insertion of the CCS system– a few modifications to the design of the steelwork (starting from a different operation of the gas turbine of the power plant if a combined cycle system is adopted). The post-combustion option is on the contrary favored by a less complex actualization, as it can be simply added as a tail end process to a manufacturing plant which was previously designed without carbon capture.

An example of possible pre-combustion technology applied to the power plant of an integrated steel mills is the one suggested by Gazzani et al. [2]. The CO_2 capture process used in this case consists in combining a water-gas shift reaction, which is intended to raise the ratio between H_2 and CO in the off-gases, with a sorption process, which removes CO_2 from the WGS reactor providing two benefits, namely the enhancement of the WGS reaction towards more H_2 production and the capture of carbon dioxide. Such a solution looks promising in terms of both CO_2 emission avoidance and limitation of the additional energy consumption caused by the CCS system.

As regards the post-combustion capture technologies applied to the steel production field,

MEA processes have so far gained the most prominent position among the possible alternatives, as reported by Arasto et al. [3]. These absorption processes are based on putting into contact an aqueous solution containing amines with the flue gas that flows out of the power plant. The regeneration of the solvent requires a great amount of thermal power, determining an energy consumption of approximately 3.4 MJ per kilogram of captured CO_2. Since MEA-based processes represent the most evaluated and best-known technology for this application, the energy consumption rates they are accredited with are therefore to be set as target value for any competing CCS system applied to power plants integrated within steel mills.

Adsorption-based systems for CO_2 separation, both in the form of pressure swing adsorption (PSA) and temperature swing adsorption (TSA) cycles, have been extensively investigated in the last decade, as they represent a promising alternative for all those pre- and post-combustion applications where the suitability of absorption-based methods has already been proven. In fact the integration of an adsorption process into the steelworks could be realized following the same approach which has been suggested for absorption processes. Moreover, both PSA and TSA cycles allow achieving very high CO_2 recovery rates, meeting at the same time the purity requirements established by CO_2 storage methods; at the same time, the specific amount of energy required by the regeneration of a solid adsorbent is generally lower than that commonly registered for an aqueous solution of amines; this feature could be exploited to reduce the impact of the CCS system on the overall consumption of the steel factory, without compromising the effectiveness of the carbon capture.

1.5 Flue gas drying

On the purposes of this investigation, the flue gas exiting from the power plant is always assumed to enter the carbon capture system with a water content equal to zero. This is due to the characteristics of the TSA processes for CO_2 capture, which require the treated gas flow to be completely dried before it interacts with the solid sorbent. The reasons for this requirement are related to the complex behavior of water in the adsorption processes, which many researches have recognized to be not only problematic to model, but also undoubtedly unfavorable towards CO_2 adsorption. The details of this issue will be further discussed in depth in Chapter 2. Here a few words are spent instead to explain through which procedures the water content of the flue gas can be reduced to the required extent.

Considering the fact that the flows at issue are characterized by huge flow rates, two main routes can be followed in order to dry the gas:

- a cooling-based process, which consist in reducing the temperature of the gas flow until all the water contained condenses and can be easily separated from the other species, which have not left the gaseous phase;
- an adsorption-based process, which exploits the selectivity of some sorbent materials towards water to separate it from the other gas species.

Even if it would be interesting to investigate which of the two solutions would suit best the application dealt with in these pages, it is out of the intention of this work to discuss this

issue in details. However, since it is here assumed that a drying process is mandatory in the context of the considered TSA application for carbon capture, it is important to give at least a few indicative values of the impact the introduction of a drying section would cause on the system and on its final performances. In fact, in order to globally assess the operation of the proposed TSA solutions, they are to be compared to the most common post-combustion application, which in many cases do not required the flue gas to be dried.

As regards the cooling-based process, a possibility is to operate the cooling by means of a sequence of chiller. If the flue gas is already saturated, an advisable solution is to employ direct contact coolers, in which the gas exchanges heat with a shower of vaporized water at lower temperature. Since the gas is already saturated in water, there is no possibility for the vaporized water to evaporate. Valenti et al. [7] have suggested this cooling procedure to dry a flue gas flow directed to a CAP unit for carbon capture. The flue gas treated in this application is produced by an ultrasupercritical steam cycle power plant, has a volumetric fraction of CO_2 of 14.5% and is saturated in water, as said; it is supposed to enter the first chiller at a temperature of 49°C ; at the last chiller, heat is removed from the system by an evaporating fluid at the temperature of -1°C. The total amount of electric power required by the cooling system is estimated in about 0.05 kWh (0.18 MJ) per kg of CO_2, i.e. approximately a fifth of the thermal energy that has to be removed from the refrigerating fluid (which means considering a COP of about 5). In comparison with the the scenarios investigated in the present study, a much lower temperature of the flue gas is considered though. Adapting this technology to the cases at issue, undoubtedly higher specific consumption would be found (an indicative amount of 0.5 MJ of electric energy may be realistically assumed as reference value, according to the temperature of the flue gas streams considered in this study).

An adsorption-based process, instead, might consist in operating a TSA cycle with a proper sorbent that shows selectivity towards water. Some calculations have been done at Separation Processes Laboratory (ETH, Zurich) for a TSA process performed at a pressure of 2 bar using silica gel as adsorbent, which is assumed to adsorb water only, while all other components behave as inerts. Initially the flue gas is pressurized up to 2.2 bar in a compressor, then is cooled down to 30°C partially condensing water. At this point the drying is completed by sending it to the adsorption column. A schematic sketch of the process layout can be observed in Figure 1.2. The total energy requirement is given by the sum of three terms:

- the heat exchangers required to heat the purge stream for the desorption column and the flue gas;
- the compressor used to pressurize the gases;
- the heating of the column during the desorption step

On the whole, considering a standard flue gas, it can be approximately estimated in 5 kJ of heat per mol of dry product, which would roughly correspond to 1 MJ for kg of CO_2.

To sum up what have just been explained, including a gas drying process is mandatory to perform a TSA cycle for CCS; it should reduce the content of water as much as possible, since even a limited amount of steam in the flue gas worsens inevitably the effectiveness of the adsorption process. Any drying system cause an additional energy consumption, which

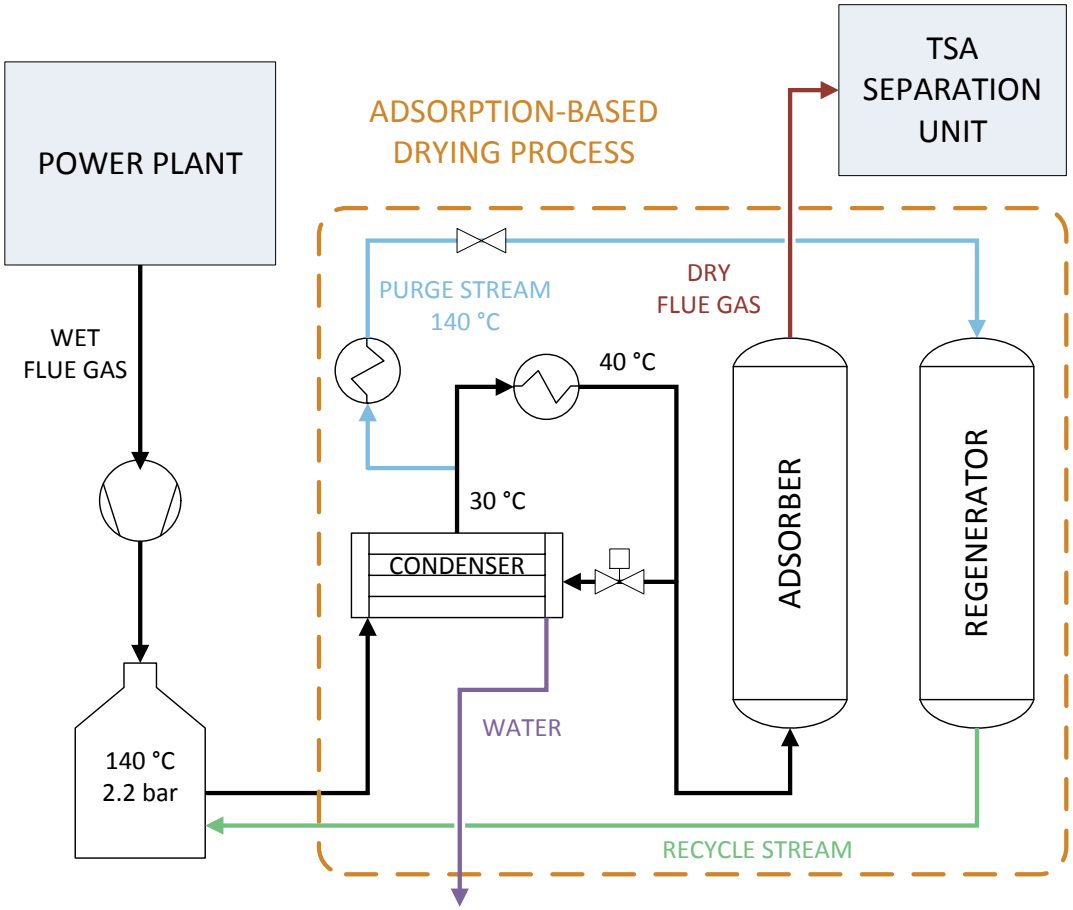

Figure 1.2: Schematic layout of an adsorption-based drying process [31]

should be sensibly taken into account when assessing the overall performances of the carbon capture system; the last mentioned value of 1 MJ of heat duty per kg of captured CO_2 appears to be representative of the best performing drying systems and can be therefore conveniently assumed as reference value.

Chapter 2

Temperature Swing Adsorption

Adsorption is the phenomenon at the basis of TSA processes. The next section briefly illustrate what adsorption is, which reasons arouse interest towards them with respect to CCS applications, how it can be modeled for the purposes of this work and what a temperature swing adsorption process consists in.

2.1 Adsorption

Adsorption is the process whereby ions, atoms or molecules of a gaseous or liquid species interact with a solid surface. Some solid materials have the property of strongly attracting a large amount of those particles and of making them adhere to their surface via chemical or physical bonds; they are called 'adsorbents', while the adsorped phase is usually indicated as 'adsorbate'. Depending on the type of bonds (chemical or physical) established between the solid surface and the adsorbate, a distinction is commonly drawn between chemisorption and physisorption. Differences deriving from the interaction nature extend to a wide variety of properties; for the sake of brevity, it might be simply stated that in physical adsorption weaker binding forces occur, in comparison with chemical adsorption.

A sorbent can be said to be 'selective' towards a certain species when it attracts the gas or liquid molecules of that compounds to a significantly wider extent rather than those of others. The selective nature shown by some solid materials has been broadly investigated to be exploited in the context of gas separation processes and nowadays a wide variety of technologies resorts to adsorption phenomena.

Recently a certain interest has arisen towards adsorption in the context of both pre- and postcombustion CO_2 capture and some substances have been found to be highly selective sorbents towards carbon dioxide out of mixtures formed with H_2, O_2 and N_2. The most attractive applications involve physisorbents, that offer the opportunity to recover the solids after adsorption by means of a regeneration process which requires a limited amount to be performed. During the regeneration the adsorbed species are in reverse desorbed from the solid surface. This is possible owing to the relative weakness of the physical bonds, which thus require a limited amount of energy to be broken; it might represent a remarkable

advantage, if the sorbent material has a notable cost or cannot be easily dismissed.

2.2 Adsorption modeling

The most common and immediate way to describe an adsorption process is to outline its related isotherm. An adsorption isotherm is a curve that indicates the specific amount of adsorbate collected on the sorbent surface as a function of the partial pressure (if gas) or concentration (if liquid) of the fluid phase. Typically for gases, an 'adsorbed amount–partial pressure' diagram is employed. Each curve is drawn for a specific fluid species interacting with a specific solid sorbent at a fixed given temperature; each point forming the curve represents an equilibrium condition reached by the adsorbent-adsorbate system for a given partial pressure of the fluid phase. Isotherms are defined as 'favorable' when concave (like in Figure 2.1d) and 'unfavorable' when convex.

Isotherms are usually traced to describe a single adsorbate–single adsorbent interaction. However, it is evident that many different fluid species may interact simultaneously with the same solid material and they will mutually affect their adsorption behaviors, so that many curves could be ideally drawn for different compositions of the gas phase, depending on the ratios between the partial pressures of the single components. Even if it might be often preferable to look at the single-species isotherms in order to consistently consider only one reference, for most applications it is necessary to take into account these mutual incidences between different components, as they may significantly affect the results. This is undoubtedly the case for CCS application, where CO_2 has always to be captured out of a gas mixture.

Numerous models have been suggested to detail the adsorption process for gas mixtures. For the purpose of this study, the socalled 'Sips' equation (2.1) model is employed, consistently with what has been already suggested for binary, ternary and other multi-component mixtures [8][9]. According to the model, for a mixture of $N_{species}$ components considered as perfect gases, the specific amount of i-th component adsorbed for sorbent mass unit at equilibrium conditions $n_{eq,i}$ can be computed by means of the following expression:

$$n_{eq,i} = n_{\infty,i} \frac{(\kappa_i \, y_i \, p)^{\gamma_i}}{1 + \sum_{i=1}^{N_{species}} (\kappa_i \, y_i \, p)^{\gamma_i}} \qquad \left[\frac{mol}{kg}\right] \tag{2.1}$$

All three parameters $n_{\infty,i}$, κ_i and γ_i describe the dependence on the system temperature [9]. The first is the saturation capacity of the solid, that is the maximum adsorbable amount at that temperature level; it is a function of T through an Arrhenius-type equation

$$n_{\infty,i} = A_{\infty,i} \exp\left(-\frac{B_{\infty,i}}{RT}\right) \qquad \left[\frac{mol}{kg}\right] \tag{2.2}$$

as well as the affinity coefficient κ_i, which mainly determines the shape of the isotherm

$$\kappa_i = A_{\kappa,i} \exp\left(-\frac{B_{\kappa,i}}{RT}\right) \qquad \left[\frac{1}{Pa}\right] \tag{2.3}$$

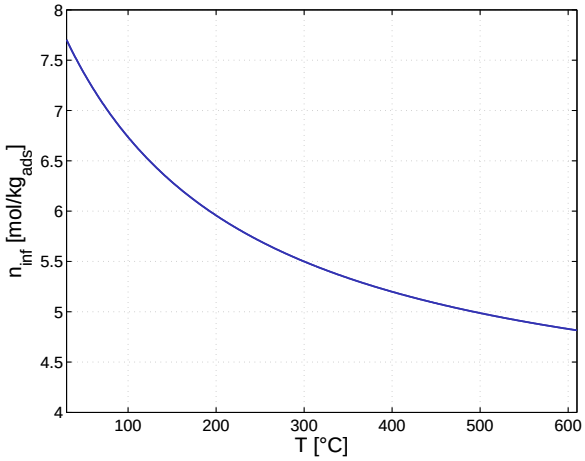

(a) n_∞–T curve for pure CO_2 adsorption over Zeolite 13X

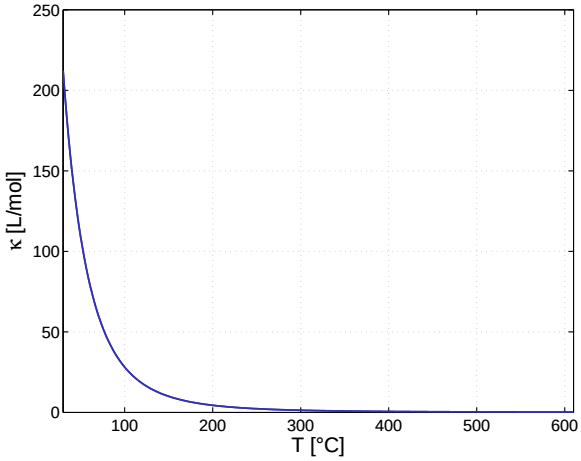

(b) κ–T curve for pure CO_2 adsorption over Zeolite 13X

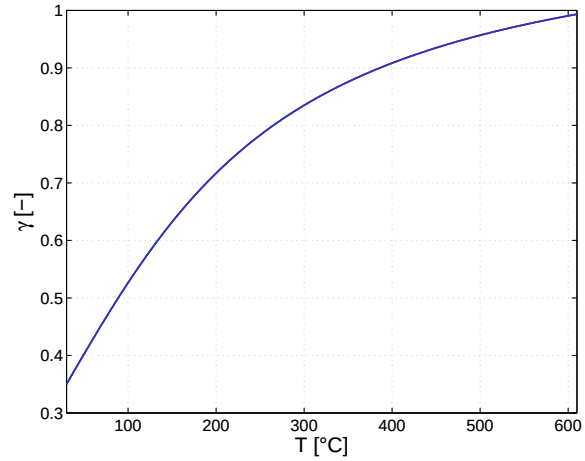

(c) γ–T curve for pure CO_2 adsorption over Zeolite 13X

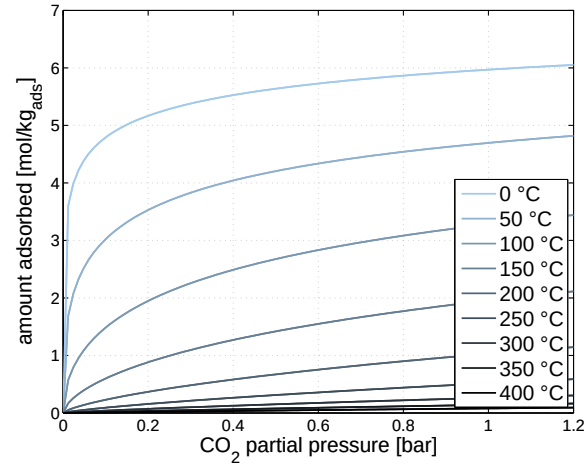

(d) Isotherms at different temperatures for pure CO_2 adsorption over Zeolite 13X

Figure 2.1: Isotherms dependence on temperature

The coefficient γ_i accounts for inhomogeneity of the sorbent surface; its dependence on temperature is evident only for certain species and can be formulated as suggested by Schell et al. [9]:

$$\gamma_i = A_{\gamma,i} \operatorname{atan}\left(B_{\gamma,i}\left(T - T_{ref,i}\right)\right) + \gamma_{ref,i} \qquad 0 < \gamma_i \leq 1 \qquad [-] \tag{2.4}$$

Adsorption is an exothermic process, as it could be discerningly deduced by the fact that it causes bonds to be established. Consequently, high temperatures must be expected to have a negative effect on it. As a matter of fact, the mentioned coefficients are affected by temperature as shown in Figure 2.1: since $B_\infty \leq 0$ and $B_\kappa \leq 0$ always, saturation capacity and affinity parameter tend to decrease as temperature rises up, though less and less steeply. The inhomogeneity coefficient shows a counteracting trend, but its influence appears to be secondary. All in all, isotherms become lower for increasing temperatures, but they get also

closer one to the other, until they theoretically collapse on a 0-valued horizontal line for $T = \infty$. The Sips equation can also be framed in terms of concentrations C_i instead of partial pressure $y_i\, p$ adopting proper coefficients.

Once the equilibrium conditions are known, they act as an asymptotic value that may be reached only after an infinite time. If under certain conditions $n_{eq,i}$ represents the maximum adsorbable amount, it can be assumed to correspond to the ultimate conversion degree of the solid; the conversion degree of the solid χ_s can be then computed as

$$\chi_{s,i} = \frac{n_i}{n_{eq,i}} \qquad [-] \tag{2.5}$$

for that fixed set of conditions. The kinetics of the adsorption process are described by a quantity, the rate of adsorption r_i, which is function of the conversion degree of the sorbent; out of the many different models that can be found in literature to determine this adsorption rate, after Jee et al. [8] a linear driving force (LDF) model has been chosen, which is stated as being frequently and successfully adopted for gas adsorption kinetics:

$$r_i = \frac{dn_i}{dt} = \omega_i\, n_{eq,i}\,(1 - \chi_{s,i}) = \omega_i\,(n_{eq,i} - n_i) \qquad \left[\frac{mol}{kg\, s}\right] \tag{2.6}$$

being ω_i the single lumped mass transfer parameter for the LDF model.

The integration of the adsorption rate differential equation allows evaluating the adsorbed amount with which solids are loaded after a given residence time under fixed conditions, starting from an initial conversion degree $\chi_{s,0}$:

$$n_{i,0} = n_{eq,i}\, \chi_{s,0,i} \qquad \left[\frac{mol}{kg}\right] \tag{2.7}$$

$$\int \frac{dn_i}{n_{eq,i} - n_i} = \int \omega_i\, dt \tag{2.8}$$

which yields

$$n_i(t) = n_{eq,i} - (n_{eq,i} - n_{i,0}) \exp\left(-\omega_i\, t\right) \qquad \left[\frac{mol}{kg}\right] \tag{2.9}$$

By means of this last expression a solid sorbent particle can be completely characterized in terms of amount of adsorbed species, once it is known which conditions it has been subjected to and for how long.

2.3 Temperature Swing Adsorption processes

As already stated, physisorbents allow operating a reversible adsorption. In order to put into practice such a procedure, the solid sorbent must be subjected to two different environments in sequence, the first promoting adsorption and the latter promoting desorption. This means two different points might be identified in a $n_{eq,i}$–p_i diagram, each of them representing the equilibrium conditions of one of the two environments.

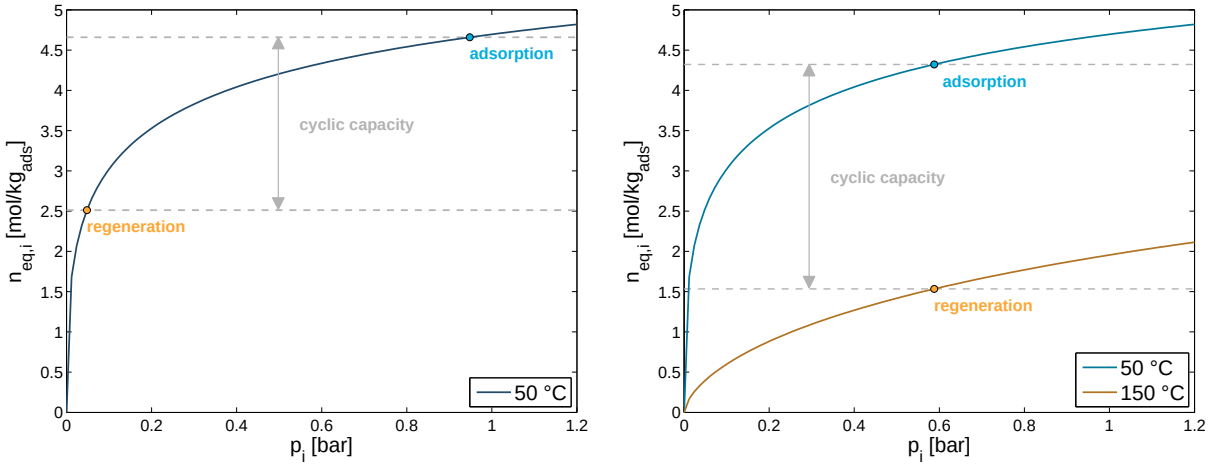

(a) Theoretical PSA cycle **(b)** Theoretical TSA cycle

Figure 2.2: PSA and TSA process concept

Since more than one parameter affects the equilibrium adsorbed amount, there are different possibilities to recreate favorable conditions for each processes. For example, pressure swing adsorption processes exploit the effect of the component partial pressure: adsorption is conducted at high pressures, so that partial pressures of the adsorbate are elevate even if it holds a limited content in the gas mixtures, whereas in the regeneration phase the pressure is reduced to lower the partial pressure of the component. This means a PSA process can be theoretically performed without changing the temperature of the system at all, i.e. remaining on the same adsorption isotherm (Figure 2.2a).

TSA processes, instead, use a difference in temperature to determine the two points, which means they operate regeneration moving the system from an adsorption isotherm to a lower one. As a consequence, they could theoretically be implemented without any change of the partial pressure of the gaseous component (Figure 2.2b)

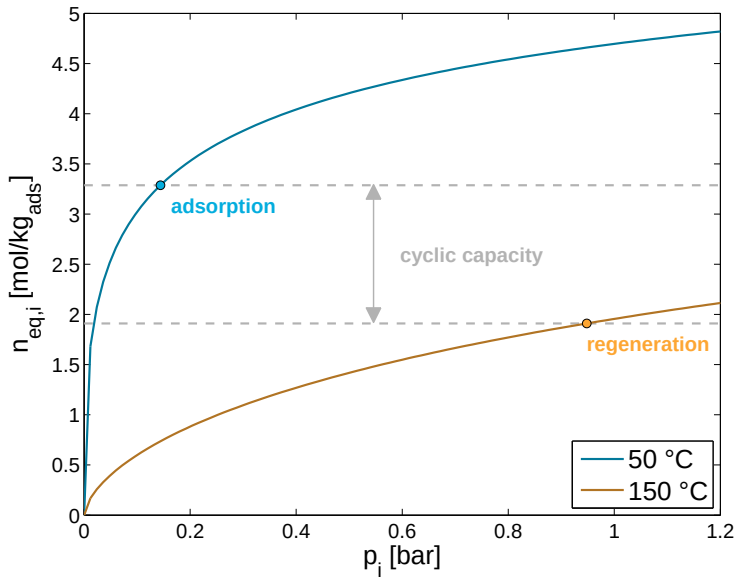

Figure 2.3: Example of TSA cycle points for CCS application

In both cases, once the regeneration step has been completed, the system can be pushed back to adsorption point and the process can start again. By repeating this sequence many times alike, a cyclic process is established.

Looking more carefully into the application of temperature swing adsorption cycles for CO_2 capture, a few observation might be done. First of all, as far as CCS systems for industrial applications are concerned, CO_2 concentrations in the gas flows to be

treated for carbon removal are usually limited under 30%, which means the adsorption condition are likely to feature a relatively low partial pressure of CO_2. At the same time, during the desorption stage the solid will probably interact with a CO_2-rich gas phase, because a certain purity is generally desirable for the recovered adsorbate product. Moreover, since in principle no particular specification about pressure levels are required, the processes are run at a system pressure available in the gas flow, which for postcombustion application is around ambient pressure. Owing to this reasons, the typical TSA cycle for a postcombustion CCS unit will use points somewhat closer to the ones shown in Figure 2.3.

This figure has an only illustrative purpose, but since it has been sketched using real data for pure CO_2 adsorption over a commercial sorbent, two precious hints might be already collected from it: A change of only 100°C is already enough to create the prerequisites of a TSA cycle for CCS and the interesting temperature range does not extend towards very high values. In fact, it has already been explained how, as regards the regeneration phase, the performance of the desorption process would improve more and more slowly while moving in the direction of higher temperatures, while the technical efforts would rationally rise more and more significantly, as well as the exergetic value of any required heat amount.

Therefore, in comparison with other separation technologies applied in the field of CCS, a very promising feature of the adsorption processes consist in the low temperature levels they require, which make them suitable for recovery of low-value heat fluxes. Moreover, since no high pressure levels are required, they appear to be more suitable than the PSA processes for those many postcombustion applications, in which the flue gas has already been expanded.

2.4 Choice of the adsorbent material

A solid material should be characterized by a combination of desirable features in order to be considered a suitable adsorbent for a specific separation application:

- First of all it should be highly selective towards the components whose separation the process is aimed at, which means that its capability of attracting those particles is significantly higher compared to that of attracting all the other species forming the fluid mixture out of which the removal is performed; otherwise the composition of the adsorbate would be similar to that of the fluid phase, so that no real separation, but rather just a change in physical state from fluid phase to adsorbed phase occurs.
- It should provide the largest surface available for adsorption within the smallest volume, which for solids usually means it has to be a porous materials; its pores should moreover be wide enough to allow the adsorbate molecules to flow inside them, so that the most of the total available surface can be actually exploited.
- It should also be inexpensive, at least when a huge amount of component has to be removed and several tons of solid material are required, accounting for a significant fraction of the total set-up costs of the system; even if in many cases the sorbent can be recovered through a regeneration step, a deterioration of the adsorbent can be sensibly predicted, so that at some point replacement might be necessary.

- If possible, it should also preferably be resistant to corrosion and not dangerous to handle.

Although these specification limit the number of possible choices to a restricted class of solid materials, a wide variety of possibilities have been studied so far and many different adsorbents are commercially available.

As regards CCS applications, high selectivity towards CO_2 is necessary when operating in presence of O_2, N_2 and H_2, considering that those species might reasonably feature comparable or higher partial pressures. Furthermore, many tons of adsorbent are required to process gas flow rates inside a power plant, so it has inevitably to cost as little as possible in order to contain the total system costs.

For the purposes of this study, a single adsorbent is chosen to perform all simulations, as it would be too time-demanding to test different solid materials and it is anyway somehow apart from the aims of this work. However, a preliminary choice is made between two suitable sorbents, whose adsorption properties have been previously investigated at Separation Processes Laboratory (ETH, Zurich) and are therefore available:

- Activated carbon, a form of porous carbon with low-volume pores that can be produced through a variety of industrial processes, obtaining slightly different specifications that suit better one or another application; its high porosity provides available surfaces of many hundreds of square meters per gram (usually above 500 m^2/g);
- Zeolite 13X, a microporous material of the family of zeolites; zeolites are aluminosilicate minerals that can be artificially synthesized and that are commonly employed as both adsorbents or catalysts in a wide range of industrial fields.

Both are commercially available and both have already been suggested in literature as adsorbent for CO_2 in the very last years [10, 11, 12, 13, 14], as the proposal of adsorption processes for CCS has gained some exposure.

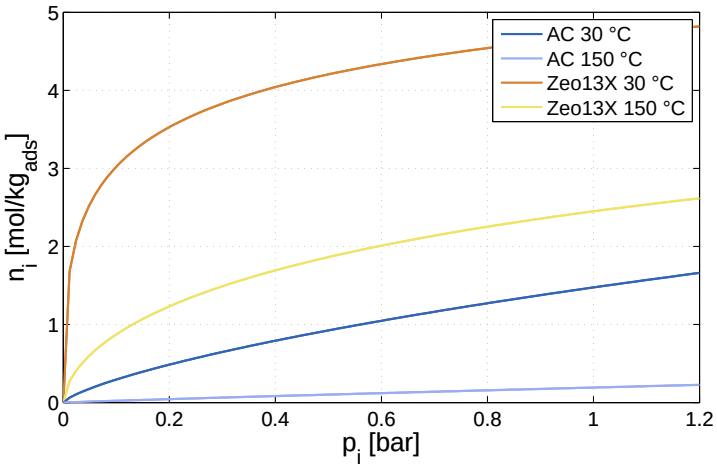

Figure 2.4: Isotherms for pure CO_2 adsorption on activated carbon and zeolite 13X

A comparison between the two activated carbon and zeolite 13X is made by looking at their adsorption isotherms for CO_2 both as pure species or as component of CO_2-N_2 gas mixtures with different compositions. In particular, the analysis is made on the bases of two assessments: First isotherms at common TSA adsorption and regeneration temperatures are outlined for different compositions; then a theoretical maximum cyclic capacity curve is drawn by varying the desorption temperature, once all the other parameters have been fixed.

Out of the many investigations done for different compositions and temperature levels, two are here reported to illustrate both the procedure and the results: Figure 2.4 depicts the isotherms at 30°C and 150°C for adsorption of pure CO_2 above both activated carbons and zeolite 13X. As it can be immediately seen, zeolite isotherms reach greater adsorbed amounts at equilibrium compared to the corresponding activated carbon ones drawn for the same temperatures; even more interestingly, zeolite isotherms show a very steep increase for low partial pressure values, followed by a flattened behavior towards higher values. Such a trend is highly desirable when TSA applications are concerned, because it allows obtaining fairly high adsorbed amount already at low partial pressure during the adsorption phase, while the higher CO_2 concentrations required to obtain a pure product during regeneration do not compromise excessively the cyclic capacities, thanks to the flattening of the curve.

Figure 2.5, instead, shows how cyclic capacities are affected by a variation in the temperature level chosen for the regeneration phase. All the other affecting parameters, as pressure levels and adsorption temperature, are kept constant. Of course cyclic capacities are negative, if desorption is performed at a temperature lower than the adsorption one, which would actually means that the adsorption step is being operated as a regeneration one and vice versa. Zeolite 13X appears once again to be preferable, as the curve gets to zero value for slightly lower desorption temperatures and, what is more important, significantly higher cyclic capacities are achieved for any desorption temperature level. After these two reasons zeolite 13X is expected to be a better solution for the CCS application here investigated and is chosen as sorbent material for all the adsorption processes that are simulated in the context of this work.

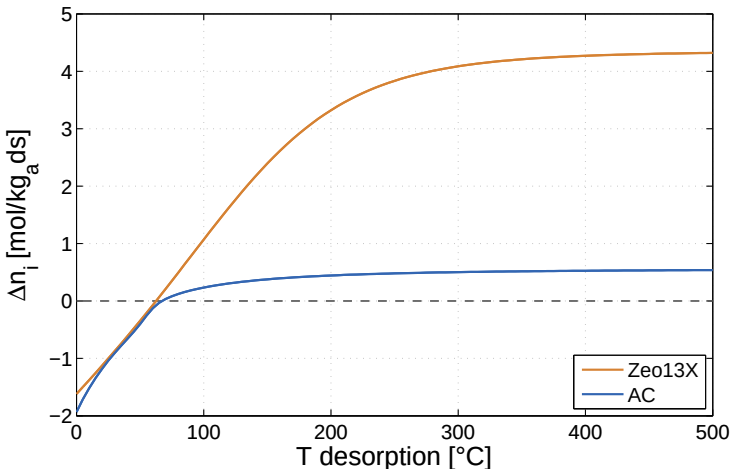

Figure 2.5: Cyclic capacity depending on desorption temperature for pure CO_2 on zeolite 13X; T adsorption 30°C, p_i adsorption 0.25 bar, p_i desorption 1 bar

2.5 Issues regarding adsorption modeling

A couple more issues regarding zeolite 13X and adsorption modeling should still be premised herein. According to the data presented in chapter 1, the flue gas which has to be treated for CO_2 removal has a composition which includes four main components: in addition to carbon dioxide, molecular oxygen, molecular nitrogen and water steam are also there. As mentioned, for the choice of the adsorbent material mixtures of CO_2 and N_2 only have been tested; the reason for it is that the experimental data available do not include any coefficient for O_2 and H_2O adsorption.

The lack of data for each component has though its own specific causes. As regards oxygen, no data are available only because no experimental session have been conducted so far at SPL for O_2 adsorption over zeolite 13X (nor over activated carbon, which could in case maybe be preferred to perform the simulations). Nevertheless, the affinities between O_2 and N_2 molecules suggest to consider the same Sips coefficients valid for both species.

A legitimate doubt might hence arise, whether oxygen and nitrogen should be treated during adsorption as a single component or as two separated ones. As one could discerningly guess, if the two were to be considered as one, the competing nature of their adsorption processes could not be observed. As a matter of fact, if the same simulations for a CO_2-O_2-N_2 mixture are performed twice, first treating O_2 and N_2 as a single component, then repeating everything with two separated species, the results show the same trends depending on the various input datasets; however in the two cases the results are always slightly different. In fact in the first case (binary mixture) the partial pressure of the O_2+N_2 component is always higher than those of single N_2 and O_2 in the second (ternary mixture) case –it is actually given by their sum. Given the shape of the isotherm curves, the increase of competitiveness of a component depending on its partial pressure is far from being linear. Therefore in the tested circumstances, in which N_2's isotherm is of the unfavorable kind, CO_2 adsorption is hindered more in the binary-mixture case than in the ternary-mixture one.

In the end, as it allows observing the competition between the two phases, it makes sense to consider O_2 and N_2 separately. It could be shown, however, that for the considered compositions of the flue gas the discrepancy between the results in the two cases is negligible, so that the choice of opting for either one solution or the other has almost no incidence on the final results, but derives rather from theoretical considerations.

The issue regarding water is, on the contrary, much more complicated. Water behavior towards sorbents cannot be modeled without a fight. Differently from the other gases here considered, water steam cannot be by any means treated as a perfect gas, which is obviously a first complication. Moreover, water adsorption is subject to complex phenomena, like, for instance, hysteresis. While many studies are currently carried out to fully understand, detail and model water adsorption, a fact has already been confirmed by the experiments performed so far: Those adsorbents which are suitable for CO_2 capture tend to adsorb water even more. Which means any postcombustion CCS adsorption process could not be performed obtaining satisfying performances, unless the flue gas is dried in advance, until containing only few water ppm.

For this reason all simulations referred to in this work are conducted imaging to feed a dried flue gas into the adsorption reactor, as already disclosed in chapter 1. As far as the available knowledge about these phenomena suggests, this limitation would of course remain once the process were to be put into practice; nevertheless this well known problem has not discouraged many from investigating the potential of adsorption processes for CCS applications.

2.6 Implementation of adsorption processes for carbon capture

With respect to the implementations of both PSA and TSA processes, the most research has been conducted using fixed beds, a well-known type of gas-solid reactor extensively employed for various processes. Although modeling of these systems is still a today's issue, detailed explanation of the phenomena that occur inside a fixed bed can be already found in literature. Nevertheless, with respect to the handling of power plant flue gas, it is still an open question whether there can be real convenience in adopting such a technology, as the results available at the present time for real implementations struggle to prove real competitiveness against other alternatives, even though theoretically the room for improvement could be vast.

Although they have been widely used in various industrial sectors starting from the first decades of the last century, fluidized bed represent a more recent technology; among the different existing kinds of fluidized reactors, circulating fluidized bed have gained a solid reputation for being compact –thanks to the high velocity of the gas flow, which requires narrower cross section– and providing good thermal and mass transfer between the gas and the solid particles. Yet some peculiar aspects related to their fluid dynamics and thermodynamics need more detailed and certain explanation to be found. Especially for what concerns thermodynamics and thermal transfer in presence of their complex fluidization regime, little and often inconsistent literature is available. As regards the use of CFBs for the capture of CO_2 through adsorption, a few studies have been published about the the topic. Theoretically, no motivation prevent circulating fluidized bed from being succesfully designed to operate in both the adsorption and regeneration phases of a carbon capture process and the good capability of controlling temperature inside this kind of reactors might be conveniently exploited for the purposes of such a system, as stated by Hoffman et al. [6]. Moreover, a very recent work by Zhang et al. [4] investigating CO_2 capture from ambient air has suggested the circulating fluidized beds to be a potentially cost-effective and promising alternative also for the handling of power plant flue gas. On the contrary, previous results obtained by Pirngruber et al. [5] have highlighted serious complications in performing TSA cycle inside CFBs, mostly due to unfavorable limitations occurring in the regeneration phase.

For both fixed beds and circulating fluidized beds more investigations are needed in order to define their actual potential as alternatives for TSA processes in the field of CCS applications. As regards the former, their optimization is at issue to prove real competitiveness against the most established technologies. For the latter, the combination of TSA processes and fluidization arouses a series of questions for which an ultimate answer has not been found yet; hence it is advisable to conduct further research about the modeling of the system, in order to be later able to assess how convenient adopting this technology might be. The most advisable way to evaluate the potential of a yet not experimentally tested process is to built a model capable of simulating its operation as realistically as possible.

The results returned by the model should be then analysed and presented in such a way to facilitate the comparison to the competiting technologies. A few indexes are commonly

taken as performance indicators to compare different CCS applications. Before starting the dissertation of the study cases, it might be thus advisable to introduce those indicators, which are also extensively employed in the next pages to evaluate the performances of the capture system.

The first parameter, called 'recovery', gives an indication of how effectively the system reduces the CO_2 content of the flue gases, as it calculates which share of the initial amount carbon dioxide is captured and which fraction is instead left at the stack. In this sense, it evaluates the effectiveness of the process. There are two ways to compute the recovery and by definition they should always return the same value:

$$\text{Recovery} = \frac{\dot{m}_{CO_2,captured}}{\dot{m}_{flue\,gas}\, x_{CO_2}^{flue\,gas}} = 1 - \frac{\dot{m}_{CO_2,stack}}{\dot{m}_{flue\,gas}\, x_{CO_2}^{flue\,gas}} \qquad [-] \tag{2.10}$$

The second parameter is indicated as 'purity'; it tells how pure is the CO_2 in the stream of the recovered product. As most storage procedures require the content of other species in the recovered flow to be as reduced as possible, this quantity is as well a strong indicator of the suitability of a certain process for a CCS application. More generally, in the field of the separation processes, the purity of the recovered species is a parameter which indicates the quality of the final product. In the context of this work it can be simply calculated as the molar fraction y_{CO_2} in the recovered stream:

$$\text{Purity} = y_{CO_2}^{recovered\,stream} \qquad [-] \tag{2.11}$$

The third parameter is the specific energy consumption, i.e. how much energy has to be spent in order to obtain a certain amount of final product. As the final product for a CCS application is the recovered CO_2, this indicator is assessed as

$$\text{Specific Energy Consumption} = \frac{\dot{Q}_{provided\,to\,the\,system}}{\dot{m}_{CO_2,captured}} \qquad \left[\frac{MJ}{kg_{CO_2}}\right] \tag{2.12}$$

The last parameter is the productivity of the system, defined as the amount of product that can be obtained by means of the process using a certain amount of solid adsorbent. Like the specific energy consumption, also the productivity is an index of the efficiency of the system, because it shows how well the capacity of the solid is used and therefore which amount of material is required to achieve a certain capture target. Productivities are computed as

$$\text{Productivity} = \frac{\dot{m}_{CO_2,captured}}{m_{solid\,in\,the\,system}} \qquad \left[\frac{kg_{CO_2}}{t_{ads}\, h}\right] \tag{2.13}$$

The first two indicators here mentioned are both indexes of the effectiveness of the process: The former holds a more quantitative meaning, whereas the latter embraces a more qualitative point of view and is related to the minimum requirements which are to be fulfilled depending on the specifications of the pipeline and of the storage site. For this reason, a 'recovery–purity' diagram is in this work widely employed to display the performances of the system in terms of accomplishment of the separation activity.

The other two parameters, instead, are merely related to the efficiency of the process, meant as the ability to operate using a limited amount of resources. For this reason the second graph that is broadly used in these pages to display the outcome of the simulations is a ‘specific energy consumption–productivity’ chart.

Chapter 3

Circulating Fluidized Beds

Fluidization has been a widely investigated issue in the engineering of gas-solid systems in the last century, its first industrial applications dating back to the 1920s. Nowadays fluidized beds are successfully employed for a various range of contexts, from refineries to metallurgical industry, from catalytic processes to combustions. In the next section their operation is described, highlighting benefits and drawbacks in comparison with the other great category of gas-solid reactor, i.e. that of fixed beds; further on their application to TSA process is discussed, starting from the description of the completely new simulation model that has been developed on the purposes of this study.

3.1 Fluidization

Gas-solid processes may be operated by means of wide variety of different technologies. Depending on the operational conditions, various fluidization regimes can be observed inside reactors. Therefore many categorizations among gas-solid reactors are applied on the basis of important features, like the velocity of the gas flow, the size of the solid particles and the mechanisms for solid inventory handling.

If the pressure drop inside a packed bed is analysed for different gas superficial velocities, the particle size being equal, after a first increase a turning point can be observed. This point corresponds to a minimum fluidization velocity, beyond which the particles are displaced by the gas flow and the bed leaves its packed configuration; as the gases have gained the capability of moving the solid particles, the frictional

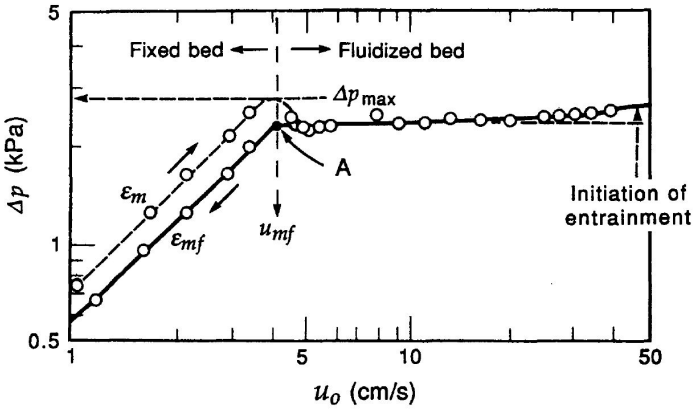

Figure 3.1: Pressure drop as function of superficial velocity at the set off of fluidization [15]

pressure Δp_{fr} drop does not increase anymore, but stays rather constant until the velocities rise enough to steadily entrain the particles along their whole way through the vessel. Therefore, plotting a Δp_{fr} curve as a function of velocity u (Figure 3.1), in the beginning a first rising section can be encountered, in which Ergun's equation has validity; at the minimum fluidization turning point a maximum pressure drop is reached, the bed loses its locked packed arrangement and minimum fluidization void fraction ε_{mf} is set, bringing Δp_{fr} down to the static pressure of the bed. If the velocity is now decreased back into the fixed bed region, a different curve is drawn, corresponding to the new void grade of the bed. If it is raised further instead, a flattened curve section follows, representing the operational range of the slower fluidized beds, where the pressure drop remains almost constant. When entrainment starts Δp_{fr} rises slightly as the only the lighter particles are entrained, before decreasing back to zero as the so-called 'pneumatic transport' becomes fully developed and no discrepancy of velocity can be observed between the gas and the solids, which means the terminal velocity u_t has been reached even for the biggest particles of the bed.

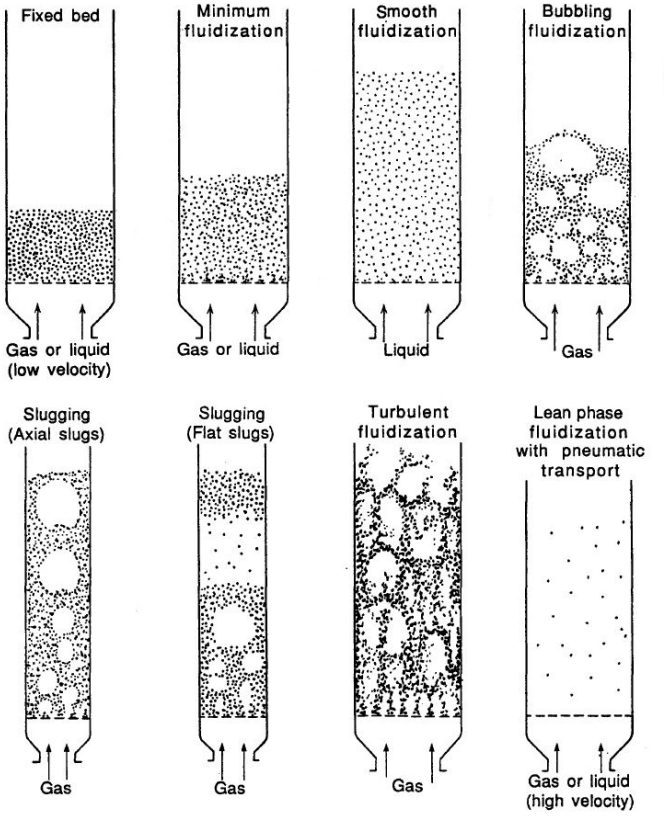

Figure 3.2: Different fluidization regimes [15]

In order of increasing gas velocity, a range of different fluid dynamic behaviors can be observed inside a reactor (Figure 3.2). The following most common types of reactor should be mentioned, each of them corresponding to a specific fludization regime:

- fixed beds and moving beds, in which the velocity of gases is always under the minimum fluidization threshold, so that there is no movement of the solid matter; the latter ones differ from the first in the possibility of continuously replacing the inventory, being the solids moved in and out of the reactor through some handling mechanism;
- spouted and bubbling beds, whose distinctive feature is a fluidization of the solid operated with gas bubbles that move through and implode inside the bed mixing it, but without carrying over any solid particle, so that the inventory has to be replaced by means of other systems; for this kind of operation, gas velocities higher than the minimum fluidization one are required;
- circulating fluidized beds, whose higher gas velocities not only move particles inside

the bed mixing them, but can also entrain them out of the reactor, where they are then separated from the gas flow to be recirculated into the reactor or conveyed somewhere else.

- pneumatic conveyors, where the solid particles do not undergo any mixing, but are rather transported by the gas flow along a straight path through the reactor.

Not every particle size is suitable for every fluidization regime, so that the different types of reactors above might be linked to specific particle dimension ranges; as a matter of fact, maps of different fluidization regimes have been designed, taking both gas velocity and particle equivalent diameter as parameter, like Grace's diagram or its updated version by Kunii and Levenspiel (Figure 3.3).

It is straightforward that the higher the gas velocity, the smaller will be the cross section required, the volumetric flow rate of gas being equal. This explains the great interest for circulating fluidized beds for those application where a huge gas flow rate has to be processed. In those cases, high velocities allow reducing the total plant size to notable compactness levels, with all the resulting benefits in terms of costs. Moreover, the fluidization regime typical of CFBs on the one hand is very effective as regards the mixing of particles, on the other hand promotes the heat exchange both between gas and solid phase and between suspension and riser walls, thanks to high convective heat transfer coefficient.

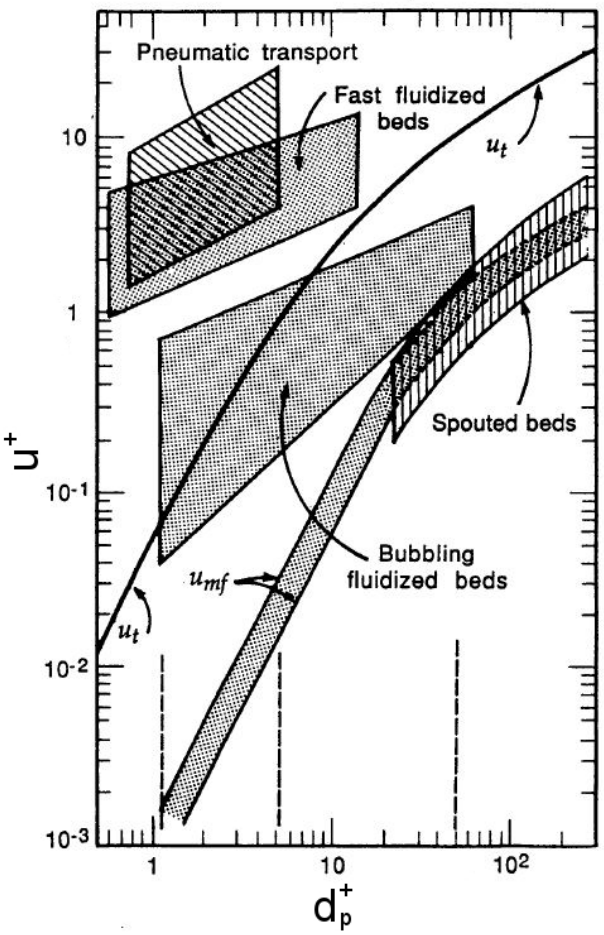

Figure 3.3: Kunii and Levespiel's version of Grace's fluidization map [15]

In a circulating fluidized bed, entrainment and elutriation act as the main mechanisms for the displacement of solids out of reactor. This means that particle size should be limited to a few hundreds of micrometers, in order to allow particles to be transported by the gas flow. In particular, the particle size chosen to set a proper behavior of the solids inside the reactor resides within the so called 'A' and 'B' groups of Geldart's classification of particles [16]; this corresponds to aeratable non-cohesive particles with a solid density ρ_s lower than 1.4 g/cm^3 and an average equivalent diameter smaller than 500 micrometers. All the solids carried over by the gases are retrieved by means of a solid separator, in most cases a cyclone, to be sent back to the reactor or to some other unit, where they undergo a different process. Figure 3.4 shows a few sketched examples of

circulating fluidized beds, from which it is possible to observe the main elements forming any CFB: a vertical elongated riser, where gases are fed at the bottom and leave from the top end; a solid separator, installed after riser outlet; a regulated system that conveys solids back into the lower part of the reactor.

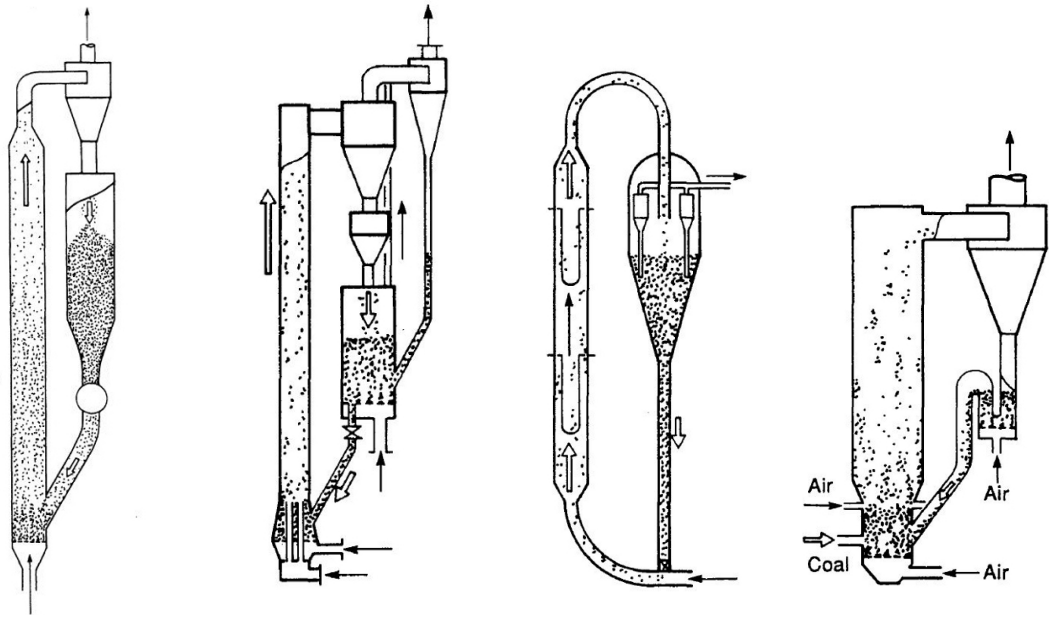

(a) Idealized setup **(b)** Experimental setup **(c)** Industrial setup for a catalytic process **(d)** Industrial setup for a combustor

Figure 3.4: Example setups for circulating fluidized bed [15]

3.2 Plant layout

Before being conveyed in the CCS system units, the flue gas leaving the steel mill power plant undergoes a drying treatment. Once its content of water has been reduced to approximately zero, the gases are driven into the adsorption unit of the TSA system, where the CO_2 is removed.

In order to operate adsorption and regeneration continuously, at least two separated reactors are required to implement a temperature swing adsorption process with circulating fluidized beds, namely an adsorber and a regenerator. As regards the gas flows used to fluidize the beds, the adsorption unit is directly fed with the flue gas coming from the driers, while in the regeneration one a gas stream with the same composition of the product is constantly recirculated from the outlet to the inlet on this purpose. On the solid side, instead, no streams enter or exit the system; the solid entrained out of each reactor are partly sent to the other reactor and partly recirculated back at riser inlet. The two solid flows traveling from one reactor to the other undergo some heat exchange aimed at recovering the heat stored in the regenerated particles; how this heat exchange should be realized, is going to be discussed in a later section of this work.

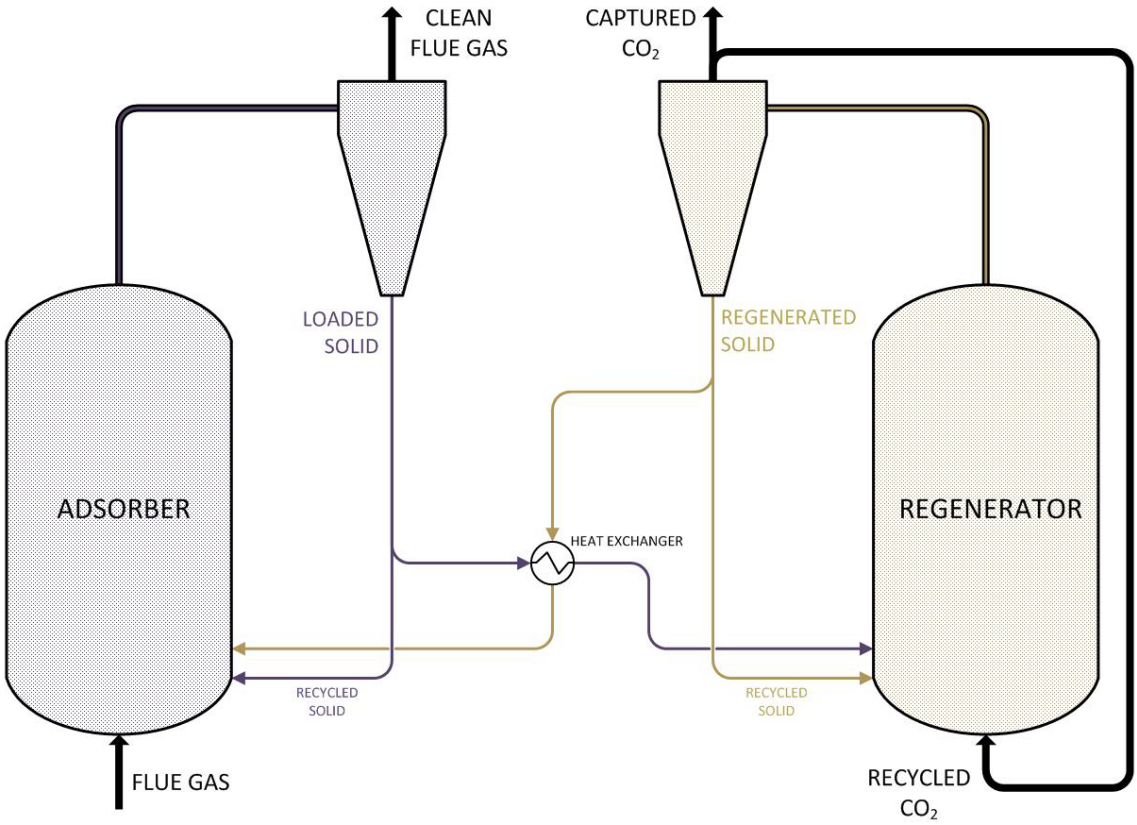

Figure 3.5: CFB: schematic plant layout

Before looking into the modelling of CFB reactors, a few words should be conveniently spent to describe the application the model is originally intended to deal with –even if it is devolped to work equally fine for other applications. Therefore here in a few lines a little information is given about the layout of a plant designed for TSA operations with circulating fluidized beds in the context of postcombustion carbon capture, as schematically displayed in Figure 3.5. On the whole the CCS system features only one entering flow, the flue gas, and two outflows, the clean flue gas –with a low carbon content– and the CO_2-rich product bound for storage.

3.3 Mass transfer modeling

The operation of the CFB reactors has been simulated by means of a completely new model, which was developed on purpose. For its implementation MATLAB®programming language has been chosen. The following sections explain in detail under which assumptions the model works, how it is structured and how calculations are done. A comment on the results yielded by the simulations follows.

3.3.1 Main assumptions and logical scheme of the model

The model for adsorption operation inside CFB reactors is a steady state one-dimensional model, where the reactor axial coordinate is discretized. It was developed in order to be valid for both adsorption and desorption processes, so that it was employed to perform simulations of both the adsorber and the regenerator of the TSA cycle for the aim of this work. It is based on two important assumptions, which are here stated and justified.

First of all, the solids inside the riser are assumed to be perfectly mixed, so that all the particles inside the reactor are at the same temperature and the average conversion degree of particles is uniform throughout the reactor (along all three dimensions, which means they are all loaded with the same amount of adsorbed phase. In this sense, as long as solids are considered, the reactor can be seen as a CSTR, where solids enter, are immediately converted to a certain uniform degree and move out after a certain residence time, with the same properties that can be found anywhere inside the reactor. This significant hypothesis is considered to be acceptable for fast fluidization regimes –like in CFBs–, since high velocities and low solid volumetric fractions provide enhance particle mixing to a great extent. From a computational point of view, thanks to this assumption no profile along the riser is needed for the average conversion degree of solid particles, so that this degree may be considered constant when computing the system of mass balance equations over the single subvolumes, reducing the number of variables.

The second strong assumption is that the reactor operates isothermally at a chosen temperature, which means that everything is at the same temperature as long as it resides inside the riser –valid for both solids and gases– and that this temperature is an input value of the model. Once again, the fast and homogeneous mixing of solids justifies this hypothesis as far as solids are concerned; consequently, temperature gradients should be negligible in the gas phase because of the allegedly high heat transfer coefficients (typical of CFBs) between gas and solid, while the possibility of exchanging heat with an external fluid allows the system to release and receive the thermal power required for its energy balance to be verified in isothermal conditions. An isothermal operation of the riser is highly desirable, because it makes possible to control the conditions under which the adsorption proceeds. Moreover, as regards the model, it has the big advantage of decoupling the energy balance of the reactor from the fluid dynamics, significantly simplifying the computation.

The last remarkable hypothesis is that of constant pressure throughout the reactor. This means, the pressure drop along the riser is neglected. Assuming this may sound like being somewhat too optimistic, but it might be observed how the low solid volumetric fractions typical of a CFB make this term undoubtedly less significant, when compared, for instance, to fixed beds. Moreover in a TSA cycle total pressure levels are not supposed to play any main role in the adsorption and desorption processes, so that there is no real need to carefully examine pressure profiles inside the reactor.

On the basis of this assumptions, the operation is modeled. While the properties of solids are uniform throughout the riser, as already mentioned, the properties of the gas flow are of course progressively changing along the riser length, according to the proceeding of the

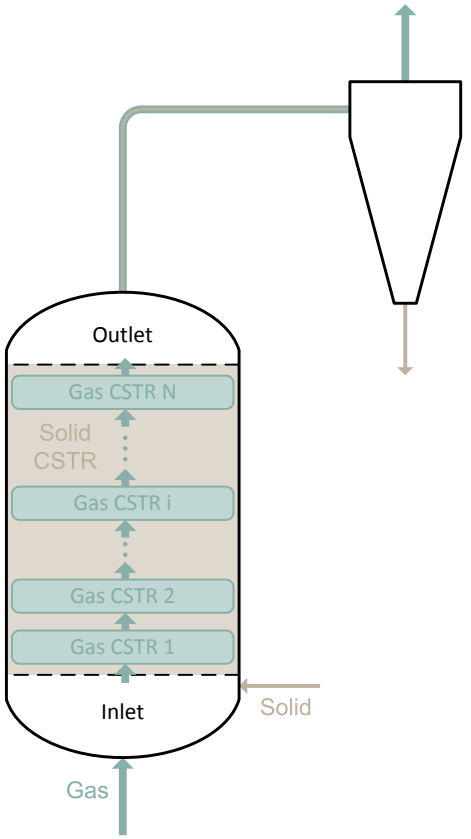

Figure 3.6: CFB: decoupling of gas-solid modelling

adsorption process. In a one-dimensional approach, it is legitimate to assume the gases inside a CFB reactor as moving forward like a plug flow. This plug flow can be approximated by means of a sequence of CSTRs, whose cross section is the same as the riser and whose length is a fraction of the riser length; these CSTRs are the subvolumes into which the reactor volume can be ideally divided. In each subvolume a certain amount of solids resides, according to the solid distribution along riser length; the gases enter the subvolume, undergo adsorption and flow out with the same properties that can be observed inside the CSTR, as it is perfectly stirred, according to theory of continuous flow stirred tank reactors. The flow exiting from the last subvolume corresponds to that getting out of the riser. This approach is rather consistent with the solid dynamics within the vessel: since the fluidization conditions are verified and there is entrainment, but the pneumatic transport regime has not been reached yet, the bed is only partially conveyed out of the reactor, while many particles slow down until they fall down at a certain height, creating some internal recirculation motion that provides such high mixing degree.

Since in the adsorption processes a certain amount of matter experiences a change in phase, a global mass balance over the whole reactor must be verified simultaneously for the gas and the solid phase. After solving the balances stepwise over all the subvolumes, the variation of the gas flow properties between riser inlet and outlet has to be consistent with the variation of the conversion degree of the solids. Figure 3.6 is meant to represent graphically this parallelized way of computing.

Following this method, the operation of the reactor is simulated starting from some input data. On the basis of these values, some assumptions are made to enter an iterative process that numerically solves the equations of the global mass balance. Inside this outer iteration loop, as many iteration loops as subvolumes are required to determine the length of each CSTR according to some fixed restrictions. Finally for each subvolume, the system of equations which constitutes the subvolume mass balance has to be solved numerically, and this is done with a last inner iterative computation. When a set of variable values that satisfies all balances and posed conditions has been identified, results are produced, in terms of profiles along the riser for the gases and of values at outlet for the solids.

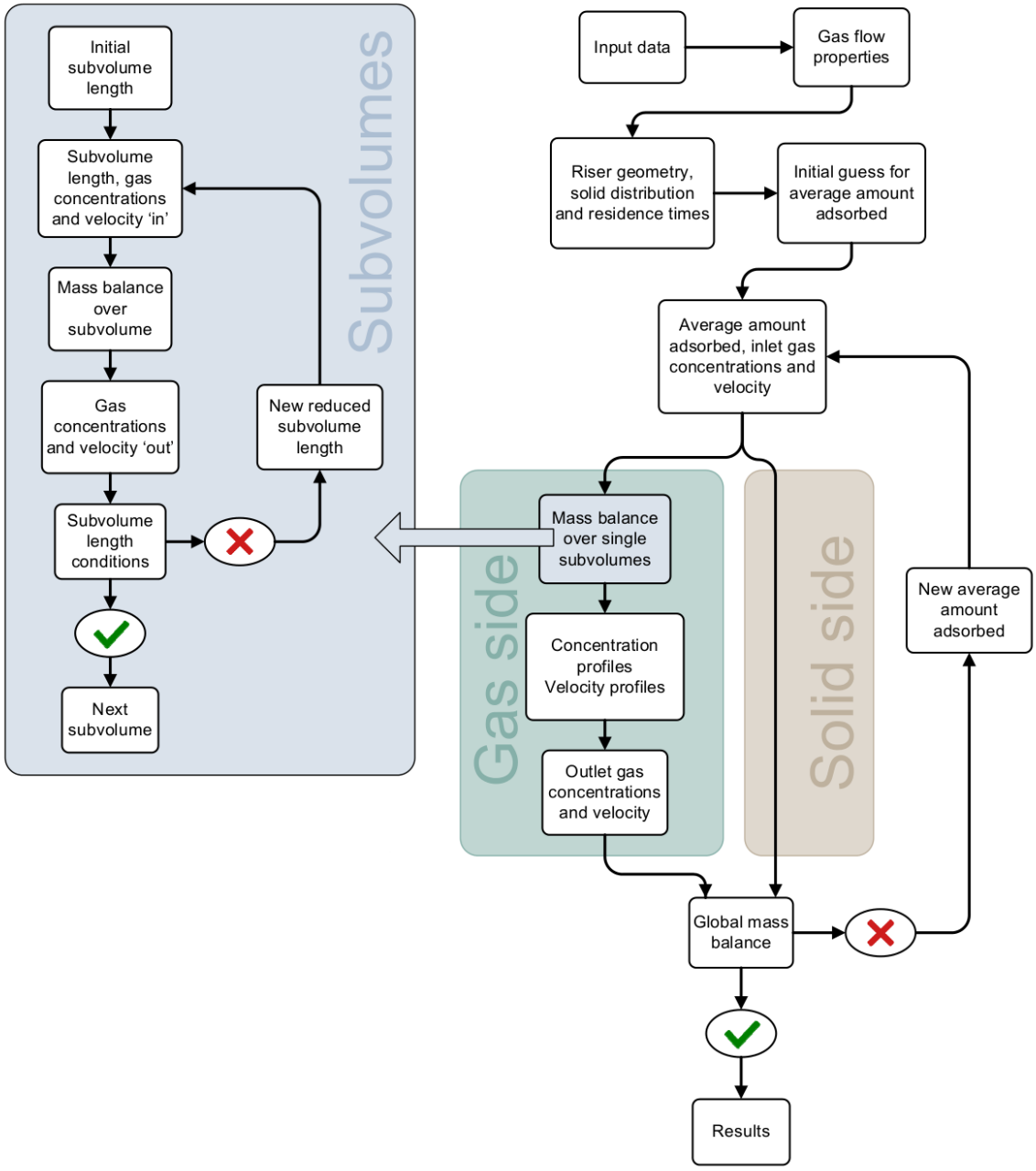

Figure 3.7: CFB: logical scheme of the reactor model

A logical scheme of how the simulations are performed is sketched in Figure 3.7: not all the features represented in the scheme have been explained yet, as the figure is intended to be a useful reference for the following paragraphs as well.

3.3.2 Input data

Any simulation model should be designed with the aim of providing a computing device as flexible as possible, i.e. a useful tool that can be properly employed in the most wide range of different situations of a certain kind. Therefore models are usually created in such a way

that some data must be given as input, to specify each time which particular application the tool is asked to recreate. The input dataset needed by this model to simulate adsorption or desorption processes consists in four different groups of values:

- flue gas data, which include
  - gas flow rate at riser inlet
  - composition of the gas flow at riser inlet
  - physical properties of the gas species
  - Sips coefficients for the adsorption of the gas species over the sorbent
- sorbent data, which mainly consist in
  - geometry of the sorbent particles
  - physical properties of the sorbent
  - average conversion degree of the sorbent particles fed at riser inlet
  - flow rate of sorbent entering the riser
- desired bed design and operational settings, which are
  - pressure and temperature conditions inside the riser
  - superficial velocity of gas at inlet
  - bed inventory
  - riser height
  - flow rate of sorbent entering the riser
  - geometry of the heating/cooling system
  - properties of the heating/cooling fluid
- desired simulation settings, in particular
  - minimum number of subvolumes
  - limit conditions for subvolume length
  - tolerances for convergences

While the first two groups of data are fixed once a specific application is considered and a certain sorbent material has been chosen, the third group of data includes all the quantities that must be modified to investigate the optimization of the process. The fourth group of data is instead only related to the operation of the simulation tool and hence should theoretically have no influence at all on the results of the computation.

3.3.3 Riser geometry, solid distribution and residence times

As a first step, pressure and temperature conditions are considered in order to compute the volumetric flow rate of gases at inlet $\dot{V}_{inlet}$, the cross section is estimated at inlet:

$$A = \frac{\dot{V}}{u_{inlet}} \qquad \left[\frac{m_{gas}^3}{s}\frac{s}{m} = m^2\right] \tag{3.1}$$

An hypothetical riser diameter is evaluated as if the cross section were circular, so that a first guess of the height to diameter ratio can be made. Should this ratio be out of the interval $3 \div 10$, a warning is printed to screen, as the riser geometrical proportions are considered out of their proper range.

Immediately after, a profile of the solid distribution inside the reactor is outlined. According to Kunii and Levenspiel's description of solid distribution inside a circulating fluidized bed [15], the riser volume can be divided into two zones, namely a bottom dense region and an upper lean region. Void fraction is to be considered constant in the dense region, while it rises progressively in the lean zone. Instead of the void fraction, for the sake of convenience here it will be always referred to the solid volumetric fraction ε_s, that is its complement to one. Therefore it can be said that ε_s is almost constant in the dense region, whereas it decreases progressively in the dense zone. Its decrease is assumed to follow an exponential law, as in eq. (3.3). Figure 3.8 shows an example of solid distribution inside a CFB riser. An initial bottom dense zone is always supposed to be present, or, at least, the value of volumetric solid fraction ε_S at inlet is always equal to $\varepsilon_{s,d}$. Any higher value of ε_S is impossible anywhere else in the riser. Thus a minimum and a maximum value for W_s could be determined, depending on H_t and corresponding to $H_d = 0$ and $H_d = H_t$ respectively.

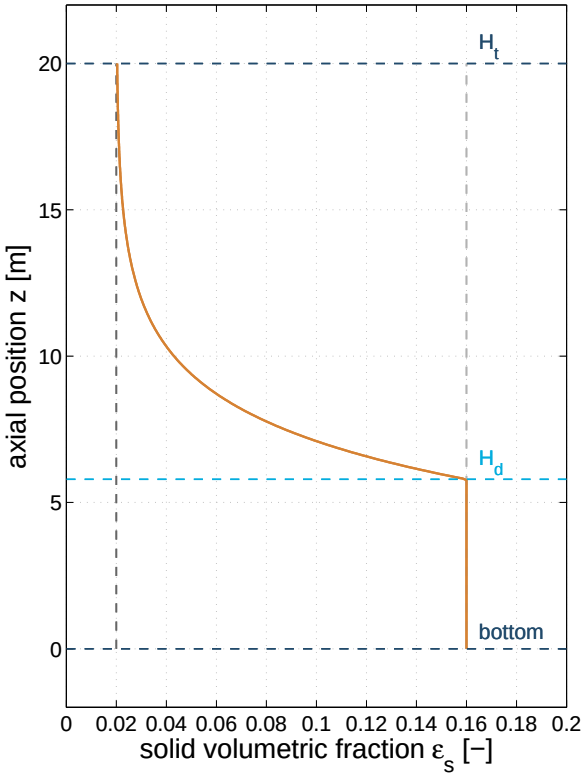

Figure 3.8: CFB: solid distribution along riser axial coordinate

The constant value of solid volumetric fraction in the dense zone $\varepsilon_{s,d}$ is set to 0.16, while the asymptotic value towards which the already mentioned exponential function tends ε_s^{asym} is assumed equal to 0.02, according to what is stated in literature [15]. The bottom dense zone height H_d is computed by means of the following equation, where it appears as the only unknown:

$$W_s = A \cdot \rho_s \left[\varepsilon_{s,d} H_d + \int_{H_d}^{H_t} \left(\varepsilon_s^{asym} + (\varepsilon_{s,d} - \varepsilon_s^{asym})\, e^{-a(z-H_d)} \right) dz \right] \qquad [kg] \qquad (3.2)$$

This expression is nothing more than the integration along the riser length of the known function that describes the volumetric solid fraction, i.e. $\varepsilon_s = \varepsilon_s(z)$ [15]:

$$\varepsilon_s(z) = \begin{cases} \varepsilon_s = \varepsilon_{s,d} & \text{for } z \in [0, H_d] \\ \dfrac{\varepsilon_s - \varepsilon_s^{asym}}{\varepsilon_{s,d} - \varepsilon_s^{asym}} = e^{-a(z-H_d)} \quad \text{with} \quad a\, u_{inlet} = const. & \text{for } z \in (H_d, h_t] \end{cases} \qquad (3.3)$$

The superficial velocity of the gas is not constant throughout the reactor (as the volumetric flow rate decreases because of adsorption); therefore the value of the constant a is set only once using a specific value of the superficial velocity, which is the one at inlet u_0. The right

value of the product $a \cdot u_0$ can be inferred from experimental data reported in literature [15], which suggest a dipendence on the average size of the solid particles.

Once the height of the bottom dense zone is known, the solid volumetric fraction at riser outlet $\varepsilon_{s,out}$ can be calculated as

$$\varepsilon_{s,outlet} = \varepsilon_s^{asym} + \left(\varepsilon_{s,d} - \varepsilon_s^{asym}\right) e^{-a(H_t - H_d)} \tag{3.4}$$

and from this the mass flow rate of solid entrained out of the reactor (G_s, per cross section unit) can be derived, when the superficial velocity at outlet u_{outlet} and the terminal velocity of particles u_t are known:

$$G_s = \rho_s \varepsilon_{s,outlet} \left(u_{outlet} - u_t\right) \qquad \left[\frac{kg_s}{sm^2}\right] \tag{3.5}$$

Heider and Levenspiel [18] indicate the following expressions to estimate the terminal velocity of solid particle:

$$u_t^+ = \left[\frac{18}{\left(d^+\right)^2} + \frac{2.3348 - 1.7439\,\phi_s}{\left(d_p^+\right)^{0.5}}\right]^{-1} \tag{3.6}$$

where

$$u_t^+ = u_t \left[\frac{\rho_f}{g\,\mu_f\,\left(\rho_s - \rho f\right)}\right]^{1/3} \tag{3.7}$$

$$d_p^+ = Ar^{1/3} \tag{3.8}$$

$$Ar = \frac{d_p^3\, g\, \rho_f\, \left(\rho_s - \rho_f\right)}{\mu_f^2} \tag{3.9}$$

where u_t^+ is the adimensional terminal velocity of solid, d^+ the adimensional equivalent diameter of solid particles, Ar the Arrhenius number and ϕ the sphericity of particles. Knowing G_s brings to another quantity, the average residence time of particles, which may be therefore evaluated as

$$\tau = \frac{W_s}{G_s\, A} \qquad [s] \tag{3.10}$$

The residence time of particles is here assumed to be represented by the following probability distribution, already adopted in literature [17]:

$$E(t) = \frac{1}{\tau}\, e^{-t/\tau} \tag{3.11}$$

Later in the calculation procedure, it is verified that at every position along the riser height conditions for fluidization are satisfied. This check is simply made by comparing the superficial velocity of gases with the minimum fluidization velocity u_{mf}, that can be derived

via the following equation, a derivation of the Ergun equation 4.1 for minimum fluidization conditions [15]:

$$Ar = \frac{1.75}{\varepsilon_{mf}^3\,\phi_s}\,Re_{p,mf}^2 + \frac{150\,(1-\varepsilon_{mf})}{\varepsilon_{mf}^3\,\phi_s^2}\,Re_{p,mf} \tag{3.12}$$

where

$$Re_{p,mf} = \frac{d_p\,u_{mf}\,\rho_f}{mu_f} \tag{3.13}$$

and the value of ε_{mf} depends on the dimension of particles and can be determined from empirical values found in literature [19].

3.3.4 Adsorption and desorption processes

The solid distribution inside the riser is defined on the main purpose of providing the information needed to describe adsorption process in the different subvolumes. As it might be intuitively deduced, adsorption is promoted by the availability of fresh unloaded solid sorbent. Therefore, the amount of gas getting adsorbed within a certain volume is inevitably linked also to the amount of solid available, i.e. to the solid volumetric fraction and to the initial conversion degree of the sorbent.

The amount of adsorbed phase $n_{i,inlet}$ carried by the solid entering the riser (which correspond to the initial conversion degree of the sorbent) is an input of the model, as it depends on external factors; for a perfectly regenerated solid (or a sorbent which never experienced any adsorption) it will be obviously equal to zero. The average amount of adsorbed phase $\bar{n}_i$ with which the solid particles are loaded as they get entrained out of the reactor is a result of the simulation; in particular, is the result of the outer iterative computation process of the model, as shown in Figure 3.7. Hence a first guess value of $n_{i,inlet}$ is required to enter the iterative process; anytime this initial value is mentioned, it is actually referred to usually more than one value (namely i values), because normally more than one gas species are supposed to be absorbed and for each of them an initial guess must be made. It is of course essential to sensibly choose this set of values, in order to conveniently reduce the number of iterations for convergence; nevertheless, it might be not so straightforward to evaluate which values to foresee at riser outlet.

In view of the fact that it is undoubtedly easier to make a rough estimation of an average gas concentration expected to be reached in the riser, the starting set of values is derived from an assumption of this quantity. This is consistent with the fact that it is possible to find a certain concentrations set, to which an average conversion degree of the solid particles would correspond for given τ, p and T; this approach has already been used for circulating fluidized beds and its application can be found in literature [17]. Equation (3.14), where the guessed average concentrations are indicated as C_i^*, shows the pathway which leads to the definition of a starting set of adsorbed amount average values, through the probability distribution already mentioned in the previous section (equation (3.11)):

$$\bar{n}_i^* = \int_0^\infty E(t)\,n_i^*(t)\,dt \qquad \left[\frac{mol}{kg}\right] \tag{3.14}$$

Once n_i^* is determined, the outer iteration loop is entered with $\bar{n}_i = n_i^*$ and the first subvolume is considered. This leads directly into the middle iteration loop (the one over subvolume lengths): the initial length for each subvolume is assessed out of the model input data as

$$(z_{out} - z_{in}) = \frac{H_t}{N_{sv}} \qquad [m] \tag{3.15}$$

where N_{sv} is the chosen minimum number of subvolumes; using this length the inner iterative process is entered for the first time.

The inner iteration loop solves a system of $i + 1$ equations, being i always the number of gas species involved in the adsorption process; each of these equation is a mass balance over the subvolume, i mass balances for the i compounds plus a total mass balance. The variables of the system are the concentrations $C_{i,out}$ and the superficial velocity of gases u_{out} at subvolume outlet. The values at inlet are for the first CSTR the same of the riser inlet. Once again, for each variable an initial guess must be made, but no relevant sensitivity was anyway observed to the value of the guess in terms of computational efforts; however, assuming both gas concentrations and superficial velocity to increase in case of desorption and decrease in case of adsorption is undoubtedly a convenient choice. After evaluating the average adsorption rates $\bar{r}_i$ depending on the average amount adsorbed $\bar{n}_i$ and on the $C_{i,out}$ concentrations –according to the assumption each subvolume works as a CSTR– with the equation already seen in the previous chapter

$$\bar{r}_i = \omega_i \left(n_{i,eq}(C_{i,out}) - \bar{n}_i \right) \qquad \left[\frac{mol}{kg\, s} \right] \tag{3.16}$$

the following system of differential equation is numerically solved between z_{in} and z_{out}:

$$\begin{cases} \dfrac{d\left(u\, C_i\right)}{dz} - \rho_s \left(\dfrac{\varepsilon_s}{1 - \varepsilon_s} \right) \bar{r}_i = 0 & \forall i = 1, \cdots, N_{species} \\ \dfrac{d\left(u\, \hat{\rho}_{mix}(p,T)\right)}{dz} - \displaystyle\sum_{i=1}^{N_{species}} \rho_s \left(\dfrac{\varepsilon_s}{1 - \varepsilon_s} \right) \bar{r}_i = 0 \end{cases} \tag{3.17}$$

It might be useful to recall that not only u and C_i, but also ε_s is a function of the axial coordinate z, whereas the molar density of the mixture $\hat{\rho}_{mix}$ is not, being pressure and temperature uniform throughout the reactor and being all the gas species considered as perfect gases. The reasonableness of the last equation of the system is grounded in this statement.

As the inner iteration loop comes to converges, all the properties of the gas flow can be assessed at the subvolume outlet. A number of conditions regarding those properties can be implemented in the simulation tool in order to decide whether it is necessary or at least convenient to reduce the subvolume length. It gets automatically reduced whenever negative concentrations $C_{i,out}$ or superficial velocities u_{out} are found as solutions of the system: it may occur if the adsorption rate happens to be very high and there is a large amount of solid in the subvolume. Although it would clearly makes no sense from the point of view of physics, the Matlab® script was programmed to firstly accept these solution (i.e., no ≥ 0

restriction is imposed for results) but then to reduce the subvolume length, because it seems to be convenient to investigate the process behavior with a denser discretization when it proceeds so fast. Moreover, optionally a more restrictive condition can be established, so that the step is shortened if the variation over the subvolume of any concentration or of the velocity exceeds a certain fraction of the entering value. When the right subvolume length is found, the middle iteration loop is finished.

The gas flow properties at the outlet of a subvolume are then directly taken as inlet input data for the following one. The computation progresses from subvolume to subvolume until the total height of the riser is reached. At this point the properties of the flow gas at riser outlet are available and the global mass balance between inlet and outlet can be verified by means of the following set of equations:

$$\dot{V}_{inlet}\, C_{i,inlet} - \dot{V}_{outlet}\, C_{i,outlet} = \dot{m}_{ads}\ (\bar{n}_i - n_{i,inlet}) \quad i = 1, \cdots, N_{series} \quad \left[\frac{mol}{s}\right] \tag{3.18}$$

where $\dot{m}_{ads}$ is the mass flow rate of sorbent fed at riser inlet and is one of the input data of the model. If the global balance does not close, a new value of $\bar{n}_i$ is calculated to start a new iteration and so forth until the iterative process converges, then the outer iteration loop is dropped.

Since this mass flow rate is different from the mass flow rate of solids entrained by gases out of the reactor, a recirculation rate R_{rec} can be calculated, so that a fraction R_{rec} of the entrained solids is recirculated back into the riser, while only the $(1 - R_{rec})$ fraction exits from the system, so that the riser can be operated in a stationary way consistently with the input data:

$$R_{rec} = 1 - \frac{\dot{m}_{ads}}{G_s} \qquad [-] \tag{3.19}$$

If R_{rec} were found to be negative (that is, if $\dot{m}_{ads} \geq G_s$) the reactor could no operate according to the input data.

In conclusion, as the outer iterative computation converges, the Matlab®code is able to provide, among others, the following information:

- location of all the interfaces between CSTRs along the riser length z
- profiles of molar fractions y_i or concentrations C_i along the riser length z for each i-th compound
- profiles of equilibrium amount adsorbed $n_{eq,i}$ along the riser length z for each i-th compound
- profiles of molar flow rates F_i along the riser length z for each i-th compound
- step profiles of average adsorption rates $\bar{r}_i$ inside each CSTR
- a profile of gas superficial velocity u along the z dimension
- combining the previous quantities, the gas flow can be completely characterized at any point along the riser length
- the variation Δn_i of the amount of adsorbed phase over the reactor for each i-th compound, which correspond to the variation of the solid conversion degree

- the total amount of matter adsorbed or desorbed

Of course, as far as the mentioned profiles are concerned, they are obtained out of an interpolation of the values at the subvolume interfaces, so that their pattern becomes more and more accurate as the chosen minimum number of subvolume increases –while the computational time becomes though longer and longer.

In Appendix B the result profiles for an example adsorption process as plotted by the Matlab® code can be observed; they refer to a typical CCS adsorption process for a postcombustion flue gas (mixture of CO_2, O_2 and N_2) over the commercial sorbent zeolite 13X. These results have been obtained adopting a limiting rule over subvolume length which reduces the length in order to limit the maximum variation of concentration in a single CSTR under a certain percentage.

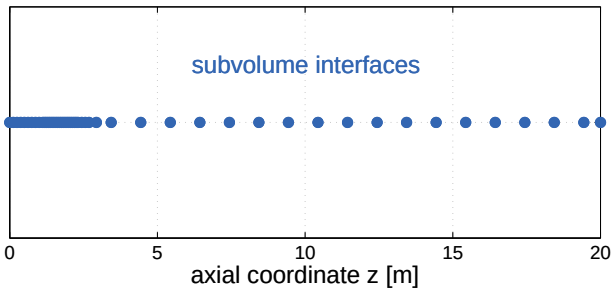

Figure 3.9: CFB: example of spacial discretization along riser length adapting variable subvolume length

Out of those two are reported here too: in Figure 3.9 an example is given of how the subvolume length adapting system provides a denser discretization where the adsorption process proceeds faster (i.e. in the bottom dense zone, where the concentration of solids is higher).

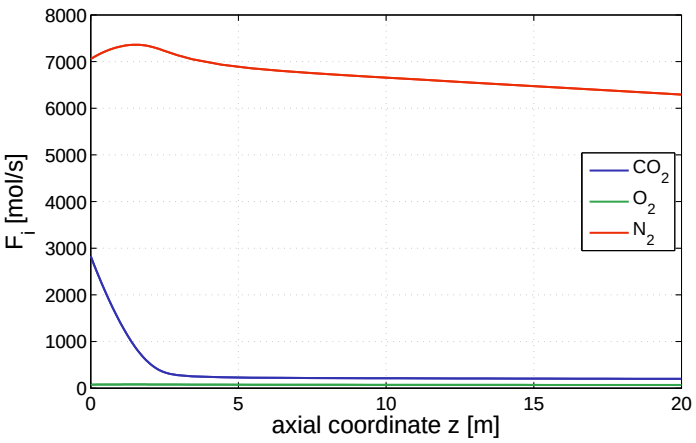

Figure 3.10: CFB: example of molar flow rates profile along riser length

Figure 3.10 instead is helpful to discuss an apparently odd computational effect, which is actually a representation of a real phenomenon which may occur inside a CFB riser. The average adsorbed amount of a certain compound in a reactor might happen to be higher than the corresponding equilibrium one only in a certain zone of the reactor, so that inside a reactor that works as an adsorber also desorption may be spotted (or viceversa); this might cause the molar flow rate of a compound not to have a monotonic curve along riser length.

This is likely to happen, for instance, in the bottom zone of an adsorber, as in figure. This weird phenomenon may be found to have a physical meaning though: in the lower part of adsorber, the higher CO_2 concentrations promote its adsorption at the expenses of the other species (being zeolite 13X selective towards CO_2), while further on along the riser, where most of the carbon dioxide has already been adsorbed and the flow is O_2- and N_2-rich, the equilibrium amount adsorbed for this last two species tends to increase. The particles which are displaced by the gas flow towards the top end, but that are eventually not entrained out

of the riser, fall back down to the dense zone. They might have remained in the upper part of the riser for a time long enough to adsorb high amounts of O_2 and N_2 though, so that when they go back to the dense zone some of those species are forced to desorb to free space for the more favored CO_2 to adsorb.

3.3.5 Model implementation for Temperature Swing Adsorption processes

As already stated, the model is developed on the purpose of working properly either in case of adsorption or desorption and it may be profitably employed for any application which requires those processes to be simulated. Regarding TSA cycles, two separated reactors are employed, one for the adsorption stage and one for the regeneration phase, as already described in section 3.2. All the input data required by the modeling of the adsorber are already available once the flue gas has been characterized the other operation conditions has been decided, except from the initial conversion degree of the regenerated sorbent fed at riser inlet, which obviously depends on the output of the regeneration process. Symmetrically, the conversion degree of solids at regenerator inlet will be defined by the output of the adsorber simulation, so that an iteration loop will be needed to find the steady state conditions under which the solids undergoes adsorption and regeneration always to the same extent. It is somehow as if a new, fresh sorbent were fed into the TSA cycle; after a certain time such an occurrence could be observed, that the loop experienced by the solid particles between the two reactors is repeated always alike.

As regards the regeneration, another input data may be only guessed at the beginning and must later be determined through an iterative process. This parameter is the composition of the flow gas at riser inlet, which according to the layout of the plant has to be identical to that at riser outlet, which is unknown until the operation of the reactor itself has been completely characterized. Therefore a reasonable starting value must be guessed to enter this iterative process, than the regeneration step has to be simulated over and over until convergence, i.e. until the all the molar fractions at inlet $y_{i,inlet}^{REG}$ correspond to all the molar fractions at outlet $y_{i,outlet}^{REG}$, adopting a certain error tolerance. Figure 3.11 displays this procedural scheme.

Regarding the results that can be inferred out of the whole cycle simulation, for a CCS application the total system recovery and purity rates can be assessed simply as

$$\text{Recovery} = \left(1 - \frac{\dot{m}_{outlet,CO_2}}{\dot{m}_{inlet,CO_2}}\right)^{ADS} = \frac{\left(F_{outlet,CO_2} - F_{inlet,CO_2}\right)^{REG}}{\left(F_{inlet,CO_2}\right)^{ADS}} \qquad [-] \tag{3.20}$$

$$\text{Purity} = y_{outlet,CO_2}^{REG} = \left(\frac{F_{outlet,CO_2}}{\sum_{i=1}^{3} F_{outlet,i}}\right)^{REG} \qquad [-] \tag{3.21}$$

while the exploited cyclic capacity of the sorbent for each adsorbed component is computed as

$$\text{Cyclic Capacity} = \bar{n}_i^{ADS} - \bar{n}_i^{REG} \qquad \forall\, i = \text{CO}_2, \text{O}_2, \text{N}_2 \qquad \left[\frac{mol}{kg}\right] \tag{3.22}$$

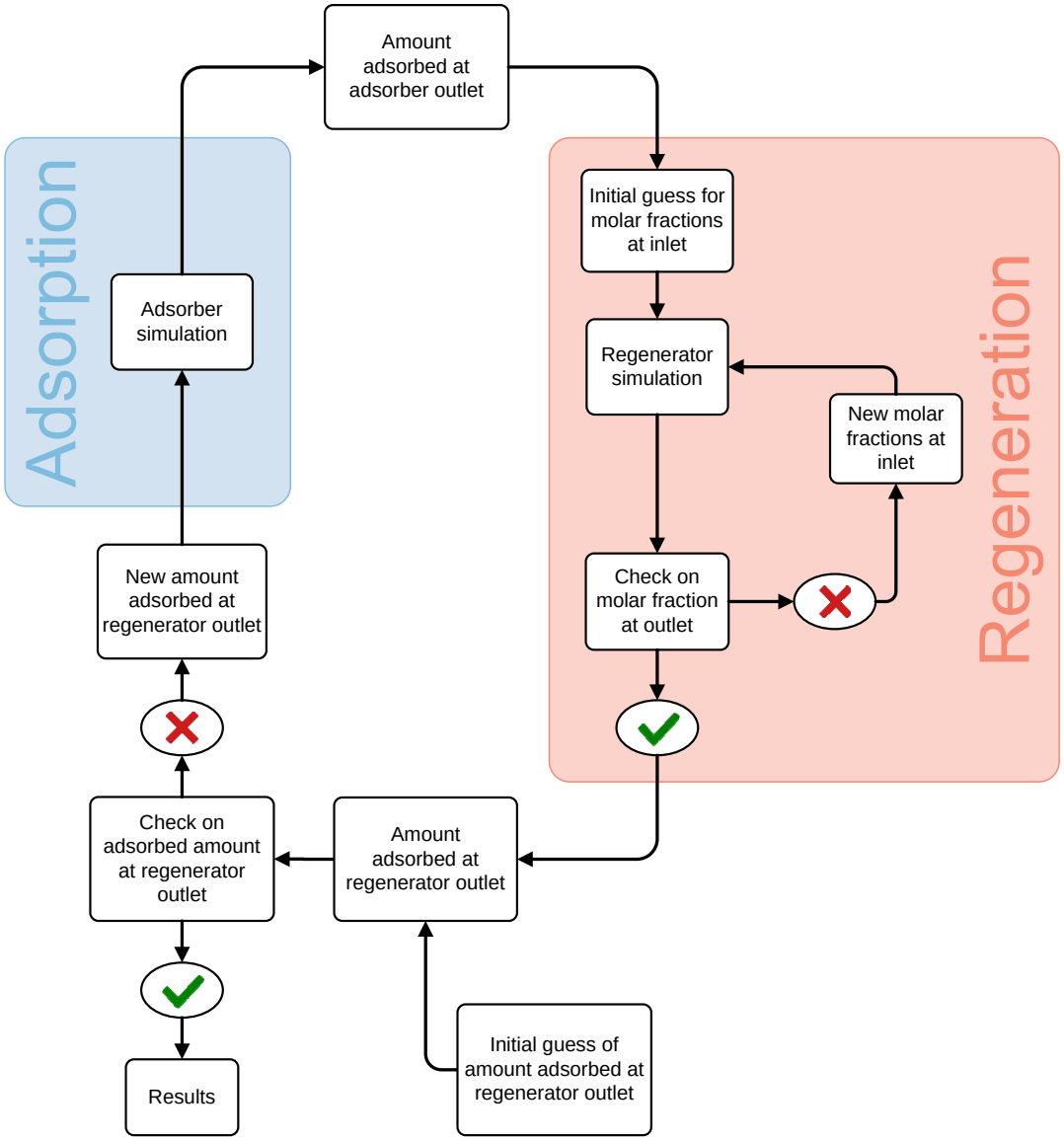

Figure 3.11: CFB: logical scheme of the TSA cycle model

The energy consumption of the system corresponds to the amount of heat provided to the regenerator. The productivity rate is calculated as

$$\text{Productivity} = \frac{\dot{m}^{REG}_{outlet,CO_2}}{W_s^{ADS} + W_s^{REG}} \qquad \left[\frac{kg_{CO_2}}{t_{ads}\, h}\right] \tag{3.23}$$

In this sense, the total productivity results being a little higher than the real one; in fact, the total inventory is underestimated, because the solids which are not inside the reactors (but instead in the cyclones, in the recirculation legs, in the solids flow control valves, as well as in the heat exchanger or in other ducts) are not included in the term W_s. Nevertheless, this neglected amount of solid usually accounts for a limited share of the total inventory (less than 10÷20%) and cannot be straightforwardly estimated; for these reasons an approximation is made considering W_s only.

3.4 Heat transfer modeling

Owing to the assumption of isothermal operation of the reactors, a strong hypothesis that will need to be validated by the results, the energy balances can be treated separately from the mass ones. The adsorption and desorption processes depend in fact deeply on the temperature on the system, and they would also normally affect it, being exothermic and endothermic respectively. Moreover, all the sensible heat related to gas and solid flows entering and leaving the reactors contributes to the total energy variation in the riser.

Nevertheless, according to the mentioned assumption, heat exchange through the walls is believed to compensate for all the other energy terms, so that the bed can operate isothermally. In the TSA cycle already presented, each reactor owns a dedicated heat exchanging system, whereby the required amount of heat is transferred in or out. The adsorber is therefore featured with a cooling system, aimed at removing the heat released by the exothermic adsorption process, while the regenerator is connected to a heating system, that balances out the energy required by desorption.

However, since the fluid dynamics is treated alike for both reactors, as far as the heat transfer coefficients inside the riser are concerned, the same method is used to determine their value. The conduction resistance of walls is here instead assumed as negligible, as it can be proved to be relatively smaller than the other resistances for thin steel walls. The thermal nature of the gas-solid reactions is believed to be initially converted into a variation of sensible heat of the solid particles that form the inventory; it is simultaneously transferred to the gas phase as well, for no temperature gradient is assumed between the solid and the gas phase –i.e., there is no thermal resistence between gas and solid particles.

Therefore, the only term left to assess is that related to the exchange between the solid-gas suspension and the riser walls. Determining the value of the suspension-to-wall coefficient inside a circulating fluidized bed is a topic still under discussion in literature. Many different explanation of this phenomenon may be found (see [20],[21],[23] and [15]): not all of them comply with each other and moreover they do not converge on the expected values of the coefficient, being all of the available correlations experimentally derived and each of them resulting properly suitable only within a narrow range of applications. Moreover, most of them have been originally written for CFB boilers, where operational conditions differ sensibly from those encountered in this work.

The different studies are though found to agree upon at least the few following points. Three different mechanism may contribute to heat transfer: conduction, convection and radiation; nevertheless, radiation can be always neglected when the temperature levels involved are sufficiently low, which is undoubtedly true for the application here investigated. Conduction and convection should, instead, both taken into account, as the particles are believed to enhance the convective heat exchange provided by gases by discontinuously getting in direct contact with the walls. This enhancement is by most correlation computed as a multiplying or an additional factor to be considered next to the convective coefficient, which is to be calculated as if only the gases were flowing inside the riser.

A correlation originally derived by Molodtsof and Muzyka [22] for gas-suspensions flow-

ing inside pipes allows calculating a multiplying factor for the only-gas convective transfer coefficient h_{og} as follows:

$$h_{susp} = h_{og} \frac{(1 + M_R C_R)^2}{1 + \alpha\, M_R C_R + \beta\, (M_R C_R)^2} \qquad \left[\frac{W}{m^2\, K}\right] \tag{3.24}$$

where M_R is the solid-to-gas loading ratio, defined as

$$M_R = \frac{\varepsilon_s\, \rho_s}{(1 - \varepsilon_s)\, \rho_g} \qquad [-] \tag{3.25}$$

ans C_R is the solid-to-gas heat capacity ratio, i.e.

$$C_R = \frac{c_{p,s}}{c_{p,g}} \qquad [-] \tag{3.26}$$

while α and β are two parameters whose value is determined looking at the fluiddynamic characteristics of the flow. In this study a correlation by Zhang et al. [23] is adopted; it is a linearization of the just presented expression and the authors state it provides better fitting for a wider range of experimental data, compared to the one used by Molodtsof and Muzyka:

$$h_{susp} = h_{og}\, (1 + \gamma\, M_R C_R) \qquad \left[\frac{W}{m^2\, K}\right] \tag{3.27}$$

In this expression γ replaces both α and β; the authors suggest an average value of 0.25 for the constant γ.

The only-gas convective coefficient is assessed by means of the Gnielinski correlation, valid for fully developed or transition turbulent flows inside cylindrical ducts within the reported intervals [20]:

- $2300 \leq Re_D \leq 10^5$
- $0.5 < Pr < 2000$

$$Nu_D = \frac{h_{og}\, D}{k_g} = \frac{\frac{f}{8}\, (Re_D - 1000)\, Pr}{1 + 12.7 \sqrt{\frac{f}{8}} \left(Pr^{\frac{2}{3}} - 1\right)} \tag{3.28}$$

$$f = \frac{1}{(1.82\, \log_{10} Re_D - 1.64)^2} \tag{3.29}$$

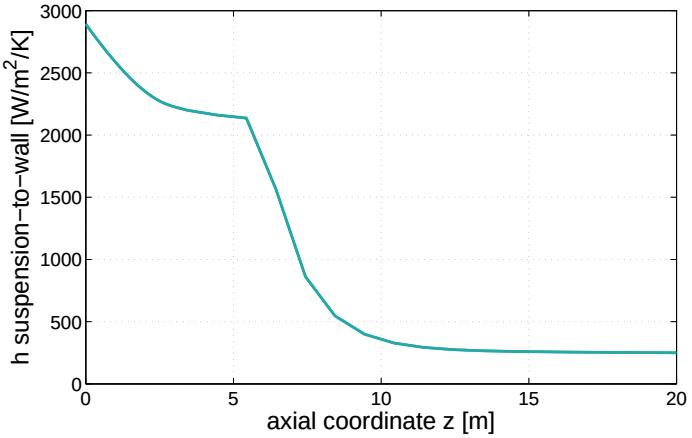

Figure 3.12: CFB: suspension-to-wall convective heat transfer coefficient along riser length

A profile of the heat transfer coefficient along the riser length obtained with these expressions looks like the one sketched in Figure 3.12: in the bottom dense zone the heat transfer can reach very high peaks, up to 2000-3000 W/m^2/K, while in the lean zone it tends to a constant asymptotic value, usually in between 200 and 400 W/m^2/K. Therefore it can be averaged out at around 400÷600 W/m^2/K throughout the whole riser.

3.4.1 Heat exchanging system geometry

Both the adsorber and the regenerator are imagined as having a rectangular cross section, with an aspect ratio of 2 between width and depth. Such a solution is meant to increase the total area available at riser walls, without causing excessive pressure drop in the gas flow. Vertical riser walls consists of tubes with an inner diameter D_{tubes} of 35 mm. Not only the waterwalls work as exchange surface, but also a set of additional wingwalls is assumed to be installed inside the riser to spread the total heat exchange surface; they are all placed parallel to the short side of the cross section, and only some of them extend full-height long from the bottom to the top of the riser, while most of them are shorter and hang over the dense bottom zone, to avoid corrosion caused by solid particles where the voidage rates are lower. The wingwalls are covered in tube bundles like the walls; they account for an overall 85% increase of the surface available for heat exchange with respect to the waterwalls-only case. This geometry of the wingwalls can be found to be implemented for CFB boilers in literature [24].

3.4.2 Energy balance over the adsorber section

Once the coefficient within the riser walls has been determined, the thermal resistance on the outside of the riser wall has to be assessed in order to evaluate the final heat transfer coefficient from the bed to the heat source.

As regards the adsorber, a stream of water at about ambient conditions works as cooling fluid to remove the heat released by adsorption. All water properties are evaluated at ambient pressure and at an average temperature T_{water} of 19°C (or 4°C under the riser temperature, if it is lower than 23°C); the water stream can undergo a maximum temperature increase ΔT_{water}^{max} of 8°C; it flows at an average velocity v_{water} of 2 m/s. The flow rate of water is determined by the cross section available taking into account all the tubes that can be placed along the riser walls and the additional wingwalls, whose total number is indicated as N_{tubes}: The convective transfer coefficient is computed by means of the Dittus-Boelter correlation for heated fluids flowing in turbulent regime into smooth pipes i.e. [20] within the reported intervals:

- $Re_D > 10^5$
- $0.6 \leq Pr < 100$

$$Nu_D = \frac{h_{water}\, D_{tubes}}{k_{water}} = 0.023\, Re_D^{0.8}\, Pr^{0.4} \tag{3.30}$$

The total heat transfer coefficient between the gas-solid suspension inside the riser and the cooling water inside the tubes is therefore computed by considering the two thermal resistances in series; among the two, the water-to-wall convective coefficients is around one order of magnitude higher than the suspension-to-wall one (roughly $5{\cdot}10^3$ versus $5{\cdot}10^2$ W/m^2/K respectively), so that the latter is the limiting term:

$$h_{total} = \left(\frac{1}{h_{susp}} + \frac{1}{h_{water}} \right) \qquad \left[\frac{W}{m^2\, K} \right] \tag{3.31}$$

The total flow rate of water depends on the number of available tubes

$$\dot{m}_{water} = \frac{\pi D_{tubes}^2}{4} N_{tubes}\, v_{water}\, \rho_{water} \qquad \left[\frac{kg}{s}\right] \tag{3.32}$$

while the maximum amount of thermal power that can be removed by the water stream can be thus computed as

$$\dot{Q}_{max} = \dot{m}_{water}\, c_{water}\, \left(\Delta T_{water}^{max}\right) \qquad [W] \tag{3.33}$$

Considering the section delimited with a dashed blue line in Figure 3.13, the mass balance applied to the adsorber section can be expressed as follows:

$$\dot{m}_{g,inlet} + \dot{m}_{R1} + \dot{m}_{E4} = \dot{m}_{g,out}^{ADS} + \dot{m}_{Y1} \qquad \left[\frac{kg}{s}\right] \tag{3.34}$$

being $Y1$, $R1$ and $E4$ the flow of solid coming out of the riser, the flow of solid recirculated back into the riser and the flow of unloaded solid coming from the regeneration unit respectively. Each solid flow includes two different terms, namely that of the solid sorbent ($_{ads}$) and that related to the adsorbed phase, so that

$$\dot{m}_{E4} = \dot{m}_{ads} + \dot{m}_{ads} \sum_{i=1}^{N_{species}} \left(\bar{n}_i^{REG}\, M_i\right) = \dot{m}_{ads} \left(1 + \sum_{i=1}^{N_{species}} \left(\bar{n}_i^{REG}\, M_i\right)\right) \qquad \left[\frac{kg}{s}\right] \tag{3.35}$$

$$\dot{m}_{Y1} = G_s + G_s \sum_{i=1}^{N_{species}} \left(\bar{n}_i^{ADS}\, M_i\right) = \frac{\dot{m}_{ads}}{(1 - R_{rec})} \left(1 + \sum_{i=1}^{N_{species}} \left(\bar{n}_i^{ADS}\, M_i\right)\right) \qquad \left[\frac{kg}{s}\right] \tag{3.36}$$

$$\begin{aligned} \dot{m}_{R1} &= G_s\, R_{rec} + G_s\, R_{rec} \sum_{i=1}^{N_{species}} \left(\bar{n}_i^{ADS}\, M_i\right) \\ &= \dot{m}_{ads}\, \frac{R_{rec}}{1 - R_{rec}} \left(1 + \sum_{i=1}^{N_{species}} \bar{n}_i^{ADS}\, M_i\right) \qquad \left[\frac{kg}{s}\right] \end{aligned}$$

As it can be seen in figure, the solid that exits from the riser is partly recycled at riser inlet ($R1$) and partly sent to the regenerator ($E1$); hence

$$\dot{m}_{Y1} = \dot{m}_{R1} + \dot{m}_{E1} \qquad \left[\frac{kg}{s}\right] \tag{3.37}$$

The two streams $E1$ and $E4$ –and the corresponding $E2$ and $E3$– differ only from the amount of adsorbed phase transported by the sorbent particles, which is given by $\bar{n}_i^{ADS}$ for $E1$ and $E3$, by $\bar{n}_i^{REG}$ for $E2$ and $E4$ instead. This gap in sorbent phase is the effected of the

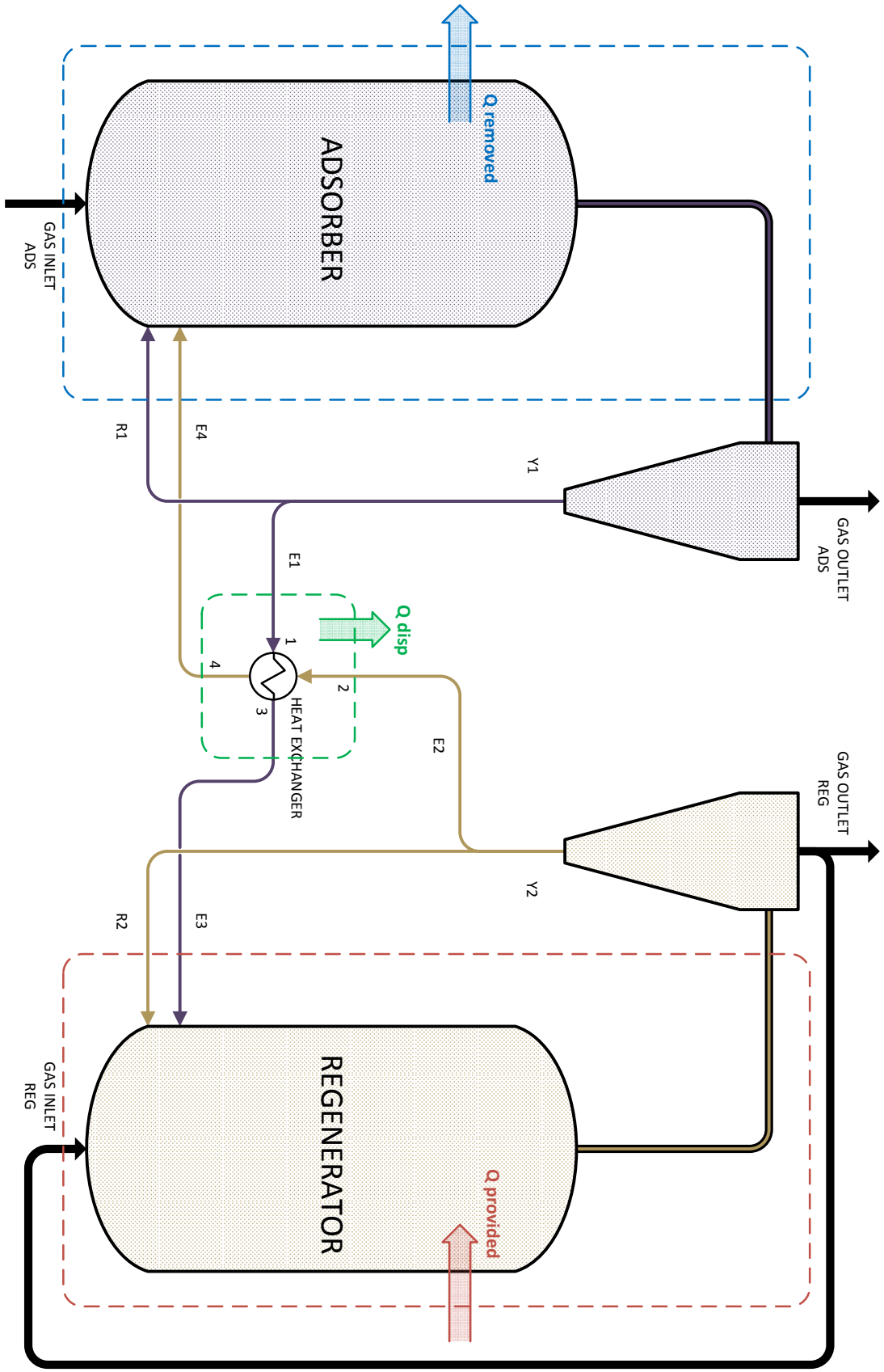

Figure 3.13: CFB: plant layout and energy balance sections

moles adsorbed and desorbed cyclically on the sorbent surface, and therefore

$$\begin{aligned}(F_g M_g)_{inlet}^{ADS} - (F_g M_g)_{outlet}^{ADS} &= \dot{m}_{E1} - \dot{m}_{E4} \\ &= \dot{m}_{ads} \sum_{i=1}^{N_{species}} \left(\bar{n}_i^{ADS} - \bar{n}_i^{REG}\right) M_i \\ &= \dot{m}_{E3} - \dot{m}_{E2} \\ &= (F_g M_g)_{outlet}^{REG} - (F_g M_g)_{inlet}^{REG} \qquad \left[\frac{mol}{s}\right]\end{aligned} \tag{3.38}$$

Coming to the energy balance across the adsorber section, it may therefore be written –using the terms defined in the previous mass equations– as follows:

$$\dot{Q}_{adsorption} + \dot{Q}_{g,inlet}^{ADS} + \dot{Q}_{R1} + \dot{Q}_{E4} = \dot{Q}_{g,outlet}^{ADS} + \dot{Q}_{Y1} + \dot{Q}_{removed} \qquad [W] \tag{3.39}$$

where the single terms are computed as

$$\dot{Q}_{adsorption} = \sum_{i=1}^{N_{species}} \left[\left(\bar{n}_i - n_{i,inlet}\right)^{ADS} \left(-\Delta h_i^{ads}\right)\right] \qquad [W] \tag{3.40}$$

$$\dot{Q}_{g,inlet}^{ADS} = (F_g M_g)_{inlet}^{ADS}\ c_{p,g} \left(T_{g,inlet}^{ADS} - T_{ref}\right) \qquad [W] \tag{3.41}$$

$$\dot{Q}_{g,outlet}^{ADS} = (F_g M_g)_{outlet}^{ADS}\ c_{p,g} \left(T_{g,inlet}^{ADS} - T_{ref}\right) \qquad [W] \tag{3.42}$$

$$\dot{Q}_{Y1} = \dot{m}_{Y1}\, c_s \left(T_{adsorption} - T_{ref}\right) \qquad [W] \tag{3.43}$$

$$\dot{Q}_{R1} = \dot{m}_{R1}\, c_s \left(T_{adsorption} - T_{ref}\right) \qquad [W] \tag{3.44}$$

$$\dot{Q}_{E4} = \dot{m}_{E4}\, c_s \left(T_4 - T_{ref}\right) \qquad [W] \tag{3.45}$$

The thermal power $Q_{removed}$ that has to be removed in order to operate the reactor isothermally at $T_{adsorption}$ can be derived out of the other quantities –which are all known after simulating the reactor dynamics– by means of this energy balance.

It must be remarked that the specific capacity of solids $c_{p,s}$ is assumed to be equal for both the sorbent material and the adsorbed phase of the different gas species involved in the process. As regards T_{ref}, it is only a reference temperature level which can conveniently correspond to the temperature at which Δh^{ads} is evaluated. The procedure used to assess T_4 is going to be explained in the next chapters.

3.4.3 Energy balance over the regenerator section

As regards the regenerator, condensing steam is used heating fluid to provide the heat required by desorption; the main feature of this solution is that as long as the heating fluid undergoes a state transition, it releases heat at a constant temperature, which suits conveniently the purpose of operating the riser isothermally.

All steam properties are evaluated at a condensation temperature T_{steam} 20°Chigher than that of the regeneration unit (down to a lower bound of 110°C); this is meant to reduce as much as possible the exergetic content of the heat used in the CCS system. The steam flows at an average velocity v_{steam} of 3 m/s; its flow rate is determined –in analogy with the cooling system– by the cross section available in the tubes that can be placed along the riser walls and the additional wingwalls: The steam is imagined as flowing downwards in the tubes –so to prevent any risk of flooding inside the pipes, which might be caused by shear effect of the steam flow on the condensate surface– with a turbulent annular pattern. The convective transfer coefficient of an annular flow of condensing steam can be computed by means of a correlation by Dobson and Chato, as reported in [25], which gives the value as a function of the vapour quality x_v:

$$Nu(x_v) = \frac{h_{steam}(x_v)\, D_{tubes}}{k_{liquid}} = 0.023\, Re_{ls}^{0.8}\, Pr_l^{0.4} \left(1 - \frac{2.22}{X_{tt}^{0.89}}\right) \tag{3.46}$$

where

$$Re_{ls}(x_v) = \frac{\dot{m}_{steam}\, D_{tubes}\, (1 - x_v)}{\mu_l} \tag{3.47}$$

$$X_{tt}(x_v) = \left(\frac{1 - x_v}{x_v}\right)^{0.9} \left(\frac{\rho_g}{\rho_l}\right)^{0.5} \left(\frac{\mu_l}{\mu_g}\right)^{0.1} \tag{3.48}$$

The total heat transfer coefficient between the suspension inside the riser and the condensing steam flowing inside the tubes is therefore computed by considering the two thermal resistances in series, being the suspension-to-wall the limiting term (approximately $5{\cdot}10^2$ W/m^2/K, while the steam condensing inside the tubes exchanges heat with a coefficient always higher than 10^4 W/m^2/K):

$$h_{total} = \left(\frac{1}{h_{susp}} + \frac{1}{h_{steam}}\right) \qquad \left[\frac{W}{m^2\, K}\right] \tag{3.49}$$

The total flow rate of steam depends on the number of available tubes, in analogy to what already seen for the cooling system,

$$\dot{m}_{steam} = \frac{\pi D_{tubes}^2}{4}\, N_{tubes}\, v_{steam}\, \rho_{g,steam} \qquad \left[\frac{kg}{s}\right] \tag{3.50}$$

as well as the maximum amount of thermal power that can be provided to the reactor

$$\dot{Q}_{max} = \dot{m}_{steam}\ (\Delta h_{lv}(T_{steam})) \qquad [W] \tag{3.51}$$

Considering the section enclosed within the dashed red line in Figure 3.13, the mass balance applied to the regenerator section can be written as follows:

$$\dot{m}_{g,inlet} + \dot{m}_{R2} + \dot{m}_{E3} = \dot{m}_{g,out}^{ADS} + \dot{m}_{Y2} \qquad \left[\frac{kg}{s}\right] \tag{3.52}$$

being $Y2$, $R2$ and $E3$ the flow of solid coming out of the riser, the flow of solid recirculated back into the riser and the flow of loaded solid coming from the adsorption unit respectively. Those flows are symmetrical to those already detailed in the previous section. Once again, the solid that exits from the riser is partly recycled at riser inlet ($R2$) and partly sent to the regenerator ($E2$), as in figure.

According to this mass balance, the energy balance across the regeneration section, is therefore defined as follows:

$$\dot{Q}_{provided} + \dot{Q}_{g,inlet}^{REG} + \dot{Q}_{R2} + \dot{Q}_{E3} = \dot{Q}_{g,outlet}^{REG} + \dot{Q}_{Y2} + \dot{Q}_{desorption} \qquad [W] \tag{3.53}$$

where the single terms are computed as

$$\dot{Q}_{desorption} = \sum_{i=1}^{N_{species}} \left[\left(n_{i,inlet} - \bar{n}_i\right)^{REG} \left(-\Delta h_i^{ads}\right) \right] \qquad [W] \tag{3.54}$$

$$\dot{Q}_{g,inlet}^{REG} = \left(F_g M_g\right)_{inlet}^{REG} \, c_{p,g} \left(T_{g,inlet}^{REG} - T_{ref}\right) \qquad [W] \tag{3.55}$$

$$\dot{Q}_{g,outlet}^{REG} = \left(F_g M_g\right)_{outlet}^{REG} \, c_{p,g} \left(T_{g,inlet}^{REG} - T_{ref}\right) \qquad [W] \tag{3.56}$$

$$\dot{Q}_{Y2} = \dot{m}_{Y2} \, c_s \left(T_{desorption} - T_{ref}\right) \qquad [W] \tag{3.57}$$

$$\dot{Q}_{R2} = \dot{m}_{R2} \, c_s \left(T_{desorption} - T_{ref}\right) \qquad [W] \tag{3.58}$$

$$\dot{Q}_{E3} = \dot{m}_{E3} \, c_s \left(T_3 - T_{ref}\right) \qquad [W] \tag{3.59}$$

The thermal power $Q_{provided}$ that has to be provided in order to operate the reactor isothermally at $T_{desorption}$ can thus be derived out of this energy balance.

3.4.4 Energy balance for the heat exchange between solid streams

According to the aim of reducing the total energy consumption of the system, it seems sensible to recover as much heat as possible out of the hot solids that leave the regeneration unit and travel to the adsorption one. An intelligent reuse of this heat would be in order to drive it into the colder solids that flow in the opposite direction; in fact, as they enter the regenerator they are heated up to $T_{desorption}$, causing a certain amount of externally provided energy to be spent to fill this temperature difference. At the same time, if the regenerated solids were fed at the adsorption riser without being cooled down in advance, all their sensible heat should be

drained out of the adsorber, increasing the total thermal power to be removed by the cooling system. It is straightforward how implementing some regenerative heat exchange between this two streams is essential to achieve adequate performances in terms of overall amount of heat required by the operation of the system.

How such a heat exchange should be operated within a real application, is an interesting as well as opened issue that will not find an answer in this work. The following aspects of the problem should be taken into account:

- although some applications of solid-solid heat exchanger do exist, they are not implemented on big scale, so that it would appear unreasonable to employ one of those devices in the CCS unit of a big power plant, like the ones investigated in this study;
- at a first sight, the most attractive solution would probably be to employ a gas flow as heat transfer fluid from one solid stream to the other, but on the one hand any gas flow available within a power plant or a still mill would not act as an inert towards the sorbent, if it were to get in direct contact with it; this means the cycle should be simulated in a complete different way to consider also the effect of this process, which could anyway hardly bring any advantage from the point of view of the global performance of the CCS system. On the other hand, it is undoubtedly difficult to operate any sort of heat exchange without direct gas-solid contact obtaining at least fair efficiency rates;
- another possibility would be that of mixing the two streams, eventually resulting in one stream of solids, whose temperature would be somewhere in between the two initial temperatures. This would allow recoverying only a limited fraction of the total heat available in the hot solids. Moreover, it would also strongly compromised the performances of the CCS system by halving the cyclic capacity of the sorbent, as the mean conversion degree of the final stream would be the average of the conversion degrees of the two initial streams.

For the purpose of this study, it is assumed that the heat exchange can be somehow operated, even if no practical solution is suggested for this issue. In this case, the balances over an idealized heat exchanger might be written looking at the section outlined with a dashed green line in Figure 3.13: The two streams get across the heat exchanger without changing their flow rates

$$\dot{m}_{E1} = \dot{m}_{E3} \qquad \left[\frac{kg}{s}\right] \qquad (3.60)$$

$$\dot{m}_{E2} = \dot{m}_{E4} \qquad \left[\frac{kg}{s}\right] \qquad (3.61)$$

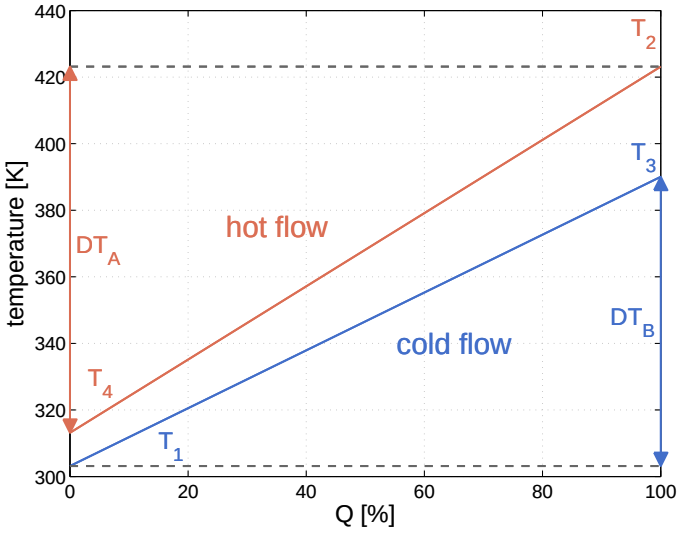

Figure 3.14: CFB: T–$\dot{Q}$ diagram of the heat exchange between solid streams

while the temperature levels achieved by the solids flowing from adsorber to regenerator – and the other way round– are to be computed by means of the energy balance, which claims

$$\dot{m}_{E2}\, c_s\, (\Delta T_A) = \dot{m}_{E1}\, c_s\, (\Delta T_B) + \dot{Q}_{disp} \qquad [W] \tag{3.62}$$

where

$$\Delta T_A = T_2 - T_4 \qquad ; \qquad \Delta T_B = T_3 - T_1 \qquad [K] \tag{3.63}$$

$$\Delta T_B = \frac{\dot{m}_{E2}}{\dot{m}_{E1}} \cdot \Delta T_A \cdot \eta \qquad [K] \tag{3.64}$$

being η the assumed recovery efficiency of the exchanger. Of course, $\dot{m}_{E1} > \dot{m}_{E2}$ because the first is loaded with a larger amount of adsorbate after adsorption while the second comes out of the regenerator; for this reason, $\Delta T_B < \Delta T_A$, even when η is assumed equal to one. Figure 3.14 shows the temperature-thermal power diagram of the heat exchange as here detailed.

Chapter 4

Fixed Bed

Fixed bed are a well-known solution for gas-solid systems, whose operation has been extensively investigated and can be nowadays detailed rather accurately, thanks to the fact that it features less complex phenomena than those found inside fluidized beds.

Since a simulation software has been already developed at SPL and it has been made available to perform all the computations needed in this study, no new modeling technique is presented in this chapter and the employed model itself is not discussed deep in details. The efforts of this work are therefore focused more on other issues regarding the plant layout and the process scheduling; they are examined extensively in these pages, for they are of much greater interest than in the CFB case and represent an important stage in the development of an actionable fixed bed system.

4.1 Fixed beds

A fixed bed consists of solid particles packed within a column-shaped vessel, through which a gas flow moves smoothly without causing any displacement of the solids.

The superficial velocity of the gases is limited in order to never reach the minimum fluidization conditions and their flow follows a rather straight path across the reactor, as it deviates only locally to surround the particles, filling all the void interstices between them. Consequently, the flow of gas inside a fixed bed may be conveniently described by means of a plug flow model, using a single-dimension spatial discretization, unless specific phenomena on the radial direction are investigated.

In comparison with fluidized bed, the lower gas velocities allow reaching longer contact times between gases and solids, for a given bed height. At the same time though they cause the required cross sectional area to be several times wider than in the fast fluidized beds, an effect which is further worsened by the high solid volumetric fraction. In this sense, they look most suitable for slowly proceeding processes operated on limited amounts of gases.

The void fraction of a fixed bed is uniform along its height and is lower than in any fluidized bed system. As presented in chapter 3, when a gas flows through a packed bed, the particles cannot be displaced by gases and therefore they hinder the flow causing a frictional

pressure drop which increases together with the gas velocity, according to the expression formulated by Ergun [26]

$$\frac{\Delta p_{fr}}{L} g_c = 150 \frac{(1-\varepsilon)^2}{\varepsilon^3} \frac{\mu_f \, u}{(\phi_s \, d_p)^2} + 1.75 \frac{1-\varepsilon}{\varepsilon^3} \frac{\rho_f \, u^2}{\phi_s \, d_p} \qquad \left[\frac{kg}{m^2 \, s^2}\right] \tag{4.1}$$

The total pressure drop across the bed can be computed as [15]

$$\Delta p = \Delta p_{fr} \pm \frac{\rho_f \, L}{g_c} \qquad [Pa] \tag{4.2}$$

where $+$ stands for upwards and $-$ for downwards flowing fluid. The second term of the last equation is anyway negligible for gaseous fluids, unless dealing with very high pressures and long beds. As inferable from Ergun's equation, the particle size is heavily affecting the total pressure drop, so that particles equivalent diameter are better kept at least in the order of magnitude of a few millimeters. For fixed particle dimensions, the pressure drops are lower than those undergone by gases in a fluidized bed and they do not play any substantial role in TSA applications, where pressure is not to be monitored very strictly.

4.2 Model

To assess the performances of a fixed bed operation a simulation tool developed at Separation Process Laboratory has been employed; the model implemented by this tool is not going to be described in details in these pages, as it does not count as an original contribution of this work. Anyway a little information must be provided to the reader, in order to present the potential of the software, intended as the range of possible process configuration the tool has been designed to recreate.

This tool has been developed to simulate the operation of a single vessel. The data it takes as input can be divided into seven groups:

- the data regarding the streams fed into the vessel, intended as their flow rate, their temperature and pressure and their composition;
- the main properties of the gas species that form the feed stream;
- the properties of the solid sorbent material;
- the geometry of the vessel, including the characterizing parameters of the related heating and cooling system;
- the configuration of the cycle, intended as the sequence of the steps the TSA process consist of, included all the specific operational settings of each step;
- the initial conditions of the system;
- a time discretization step and a space discretization step.

In fact the different phases of a complete adsorption and regeneration process in a fixed bed plant are not operated by different reactors, but they are rather undergone in sequence by the same column, following an established schedule and determining a total cycle duration t_{cyc}, which corresponds to the time lapse required by a single unit to complete the phase sequence.

Therefore each reactor undergoes continuous changes in its operation which can be outlined along the time dimension within a certain interval, that corresponds to the total cycle duration. The steady state operation of a fixed bed, in fact, does not consist in all the system parameter to be kept constant in time; it rather means those parameters are cyclically repeated alike after a time lapse t_{cyc}.

These changes concern of course pressure and temperature as well, so that no assumption of isothermal operation of the reactor can be made for a fixed bed. This means the mass balances and momentum balances cannot be decoupled from the energy balance, but they have to be solved simultaneously. At the same time, these modeling implies both a space and a time discretization must be employed to assess the behavior of the system.

As mentioned, the model takes as input a chosen step schedule; in order to build it, six different types of units can be selected and arranged forming an arbitrarily long sequence:

- pressurization unit, which operates shutting the outlet of the column and letting the gas in from the other end;
- closed heating or cooling unit, with both ends being shut so that no mass flow enters or leaves the column;
- adsorption unit, which is entered and left by a fluid stream forced into the vessel by a pressure gradient between the pressure of the gas at the inlet and the back pressure set at the outlet; this of course implies the column to be open at both ends;
- blowdown unit, where one end is shut, while the other is left open for a gas to autonomously flow out of the vessel under the effect of a pressure gradient established between the inner conditions of the reactor and the back pressure set at the outlet;
- pressure-equalization pressurization unit (not used in TSA processes), in which one end of the column is shut, whereas the other is directly connected to a pressure-equalization blowdown unit, letting the pressure equalize inside the two units, reaching an intermediate value;
- pressure-equalization blowdown unit (not used in TSA processes), which has to be coupled to a pressure-equalization pressurization unit.

Each unit can be run in either cocurrent or countercurrent flow pattern, ‘cocurrent’ meaning upwards and ‘countercurrent’ meaning downwards.

Moreover, for each step a specific time extent must chosen, as well as the temperature of the external heating or cooling fluid, the back pressure level at the open outlet and the destination of the outflow (if there). Any outflowing stream can either form a product or be totally or partially recirculated into another unit. Recirculation can be direct (which implies some time limitations for the two linked units) or can run through a storage tank, where the gas is firstly gathered to be later gradually released with a constant flow rate.

If the designed sequence is physically operable, the model computes all cycle parameters proceeding instant after instant along the vessel axial coordinate. Each step provides the initial conditions for the following one, following the given sequence. The computing procedure converges when steady state operational conditions are achieved, i.e. when the entire process cycle is repeated alike twice sequentially, considering a certain established error tolerance.

As any CCS system, the plant layout has necessarily to feature at least two outputs: the first is the clean flue gas, i.e. the flue gas after the removal of CO_2; the second is the recovered CO_2-rich stream directed to sequestration. In all the configurations analyzed in this dissertation, these two are the only two mass outflows of the system, whereas the feed stream is the only input flow. The two outflows are indicated as 'product 1' and 'product 2' respectively.

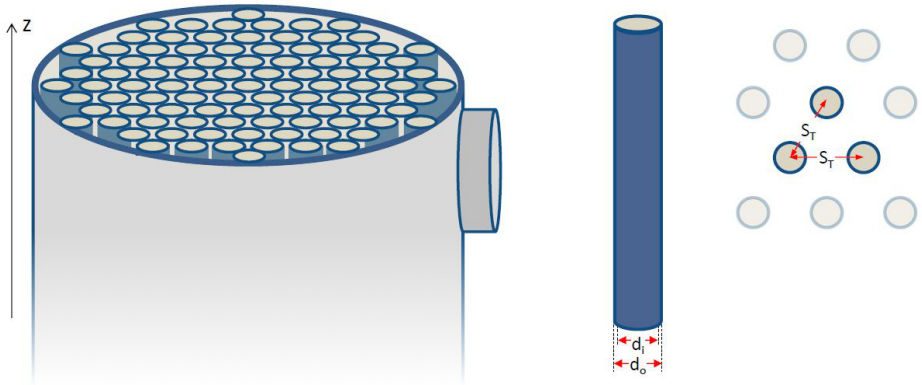

Figure 4.1: Schematic shell and tube design of fixed bed vessel

For the purposes of this study, a shell and tube reactor is modeled (Figure 4.1), in which each tube correspond to a column. The bed is equally distributed into N_{col} equidistant columns, arranged repeating a triangular pattern of side length S_T. An ideal heat exchanging fluid (which for a real implementation could be identified as water for the cooling and hot steam for the heating) flows in the shell all around the columns; it is assumed as an isothermal heat source, which means its heat capacity is ideally infinite. The heat capacity of the metal forming the column walls is instead taken into account. All the specification of the fixed bed vessel and of the heat exchange system as simulated in the context of this study are reported in Appendix C.

As regards the output of the model and, in particular, the evaluation of the assessment parameters that have been introduced in Chapter 2, the recovery and the purity of the system are assessed according to their definition as

$$\text{Recovery} = \frac{\int_0^{t_{prod\,2}} \dot{m}_{CO_2}^{prod\,2}\, dt}{\int_0^{t_{feed}} \dot{m}_{CO_2}^{feed}\, dt} = 1 - \frac{\int_0^{t_{prod\,1}} \dot{m}_{CO_2}^{prod\,1}\, dt}{\int_0^{t_{feed}} \dot{m}_{CO_2}^{feed}\, dt} \qquad [-] \tag{4.3}$$

$$\text{Purity} = \frac{1}{t_{prod\,2}} \int_0^{t_{prod\,2}} y_{CO_2}^{prod\,2}\, dt \qquad [-] \tag{4.4}$$

where $t_{prod\,1}$, $t_{prod\,2}$ and t_{feed} are the time intervals within a single cycle during which each stream flows respectively. The recovery rate is always computed following both routes, so that a possible discrepancy between the two results could be read as warning for some error

in the computation. All the results shown in these pages are characterized by a negligible discrepancy between the two results.

The specific energy consumption takes into account the amount of heat provided to the system by the hot fluid flowing on the outside of the columns in the shell and tube vessel. All the heated stages in the cycle sequence are considered. In the end it can be computed through the expression

$$\text{Specific Energy Consumption} = \frac{\int_0^{t_{heated\,stages}} \sum_{heated\,stages} \dot{Q}_{provided}\, dt}{\int_0^{prod\,2} \dot{m}_{CO_2}^{prod\,2}\, dt} \qquad \left[\frac{MJ}{kg_{CO_2}}\right] \tag{4.5}$$

Looking at a single column, the productivity of the system can be referred to its inventory if the mass flow rate of captured CO_2 yielded during a whole cycle is considered:

$$\text{Productivity} = \frac{\int_0^{t_{prod\,2}} \dot{m}_{CO_2}^{prod_2}\, dt}{W_s} \qquad \left[\frac{kg_{CO_2}}{t_{ads}\, h}\right] \tag{4.6}$$

As the whole system is actually a collection of identical columns which perform the same cycle, this result is correctly representative of the whole system as well.

4.3 Choice of a cycle configuration

The pursuit of an optimal configuration of the TSA cycle has to proceed through a series of sensitivity analyses aimed on the one hand at reaching the required specifications for the products, on the other hand at maximizing the productivity and minimizing the energy consumption of the process. While performing these sensitivity analyses only the durations of the single cycle steps are varied as independent parameters, while both the temperatures of the cooling and heating fluids (30°C and 150°C respectively) and the gas superficial velocity (0.21 m/s) are kept fixed. Sensitivity analyses are then performed over different cycle configurations in order not only to identify the best reachable operational points, but also to get acquainted with the trends, according to which the cycle performances vary after modification of the main input parameters. This is needed to develop some analytic skills, in order to predict the consequences of a change of operational conditions.

4.3.1 Basic cycle configuration

Consistently with this aim, a few simulations with the simplest possible configuration – a basic 4-step TSA cycle, as in Figure 4.2– are performed. Such a configuration allows inferring effortlessly the most standard trends, which are usually more visible if the cycle scheme is simple, because the amount of links between the different units is limited to its minimum value (together with the mutual effects those links imply).

In order to perform a classical TSA process, the system must undergo at least four separated phases in sequence. Since during operation the cycle is repeated always alike, the description of a step sequence might rightfully start from any of those steps; for the sake of simplicity, all the schemes displayed in these pages will start from a pressurization step.

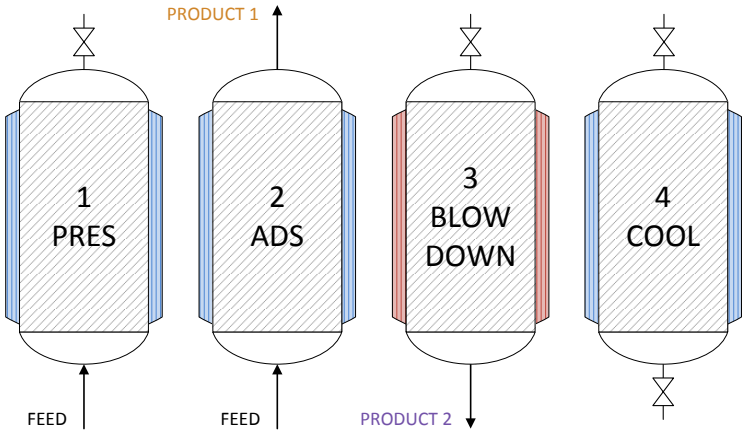

Figure 4.2: Fixed bed: basic 4-step cycle layout

A pressurization is needed to bring the system back to the standard pressure after a closed cooling step. It can be operated by conveying the feed stream directly into the column and simultaneously shutting the column outlet, so that the gas is forced and gathered inside the column, increasing pressure. Given that a TSA process is supposed to operate under almost constant pressure conditions, the gap that pressurization has to fill might accounts to a few bar at most. Hence pressurization times are always very short, if compared to the total cycle duration. At the beginning of pressurization the bed is completely regenerated and at low temperature; as a consequence the flue gas starts adsorbing already when it is fed to the reactor to pressurize it. The heat exchanging fluid removes continuously heat from the bed during the whole step, so that temperature does not increase.

After pressurization, the adsorption stage begins. The column is opened at both extremes. The flue gas is fed at constant flow rate in the column, where CO_2 is adsorbed and a N_2- and O_2-rich gas flow (the clean flue gas) is produced at outlet, forming what is here indicated as 'product 1'. During this step, the bed is progressively loaded with adsorbate. Temperature is kept low via heat exchange with the external cooling stream.

Once the bed has been loaded with the removed CO_2 –and inevitably also some O_2 and N_2– operational conditions must be switched to the regeneration mode. Which means temperatures are increased, in order to move the system towards a lower adsorption isotherm. In this basic cycle, as soon as the heating begins (by increasing the temperature of the external heat exchanging stream) the so called 'product 2' (i.e. the product sent to storage) starts flowing out of the bottom end of the column, while the top end is kept shut. Thus a countercurrent flow is set off.

When the regeneration step is concluded, the system must be brought back to adsorp-

tion conditions in order to repeat the cycle. That means the bed must be cooled down. The cooling is performed keeping both column ends shut, so that no gas flows in or out of the reactor; however, since the systems move to an higher isotherm, adsorption occurs changing the composition of the gas phase left inside the reactor and the adsorbed amount on solid surface. Consequently also the amount of gas inside the reactor changes, because it is partially adsorbed, and this causes the pressure to progressively decrease; to bring the column back to the proper conditions for the adsorption step, the pressurization stage is inserted.

Figure 4.3 shows example profiles of p, T and y_i in time for an operational point of this basic 4-step cycle, point that will be adopted as reference case for the next analyses. This operational point features the following step durations shown in Table 4.1.

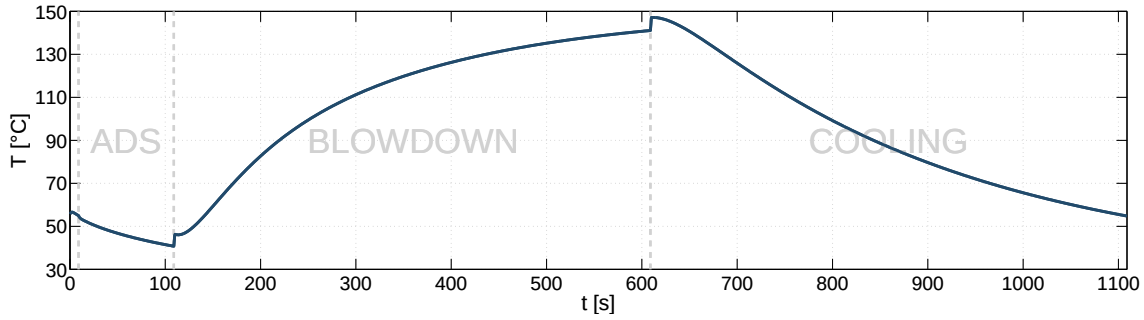

(a) Temperature profile in time

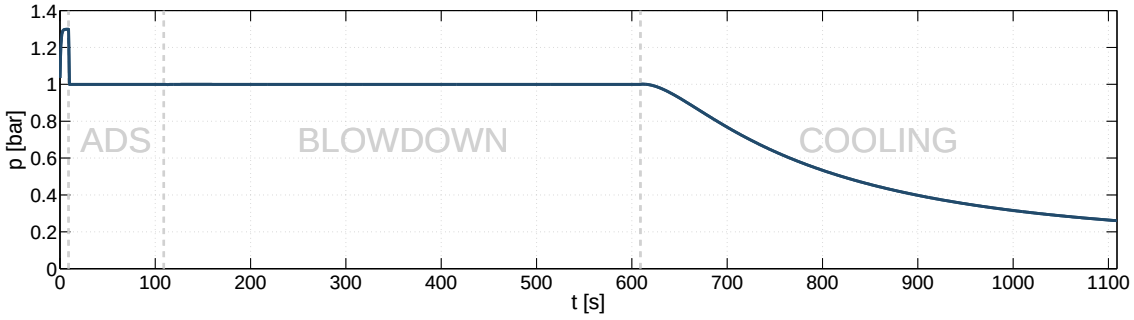

(b) Pressure profile in time

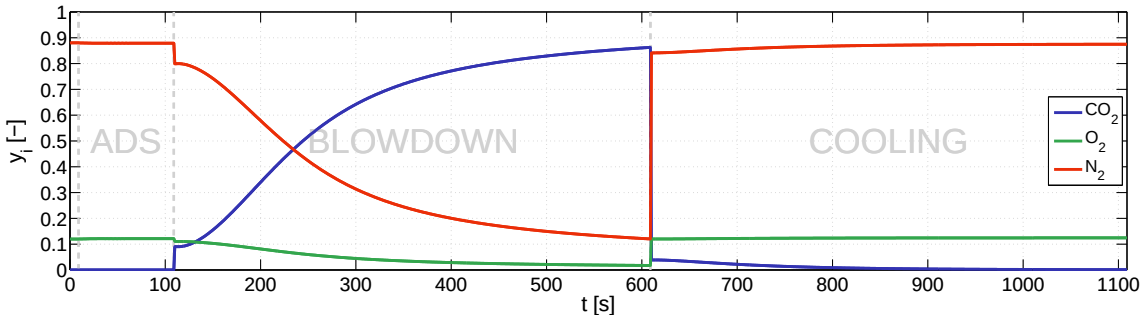

(c) Molar fraction profile in time

Figure 4.3: Fixed bed: example profiles in time for basic 4-step cycle, referred to the outlet section of the column (top end for upward flow, bottom end for downward flow)

Table 4.1: Reference case for basic 4-step cycle: step durations

Unit 1 Pressurization	Unit 2 Adsorption	Unit 3 Blowdown	Unit 4 Cooling
10 s	100 s	500 s	500 s

T, p and y_i are measured at the column outlet (top end for cocurrent and shut-column steps, bottom end for countercurrent steps). When the column is shut down, the gas phase inside is almost perfectly mixed, because both heating and cooling proceed at rather slow speeds; therefore the values at outlet are representative of the state of the whole bed. Please note that when a gas flow is entering or leaving the column, its flow rate is not generally constant, unless differently specified.

Once the layout of a cycle (read: number and type of units, interconnections between them) has been fixed, step durations are the first parameter to modify, in order to observe appreciable variations of the cycle performance.

Focusing on this basic 4-step cycle, three sensitivity analyses have been conducted, in order to outline the most basic trends. The parameters which have been modified are the duration of the adsorption step, of the heated blowdown step and of the cooling step, while no sensitivity analysis has been made over the pressurization step, as it makes no sense to have a different pressurization duration once the proper pressure is reached, unless a different pressure level is to be set inside the reactor, which is not the case for these TSA cycles that are all to be performed at approximately ambient pressure. Figure 4.4 represents the results in the 'recovery–purity' diagram, which are meant to be observed in relative more than absolute terms, only to infer some major trends.

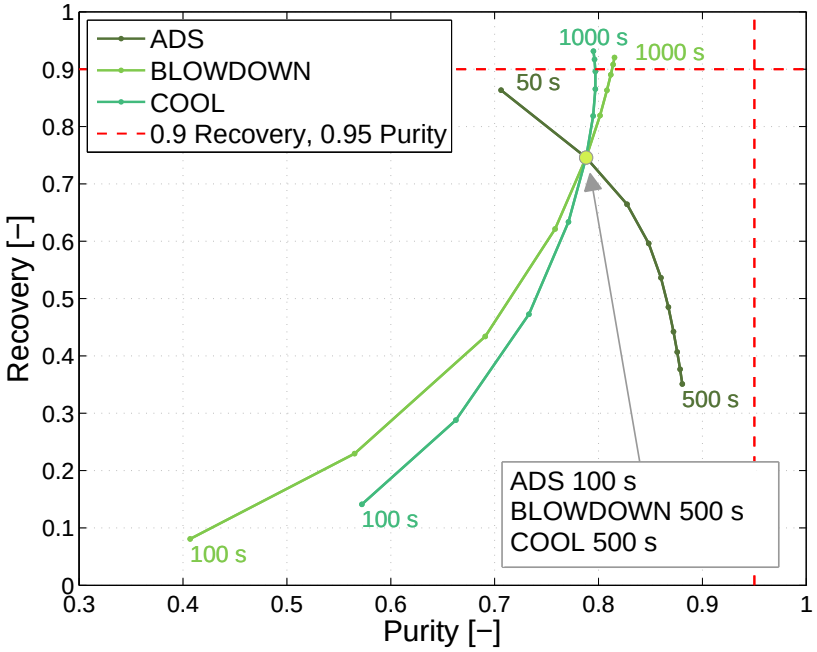

Figure 4.4: Fixed bed: sensitivity analyses results for basic 4-step cycle in 'recovery–purity' diagram

At first glance, it can be observed how both longer heating and cooling steps bring towards higher recovery rates, for they mean a closer approach to the low and high temperature levels fixed by the heat-exchanging external fluid and therefore they extend the cyclic capacity of the solid. The purity is also generally enhanced, but only up to a certain cooling time, after which it slowly starts decreasing, because, while the column is shut, the concentration of CO_2 reaches so low values, that the adsorption of O_2 and N_2 starts gaining relevance.

Moreover, the longer the heating or cooling steps become, the more slowly recovery and purity increase, since the temperature difference between the bed and the heat source gets reduced (as well as the change in bed temperature, consequently). It can also be remarked that the curve representing the variation of cooling time is always steeper than the heating one, owing to the fact that the effect of a temperature change on $n_{eq,i}$ values (which are strictly related to the recovery rate, as somehow determines the maximum cyclic capacity) is stronger at low temperatures, as it can be inferred comparing adsorption isotherms drawn at different temperatures (see Figure 2.1).

As regards the variation of the adsorption time, it can be remarked that longer step length produces higher purity rates and lower recovery rates: the explanation for this trend is to be found in the position reached by the mass transfer zone in the bed at the end of the step. The shorter the duration of the step, the further the mass transfer zone will be from the end of the bed, which indeed corresponds to higher recovery rates, because some sorbent capacity is still available for adsorption; shorter adsorption times correspond to lower purity rates as well though, since the concentration of O_2 and N_2 in the gas phase results being eventually higher.

As far as energy consumption and productivity are concerned (Figure 4.5), the effect of a cycle modification can often play opposite effects on these two parameters. If, for instance,

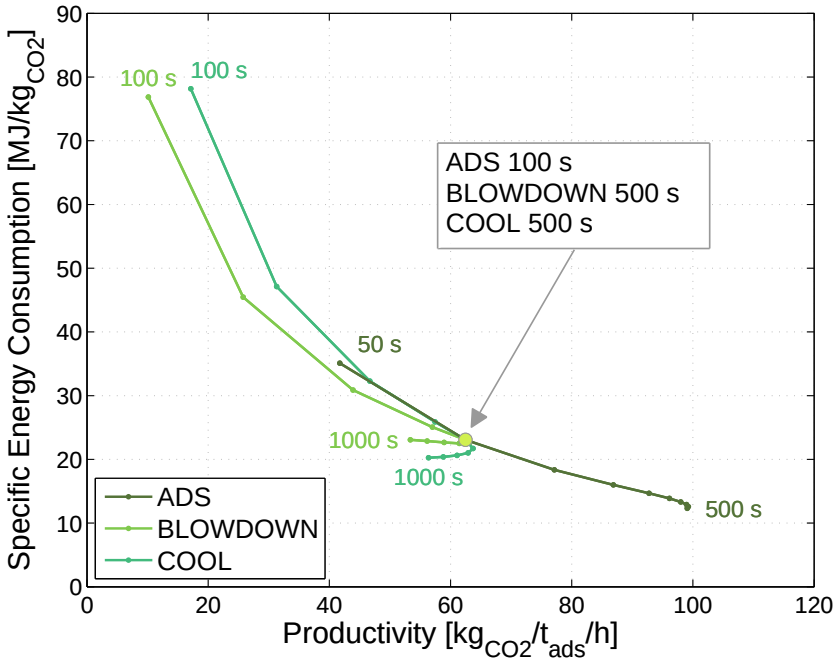

Figure 4.5: Fixed bed: sensitivity analyses results for basic 4-step cycle in 'specific energy consumption–productivity' diagram

the heating step duration is extended, one the one hand the total energy consumption unquestionably increases, but the sorbent capacity is better exploited thanks to a higher temperature –that leads to better regeneration– and therefore the specific energy consumption even decreases, when the advantage on the adsorption side overcomes the drawback on the energetic side. The productivity of the cycle (in terms of amount adsorbed per adsorbent mass unit) also increases, unless its value specific to total cycle duration is considered: in this case the curve is characterized by a maximum reachable value of productivity, because at some point the benefits on productivity are overwhelmed.

The positive effect of longer adsorption steps over productivity can be easily explained by the fact that if the mass transfer zone gets closer to the end of the bed (up to the breakthrough of the adsorption front at reactor outlet), the bed is then fully loaded with CO_2 up to its maximum capacity, which corresponds to a better exploitation of its adsorbing potential. Since the adsorption phase is not heated, if only the adsorption time is increased more CO_2 is adsorbed while the total amount of energy provided to the system remains unchanged: hence the specific energy consumption is reduced.

However, it can be noticed that none of the settings tested by these sensitivity analyses meets both the requirements of a realistically operative CCS application, namely 90% recovery and 95% purity. Although the amount of operational points tested for this cycle is undoubtedly insufficient to draw any conclusion, predictably with such a cycle configuration it is not possible to reach those aimed performances and to keep at the same time the energy consumption and the productivity levels within an interesting range.

4.3.2 More complex cycles

Other possible configurations are tested by means of similar sensitivity analyses, always varying the length of the steps (pressurization excluded). In this way a high number of possible different operational points are identified by means of their performance as computed by the software, in order to define a range of reasonable values and to observe how the complexity of the cycle layout affects the trends detected with the basic 4-step cycle. The following schemes have been tested (they are represented in Figure 4.6):

- a 6-step scheme (configuration **a**) with two adsorption steps and a purge step after the blowdown. The purge is aimed at pushing regeneration to a deeper extent and for this reason is operated heating the reactor and feeding a recirculated fraction of the O_2- and N_2-rich product 1, so that desorption of CO_2 is enhanced by its low concentration in the gas phase. The purge is indeed an effective sweeping action, but it produces a too CO_2-lean flow, which would compromise purity if directly mixed with product 2; for this reason a second adsorption step is introduced, where to recycle the product flowing out of the purge;
- a 7-step scheme (configuration **b**) derived from configuration **a**, by integrating a closed heating before the blowdown. Such a modification is meant once again to promote regeneration by increasing the total heating time, but starting with a shut-column stage, during which pressure necessarily increases;

- another 7-step scheme (configuration **c**), identical to the previous one, but with a first open-column heating stage instead, i.e. a blowdown. Since at the beginning of the blowdown O_2 and N_2 contents are rather high (because of the gas left inside the column at the end of the adsorption step and because they are the first species to be desorbed), the product of the first heating phase (which is actually operated continuously with the second heating stage, being the column conditions identical) is mixed with the clean flue gas. This measure slightly reduced the recovery rate, whose reference target appears to be easier to achieve though, compared to the purity one;
- an 8-step scheme (configuration **d**) which combines the previous two 7-step configurations, resulting in four heating stages, one shut, two open and a final purge. The first of the two heated blowdown steps contributes forming product 1, while product 2 consists of the latter.
- a 9-step scheme (configuration **e**), further development of configuration **d**, in which the first blowdown step is recirculated back to a dedicated adsorption step, in order to remove the CO_2 before mixing the flow with product 1, so that the recovery rate of the process is not compromised. The high CO_2 content of the recycle (at least higher than that of the flue gas, although it is not high enough to directly eject the flow into product 2) allows adsorption to proceed further even on an already loaded bed.

The results produced by the sensitivity analyses performed on theses cycle schemes are not discussed in details; a quick summary of the conclusions drawn after the observed results is given here instead:

- configuration **e** is found to yield the best average performances; under some setting conditions, it could also easily meet both recovery and purity reference requirements. The other configurations are in general not prevented from reaching performances as good as the best ones of configuration **e**, but they strive more to get there. This should at least give a warning about the fact that recirculating the initial part of the blowdown is a clever solution. In fact it allows not to compromise the purity rate mixing a CO_2-lean stream with product 2, while it prevents from ejecting that little CO_2 in the flue gas directly, worsening the recovery rate;
- none of the operational points whose performances reach the reference thresholds features a reasonably low specific energy consumption; as a matter of fact, the tested schemes are all characterized by a rather complex layout and long cycle durations, characteristics which somehow tend to add to the energy requirement and to lower the productivity (in which the cycle duration is at denominator);
- adopting a purge step helps indeed improving the performances in terms of better regeneration of the bed, but it seems reasonable to allege that similar results may be obtained without such a step, by slightly extending the duration of the the previous heated stages. This would somehow simplify the cycle layout, without compromising excessively the performances;

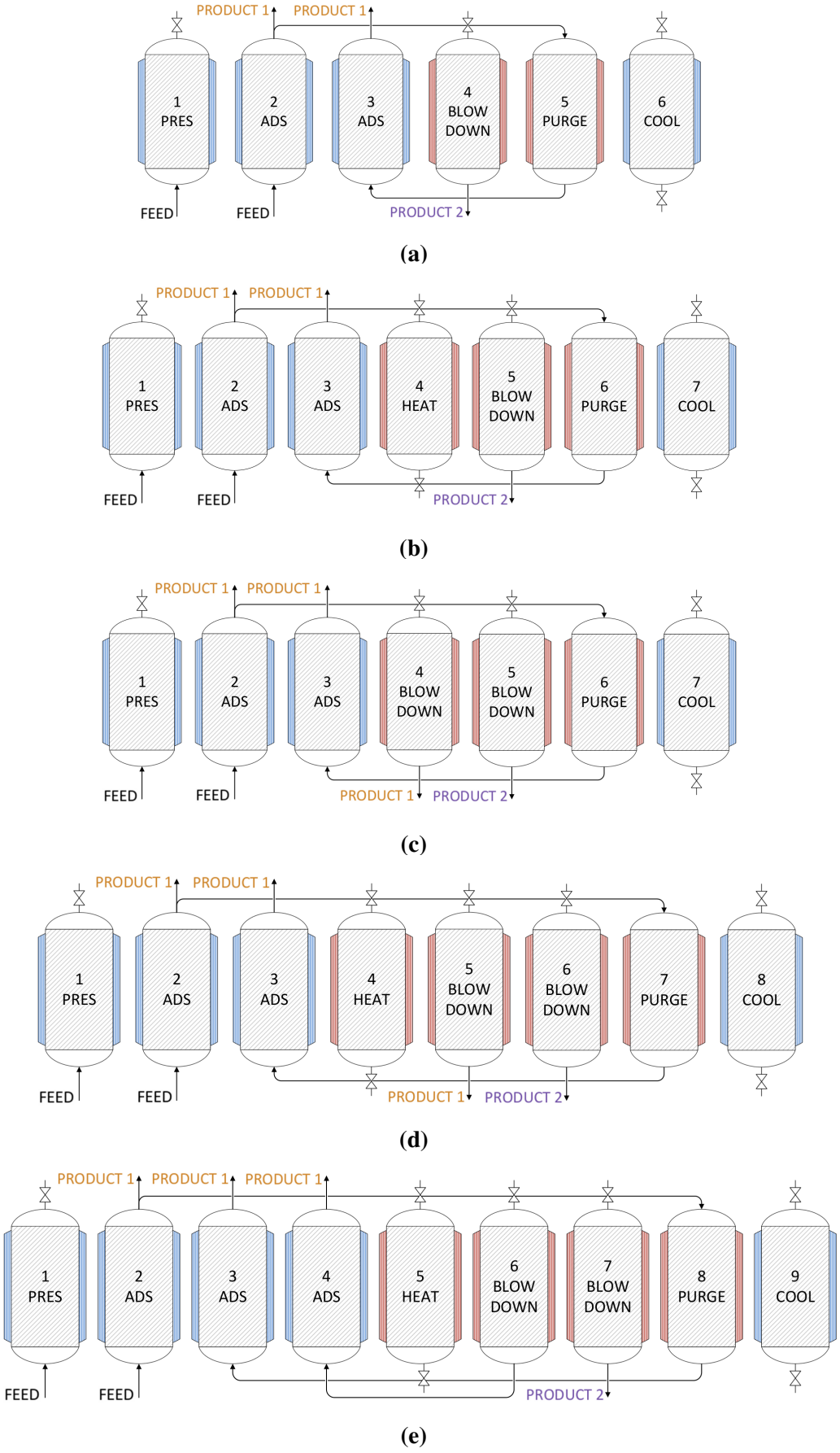

Figure 4.6: Fixed bed: cycle schemes

- there is no real need of separating the different adsorption steps, as in all these cycles. One or more recycled streams might be premixed with the feed before being driven into the column during a single shared adsorption stage. This would also promote the adsorption process, because the concentration of any recycled flow (as far as these configurations are concerned) is higher than that of the feed; therefore the bed would interact from the beginning with a higher CO_2 concentration in the gas phase. Moreover, this premixing solution would prevent different adsorption fronts to move across the bed in sequence, which may cause a larger fraction of the bed to remain unloaded;
- in general, as far as the energy-productivity graph is concerned, the sensitivity analyses show trends similar to those of the basic 4-step cycle; the same could be only partially stated for the recovery-productivity diagram instead, because the presence of recycle loops produces singular effects over those trends, because it establishes interdependencies between the units, which might be less straightforward to explain.

4.3.3 Optimal cycle configuration

After the considerations inferred from the previously mentioned analyses, a new cycle configuration is designed. It shares the double blowdown step solution –which appears unequivocally to be an intelligent and effective feature– with the first blowdown stream being always recycled back in the first adsorption unit. On the pursuit of simplification and reduction of the total duration, there is no closed heating, being all the benefits regained by recirculating the first blowdown stream; consistently the purge option is also not adopted, expecting that the same regeneration levels could be reached by means of longer blowdown extents.

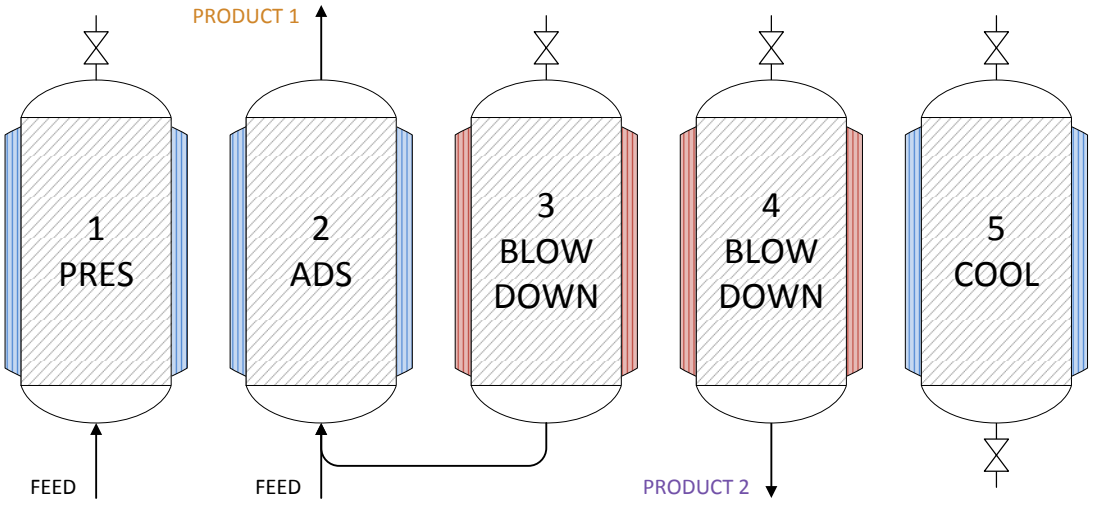

Figure 4.7: Fixed bed: 5-step cycle scheme

In the end, the layout of this cycle looks like it is displayed in figure 4.7. The pressurization step is operated in the same way as in all the other cycles previously presented, keeping

the top end shut and letting the flue gas flow upward in the column until a sufficient amount is gathered to raise the pressure at the desired level.

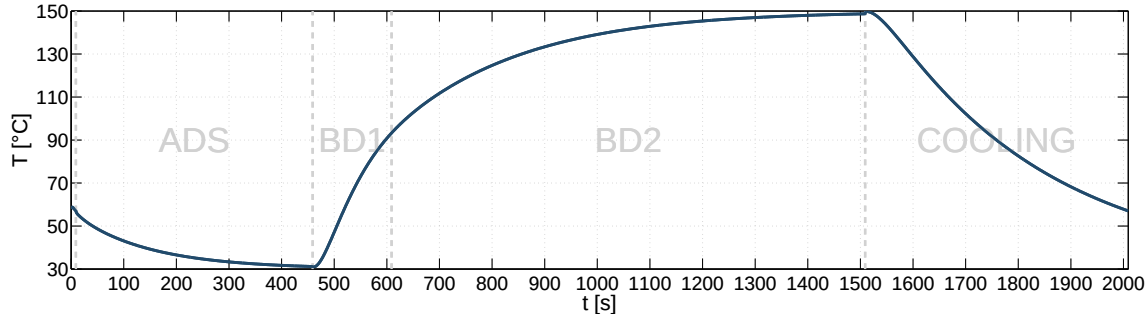

(a) Temperature profile in time

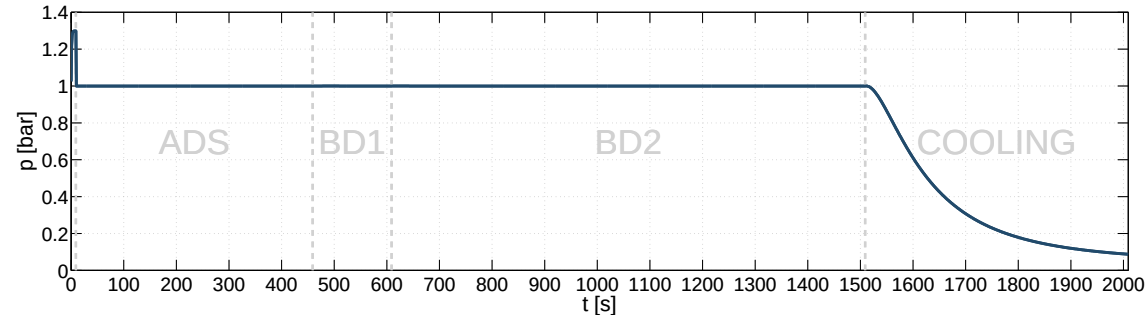

(b) Pressure profile in time

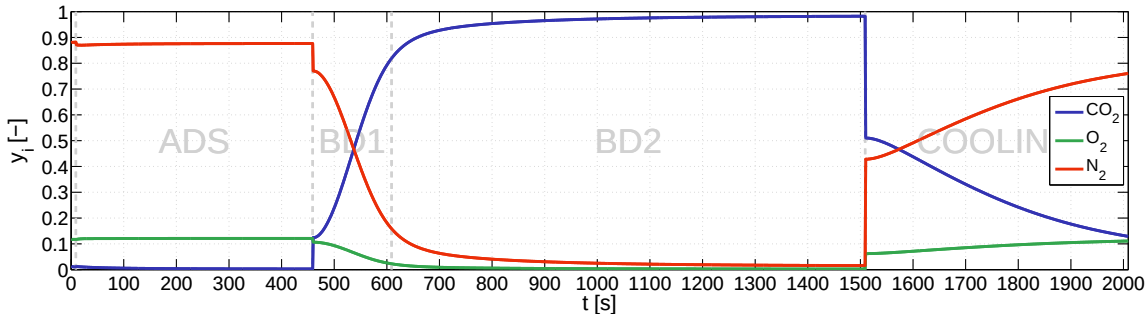

(c) Molar fraction profile in time

Figure 4.8: Fixed bed: example profiles in time for optimal 5-step cycle, referred to the outlet section of the column (top end for upward flow, bottom end for downward flow)

The adsorption step follows immediately after. During this stage the flue gas is first premixed with a recycle coming from the first blowdown, then fed continuously in the reactor. The product 1 coming out of the adsorption phase is the clean (read: CO_2-lean) flue gas which is later sent to the stack.

Following the adsorption, the heating phase begins. It is divided into two stages, which feature the same operational conditions of the column. The heat provided to the system sets off a countercurrent flow of the desorbed species out of the bottom end of the reactor, while the top end is shut. The first blowdown step is recirculated back into the adsorption unit, whereas the second forms the CO_2-rich recovered product that will be sent to storage.

The cooling stage is once again performed in shut-column configuration, allowing the bed to start adsorbing the gas left into the reactor at the end of the heating session (and therefore progressively reducing the pressure, which is then set back to the original level through the pressurization).

In Figure 4.8 example profiles of p, T and y_i in time for an operational point of this 5-step cycle are displayed. Strong similarities with the 4-step cycle profiles can be immediately observed, as well as the main difference: the heated desorption phase is divided into two units, instead of being performed in a single stage.

At first glance, the results yield by the preliminary simulations of this cycle show trends very similar to those of the basic 4-step one: This is anything but surprising, being the interconnections between the various units limited to a single recycled stream. The recirculation does not even imply any restriction in terms of duration of the steps, because a tank can be employed to gather the gas coming out of unit 3; the gas can than be progressively premixed with the feed, regulating the flow rates in such a way to obtain a constant composition at the column inlet during the adsorption phase.

As regards the performances, the preliminary simulations performed to give a first evaluation of the cycle potential let legitimately expect that results as good as the best obtained with other configuration may be reached in terms of recovery and purity rates; energy consumption and productivity levels look even more promising, as it appears to be worth reducing the total durations and opting for an overall simplification of the scheme. In this sense it could be questioned whether a single step blowdown might be enough in order to obtain similar results: if only a fraction of the stream were recycled into adsorption, only four steps would be needed to build the cycle. The answer is of course negative: an excessive reduction in purity rates would inevitably occur, due to the fact that the initial CO_2-lean blowdown product would be partially included in the recovered stream, increasing its final contents of O_2 and N_2 –which of course have to be assessed by integration of the flow rates along the whole step duration.

The recirculation of the first blowdown product is a key feature of this cycle: when varying the ratio between unit 3 and unit 4 durations, it offers the opportunity to opt for very high purities at the expenses of productivity, which is then limited by the short time frame of the second blowdown (and also of recovery, which is after a certain point necessarily compromised, when a very CO_2-rich stream is recycled into adsorption); otherwise productivity values can be favored, if unit 3 time span is reduced and a renounce in terms of purity is tolerated. Thanks to the low number of interconnections between the units (which cause always some kind of restriction), each step extent can be easily adapted, according to the conditions of the feed or aiming at different desired outputs.

In conclusion, the main features of this optimized 5-step cycle are on the one hand the flexibility, for a wide range of various targets may be reached by differently setting the phase durations, on the other hand the simplicity, as it consists of only five units, although it is structured enough to promise outstanding performances.

4.4 Process scheduling

An important phase in the design of an adsorption process using a sequence of fixed bed columns is to define a schedule according to which the real plant could operate.

In fact, the number of units which form a cycle configuration in general does not correspond to the number of real columns required to actually perform the process. As long as the previously displayed cycle configurations for TSA processes are concerned, any step sequence could be theoretically performed using only one single column; it should undergo in order all the stages that build up the cycle, gathering and storing the gases in tanks whenever a recirculation flows needs to be conveyed from the outlet of a step to the inlet of a later one (while this could not be done, instead, for the pressure equalization steps used in PSA cycles).

However, there are usually tight constraints and sensible considerations that prevent from adopting such a solution. The main restriction in this sense is, usually, that the flow of feed gas conveyed into the system cannot be interrupted and should instead be not only continuous, but also characterized by a constant flow rate. This implies two different requirements that should be met by the scheduling of the process and by the overall layout of the plant:

- first of all, the steps that take as inlet flow the feed should be performed continuously, which means that in every single moment the number of columns fed with the flue gas should be exactly the same;
- moreover, the number of columns simultaneously undergoing a feed stage should be large enough to provide on the whole the right cross section area required by the flue gas stream to flow, accordingly to the superficial velocity of the gas for which the columns have been designed.

Beside this constraint, which commonly represent a real limitation for almost all the applications of fixed bed for multi-step processes, many other bonds might be posed by the configuration of the cycle itself or by other requirements of the specific case:

- a product might be necessarily yielded with continuity, similarly to what happens with the feed –while it is more difficult to keep a constant flow rate for the products, because the proceeding of adsorption and desorption causes in general the flow rates to vary during the step;
- a recirculating stream might be operated without inserting a tank between the source and the destination unit; if no tank is employed, there is no other way to compensate the discontinuity of the source feed than programming the sequence in such a way that forces the same number of source and destination units to be always operated simultaneously;
- if pressure equalization is implemented, as already said, the pressurization and blowdown steps need to be matched in the time schedule in order to be physically connected one to the other;
- availability considerations or safety reasons might require more than one column to perform the same operation at the same time, in order to prevent the whole process to be arrested because of a malfunction or a failure.

Many and various approaches have been proposed to this issue. In literature a variety of analytical as well as graphical methods can be found to accomplish the target in the context of adsorption processes; some of them are rather basic and do not consider some cycle specifications which are actually quite likely to be found in real applications; some others are more refined and can be successfully employed even for very complex cycle schemes. Most of them, unsurprisingly, have been developed for PSA processes, which not only have been historically more common than TSA cycles, but feature on average a greater number of interconnection between the units, so that more restrictions are placed for the scheduling. All these approaches are based on the translation of the constraints into simple equations and inequalities, which eventually form a system, whose solution provides the number of columns required for the operation of the system and their organizing in terms of time.

According to what is suggested in literature [28, 29, 30], the scheduling of the fixed bed cycle is realized starting from the conversion into equations of the constraints. For this optimal 5-step configuration, the only active constraint is that the feed must be driven into the system with a constant flow rate (equal to that flowing off the power plant, $\dot{V}_{in}$) and at the inlet of every column a fixed volumetric flow rate $\dot{V}_{col}$ must be provided in order to mantain the conditions established by the cycle definition in terms of velocity of the as u. A shell and tube reactor contains N_{col} columns, so that the total flow rate that can be fed in a reactor is

$$\dot{V}_{st} = \dot{V}_{col}\, N_{col} \qquad \left[\frac{m^3}{s}\right] \tag{4.7}$$

The columns of a shell and tube vessel must of course all operate in the same stage. Therefore the minimum number of shell and tube reactors which must be entered by the feed simultaneously is given by

$$N_{st}^{feed} = \left\lceil \frac{\dot{V}_{in}}{\dot{V}_{st}} \right\rceil \tag{4.8}$$

The total duration of the feeding phase is given by the sum of the pressurization and of the adsorption steps

$$t_{feed} = t_{unit\,1} + t_{unit\,2} \qquad [s] \tag{4.9}$$

and it must be a integer multiple (J times) of the minimum time unit U that defines the scheduling

$$t_{feed} = J \cdot U \tag{4.10}$$

In fact, each U correspond to a shell and tube vessel. If in every train of vessels J reactors are simultaneously entered by the feed, the total number of trains of vessels needed is

$$N_{tr} = \frac{N_{st}^{feed}}{J} \tag{4.11}$$

The total number of vessels in a train, K, is thus equal to the minimum number of units U needed to cover the length of a whole cycle, i.e.

$$K = \left\lceil \frac{t_{cyc}}{U} \right\rceil \tag{4.12}$$

so that the total number of vessels required by the system is

$$N_{st} = K \cdot N_{tr} \tag{4.13}$$

Since K has to be an integer number,

$$t_{cyc} \leq K \cdot U \tag{4.14}$$

and therefore there can be a time lapse left in the cycle. This time lapse is called 'idle time' t_{idle} and can be positioned anywhere between to cycle steps –also divided between more step couples–, except from the first two steps, which form the feeding stage that cannot be interrupted. Of course t_{idle} is equal to

$$t_{idle} = K \cdot U - t_{cyc} \qquad [s] \tag{4.15}$$

and its extent depends on how close K is to the real ratio between t_{cyc} and U. This procedure defines in the end a new operative duration of the cycle, which is

$$t_{cyc}^{new} = t_{cyc} + t_{idle} \qquad [s] \tag{4.16}$$

and therefore a new productivity value can be computed as

$$\text{Productivity}^{new} = \text{Productivity}\frac{t_{cyc}}{t_{cyc}^{new}} \qquad \left[\frac{kg_{CO_2}}{kg_{ads}\, h}\right] \tag{4.17}$$

The parameter J, which correspond to the number of vessels within a train that are simultaneously fed with the flue gas, can vary from a minimum value of 1 (which implies N_{tr}=N_{st}^{feed}) to a maximum value equal to N_{st}^{feed}, beyond which the flow rate of gas inside each vessel would be lower than the required $\dot{V}_{st}$. Figures 4.9a, 4.9b and 4.9c outline the behavior of the idle time t_{idle}, of the total number of vessel N_{st} and of the adjusted productivity for increasing values of the parameter J.

Looking at the idle time, of course it can only decrease for higher values of J, because U becomes shorter; the cycle duration can be then approximated with a smaller error (and this error is the idle time) if it is fitted with a larger number of smaller time units. In the plot both axes are logarithmic, which means after a certain point the idle times are almost insignificant.

As regards the adjusted value of the productivity, it is strictly correlated to the idle time, as it can be inferred from the expression reported above. As soon as the idle times are small enough, their negative effect on the productivity becomes secondary. As a matter of fact, the points in the graphs are almost aligned after a certain J value.

The total number of vessels plot shows a series of points groups; each of them corresponds to a certain number of trains. The number of trains is almost inversely proportional to the parameter and the number of column fed with the flue gas should always be nearly constant, being the product of N_{st} times J, except from the rounding due to the discrete variables. For higher values of the parameter, though, the number of trains becomes small

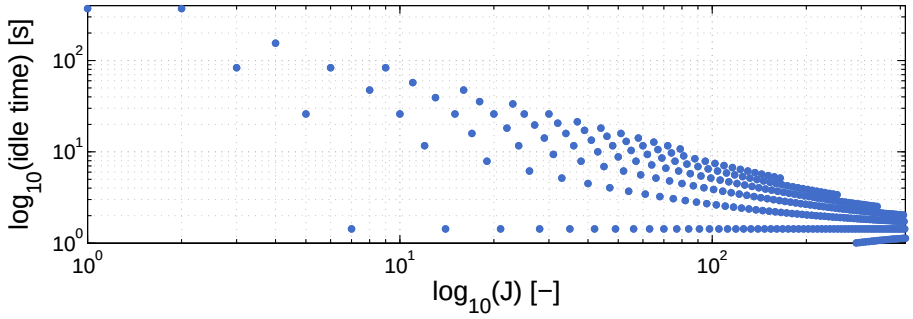

(a) Idle time

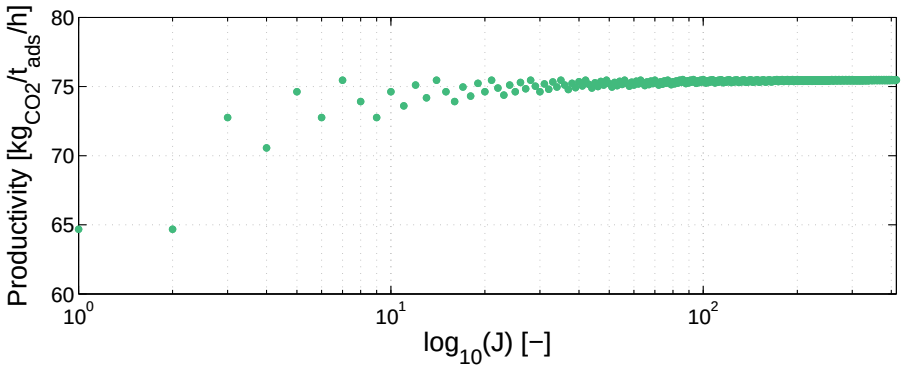

(b) Adjusted productivity

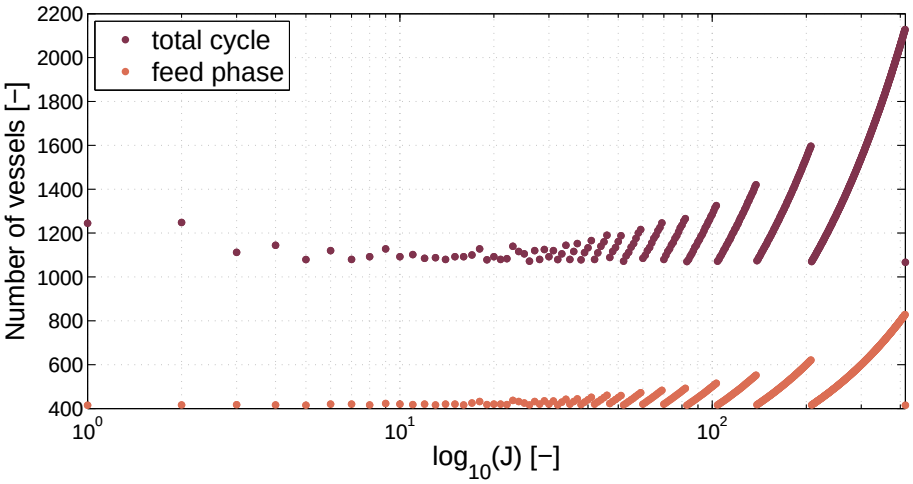

(c) Number of vessels

Figure 4.9: Fixed bed: profiles of scheduling variables

and the total number of columns increases when the approximation of the discrete variable N_{tr} is unrefined. Therefore out of all the points displayed only the one in which the number of fed vessels N_{st}^{feed} is close to the minimum can be adopted; for all the others the flow rate of gas inside the single vessels is too low and the requirements about the desired velocity of gas are not met.

Chapter 5

Results

This chapter is intended to report the main results obtained simulating TSA processes to capture CO_2 out of the flue gas coming from the power plant of an integrated steel mill. Both the two reference cases presented in Chapter 1 are analyzed, arranging a parallelism between fixed bed and circulating fluidized bed simulations. All in all, four simulation series are therefore performed.

5.1 CFB: simulations

Simulations of the CFB system have been performed varying eight of the parameters which are taken as input by the model, namely:

- temperature in the isothermally operated adsorption riser
- temperature in the isothermally operated regeneration riser
- mass of regenerated sorbent fed in the adsorption riser
- inventory in the adsorption riser
- inventory in the regeneration riser
- superficial velocity of gas at adsorption riser inlet
- superficial velocity of gas at regeneration riser inlet
- flow rate of gas at regeneration riser inlet

All of them may be varied independently, so that the incidence of any single parameter can be analyse separately. For each technology the results are first presented for one scenario, then the other situation is discussed by highlighting differences to the first case.

5.1.1 Combined cycle case

The number of different operational points that are investigated is restricted, due to the quite long duration of a single process simulation (up to about 30 minutes). About 150 simulations are performed for each of the two different reference scenarios that have been adopted for this work.

Overview of the results

To start the assessment of the analysis outputs two graphs are presented at the beginning of the dissertation of each series of simulations. They display how the performances of the simulated processes stand in the two diagrams which are chosen to represent the results and that have already been mentioned in the Introduction. Of course, process performance indexes refer to the component whose removal is the main goal of the process (i.e. CO_2).

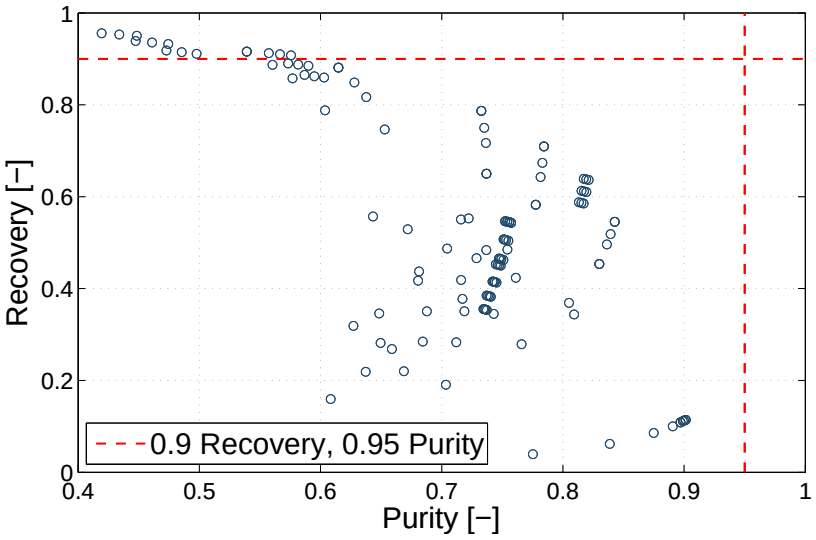

Figure 5.1: CFB, combined cycle: 'recovery–purity' diagram

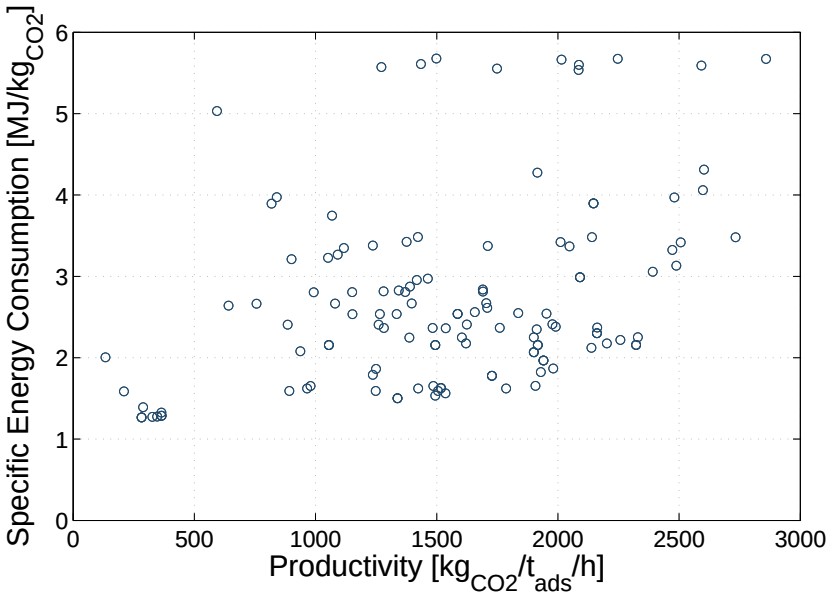

Figure 5.2: CFB, combined cycle: 'specific energy consumption–productivity' diagram

As shown by Figure 5.1, only a few points reach high recovery rates, while most of them stand within a 80% threshold. Purity are in most cases over 60% (only very high mass of sorbent cause them to be lower, as later explained), but do not show any peak up to very high levels.

Productivities are for CFB technology always very high (Figure 5.2), thanks to the fact that the continuous looping of the solids reduces the total amount of solid material necessary to adsorb the target amount of CO_2. In fact the solids inside the system are almost always undergoing either an adsorption or a desorption process and they get through only very short dead times.

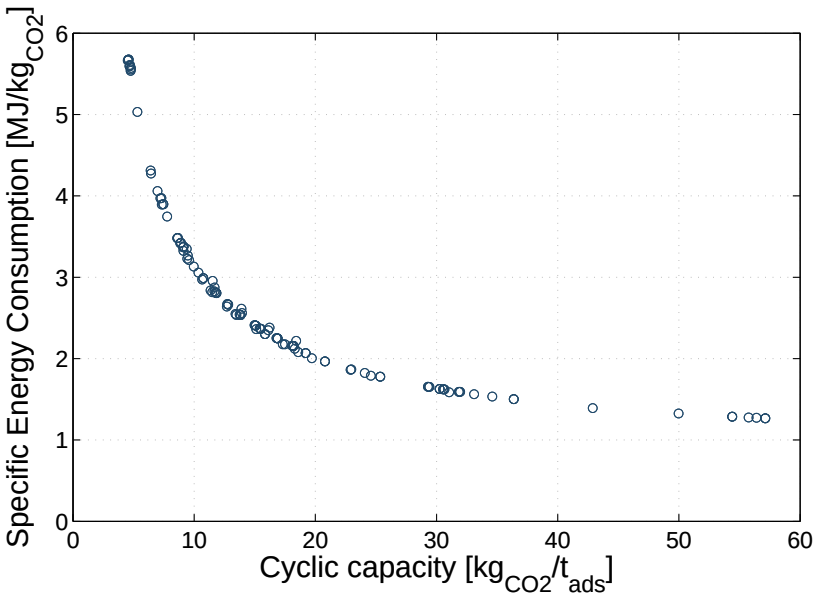

Figure 5.3: CFB, combined cycle: 'specific energy consumption–CO_2 cyclic capacity' diagram

Cyclic capacities are somewhat limited by the CO_2 content of the flue gas (Figure 5.3). They are to be compared with the equilibrium adsorbed amount at adsorption (concentration in the flue gas, ambient pressure) and regeneration conditions (i.e. hypothesized 90% molar fraction of CO_2, ambient pressure), namely around 155 and 80 kilograms of CO_2 per ton of adsorbent (3.5 and 1.8 moles per kg) respectively, which suggest the maximum possible cyclic capacity to be approximately equal to 75 kilograms per ton of adsorbent (1.7 moles per kg). This value highlights a first feature of the CFB systems: the cyclic capacities are always rather low, owing to the hindrance to regeneration represented by a high CO_2 concentration at ambient pressure.

The results here shown refer to a standard configuration of the heat exchanging system, according to which part of the sensible heat of solid is recovered from the hot-regenerated solid flow and sent to the cold-loaded one. The input data for this standard case are reported in Table 5.1.

Table 5.1: CFB, standard configuration of the heating exchanging system: data

Temperature of flue gas at adsorber inlet	20°C
ΔT at cold side of the heat exchange between solid flows (minimum ΔT)	20°C
Heat exchange efficiency	1.0
Addiotional wingwalls	yes

The ‘recovery–purity’ diagram

If the ‘recovery-purity’ diagram is considered, it is possible to straightforwardly observe some major trends among all the points depending on some parameters, namely

- temperature in the isothermally operated regeneration riser
- mass of regenerated sorbent fed in the adsorption riser
- flow rate of gas at regeneration riser inlet

While the other parameters seem to affect the results only by moving them towards slightly lower or slightly higher recovery or purity rates, these three quantities show to have a stronger influence on the final performances, since they allow to identify quite clearly some finite regions on the ‘recovery-purity’ diagram depending on the value they hold.

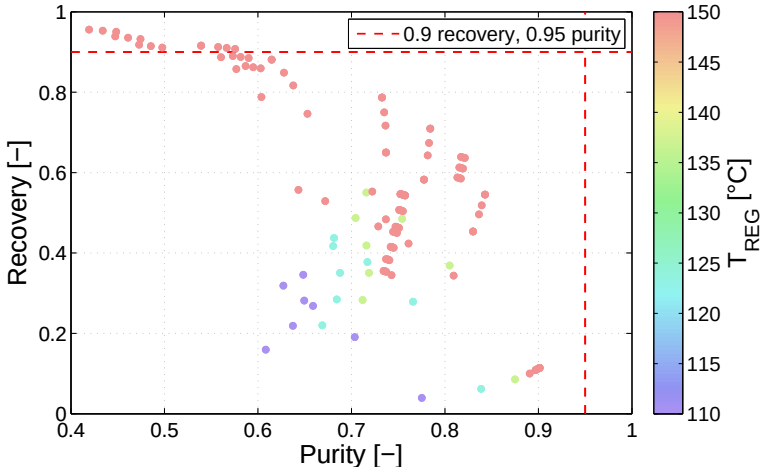

Figure 5.4: CFB, combined cycle: ‘recovery-purity-regeneration temperature’ diagram

As far as the desorption temperature is concerned, its increase drives towards higher purity and recovery rates (Figure 5.4). Its influence is great over the cyclic capacity, because the higher the regeration temperature is, the lower the associated isotherm gets, so that the bed is regenerated more in depth (Figure 5.5).

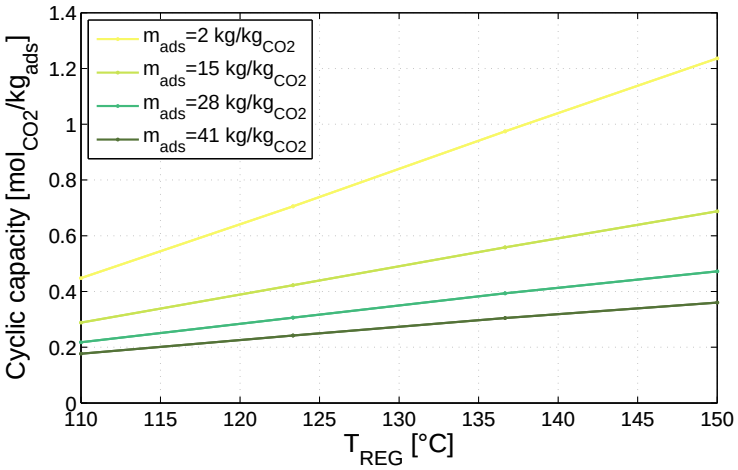

Figure 5.5: CFB, combined cycle: cyclic capacity as function of regeneration temperature

Among the eight parameters, the mass of sorbent fed in the adsorber shows the strongest influence on performances. If a higher flow rate of sorbent flows through the riser, the total amount of CO_2 that can be captured out of the flue gas increases proportionally, while the average residence time of particles decreases, the inventory being equal; the total cyclic capacity is stricly related to the residence time of particles and follows the same trend (see Figure 5.6b and Figure 5.6c).

However recovery tends to rise together with this parameter, as shown by Figures 5.6a and 5.7. This is due to the fact that increasing $\dot{m}_{ads}$ causes indeed a loss of cyclic capacity, but it is overcompensated by the greater amount of material available for adsorption. Purity is affected negatively instead for higher sorbent flow rates; in fact oxygen and nitrogen are the first species to be desorbed during the regeneration, and even if the cyclic capacity decreases significantly for CO_2, it does not for O_2 and N_2; their molar fractions are consequently higher in the regeneration phase, causing the purity to drop (Figure 5.6a).

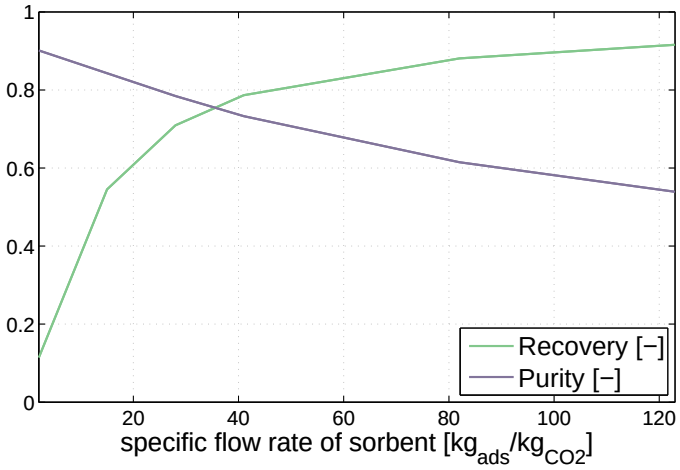

(a) Recovery and purity

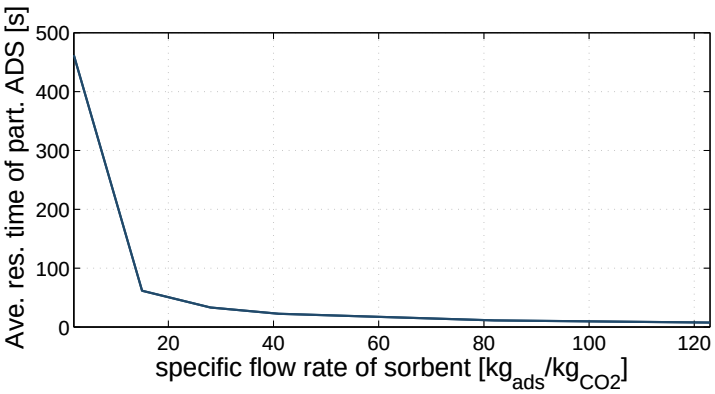

(b) Average residence time of solids in the adsorber

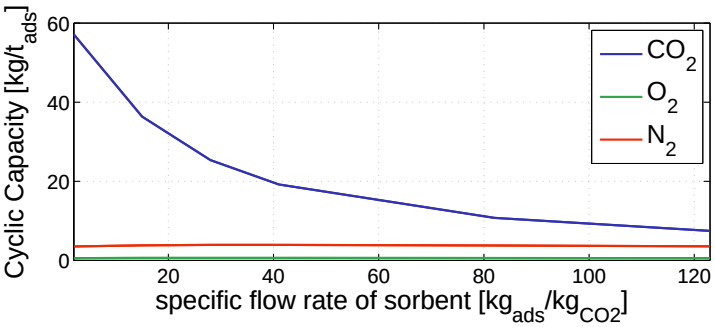

(c) Cyclic capacities

Figure 5.6: CFB, combined cycle: incidence of sorbent flow rate

It can be arbitrarily set how much gas is recycled from regeneration outlet into regeneration inlet to fluidize the bed. As the amount of recycled gas increases, a wider cross section is necessary at the regenerator to allow the stream to flow inside the riser at the fixed initial superficial velocity. At the same time the total inventory rises (for in the simulations the inventory value is always defined per cross section unit) together with the average residence time of particles. As a consequence, both recovery and purity appear to be enhanced by higher gas flow rates in the regenerator (Figures 5.8 and 5.9).

All other parameters affect performances to a secondary extent, so that their variation produces a higher concentration of points in the central part of the 'recovery-purity' diagram. Their variation produces expected consequences: lower velocities and higher inventories stretch the average residence times, so that the processes (adsorption or desorption)

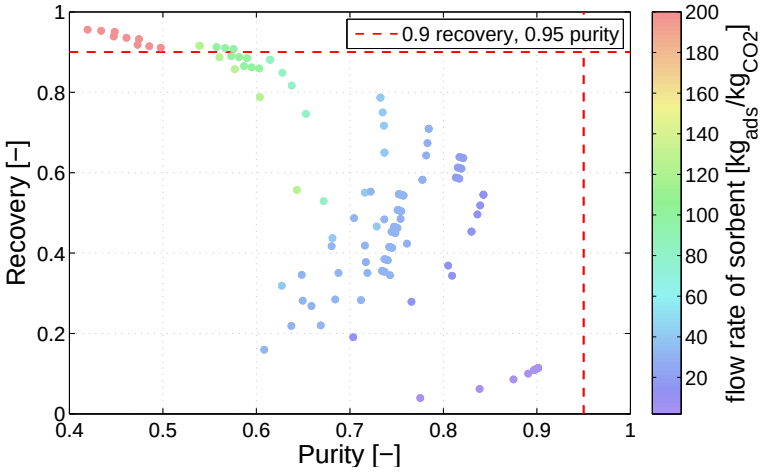

Figure 5.7: CFB, combined cycle: 'recovery-purity-sorbent mass' diagram

proceed further on (and lower velocities also increase inventories in the simulations because they cause cross section to be wider, as already explained); a lower adsorption temperature promotes the adsorption process, given its exothermic nature, but the present analysis is not going to be highly focused on this parameter, given the obvious difficulties connected to a variation of this temperature outside a certain range (over 40°C the performances are inevitably too compromised, whereas under 30°C major issues with the cooling system occur).

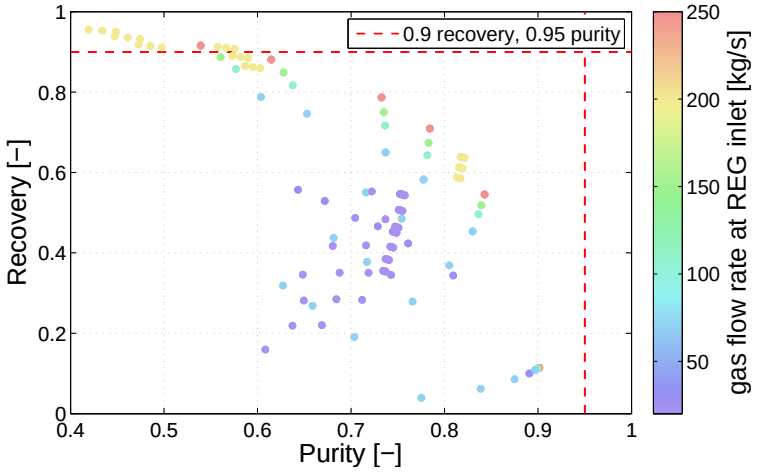

Figure 5.8: CFB, combined cycle: 'recovery-purity-regeneration gas flow rate' diagram

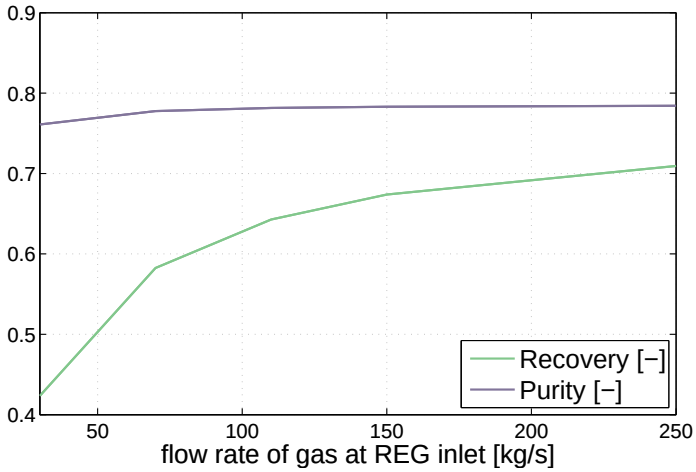

Figure 5.9: CFB, combined cycle: recovery and purity as functions of the flow rate of gas at regenerator inlet

The 'specific energy consumption–productivity' diagram

As regards the energy consumption and the productivity, the only parameter which shows a noticeable effects in terms of identifiying regions in the diagram is once again the flow rate of solid sorbent. Unsurprisingly, for lower adsorbent flowrates higher productivities can be reached, as the cyclic capacity grows thanks to longer mean residence time for solid particles. At the same time the total energy consumption –a great fraction of which is due to the heating of solids before the regenerator– becomes worse (Figures 5.10 and 5.11).

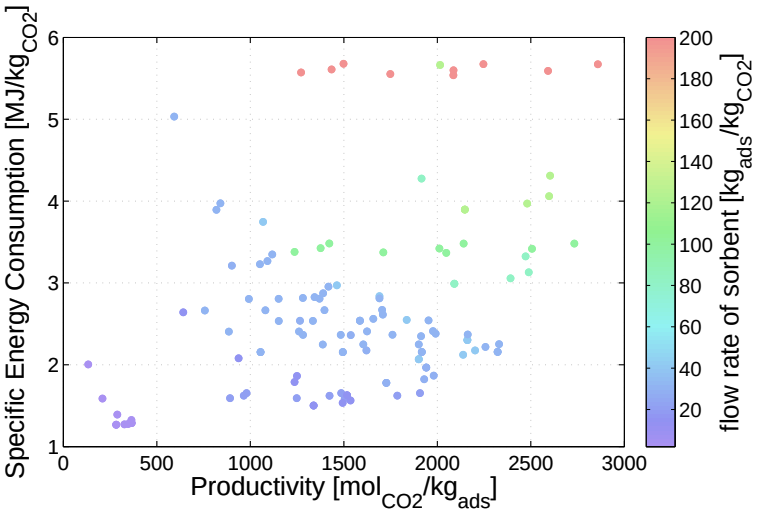

Figure 5.10: CFB, combined cycle: 'specific energy consumption–productivity' diagram

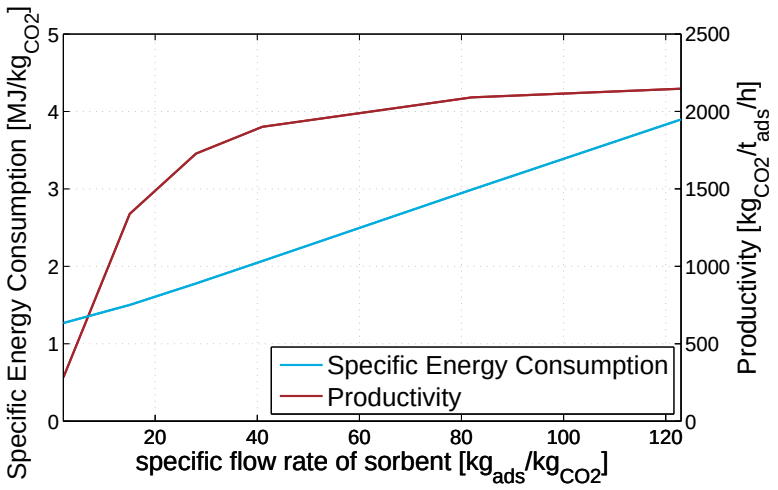

Figure 5.11: CFB, combined cycle: productivity and specific energy consumption as functions of the specific flow rate of sorbent

5.1.2 Operational issues

All the simulations whose results are here shown have been conducted assuming that the risers could operate according to the specified input data. However, many of them actually

represent unrealistic operational condition under the assumptions employed for the model, as is going to be explained here.

First issue: surface availability for heat exchange

Out of all the points shown in the previous plot, only few manage to stay within the feasibility limits (ratio<1), when the ratio between required and available surfaces for heat exchange is taken into account. Figure 5.12 shows how problematic is this issue for both the adsorption and the desorption riser. Moreover it has to be remarked that the few feasible operational settings correspond to very low recovery values and are therefore practically of no interest. By comparison with Figure 5.7 it can be also inferred that sorbent flow rates are mainly responsible for the feasibility of the heat exchange: higher sorbent flow rates make thermal capacity of the solid stream bigger, which means a greater amount of energy has to be provided to the regenerator for the heating of solids in order to keep the temperature at the desired value, as well as in the adsorber a higher thermal power has to be transferred out of the reactor (being all temperature levels set constant).

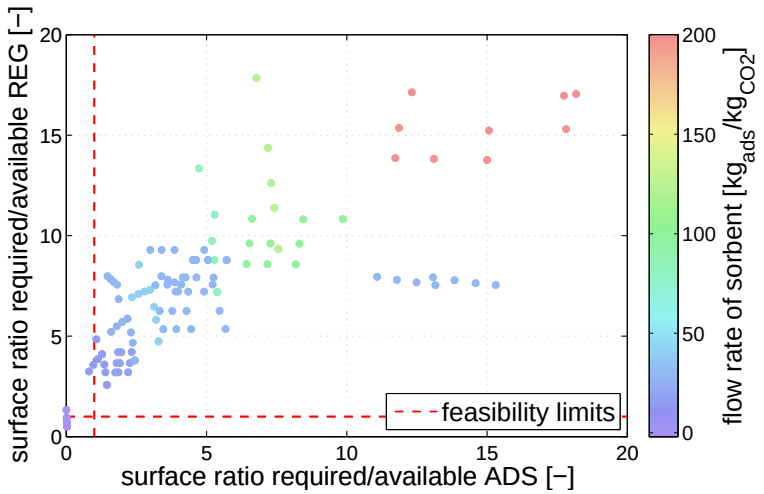

Figure 5.12: CFB, combined cycle: available surface ratio for adsorber and regenerator

Taking into account the variation of the two parameters whose variation appears to be most affecting –flow rate of gas at regenerator inlet and mass of sorbent–, it can be shown how only very low mass of sorbents allow to operate the process transferring heat only through the available surfaces (Figure 5.12). Higher flow rates of gas in the regenerator improve the situation for the regeneration outlet (because they go together with wider cross section, i.e. larger surfaces), but increase the inventory promoting the regeneration, so that also the total amount of heat released by adsorption ends to be greater and the situation in the adsorber becomes more critical (Figures **??** and 5.13). The feasible operating conditions, as already said, correspond anyhow to high purity rates, yet very low recovery performance (Figure 5.14). If a variation of superficial velocity is considered, two counteracting effects can be observed (here the adsorber case is presented as an example): decreasing the velocity the cross section necessarily increases, and therefore the total surface available for heat exchange increases proportionally; at the same time the average residence time of particle rises, so that the process can proceed further on, which means a greater amount of heat is released by adsorption and has to be removed; moreover, for higher velocities the Reynolds number and the length-diameter ratio rise, enhancing the convective heat transfer coefficient between the suspension and the

wall. The two effects are counteracting, which means that at a certain point a maximum value of the ratio between the surface available in the adsorber and the available one can be found depending on the superficial velocity (Figure 5.16).

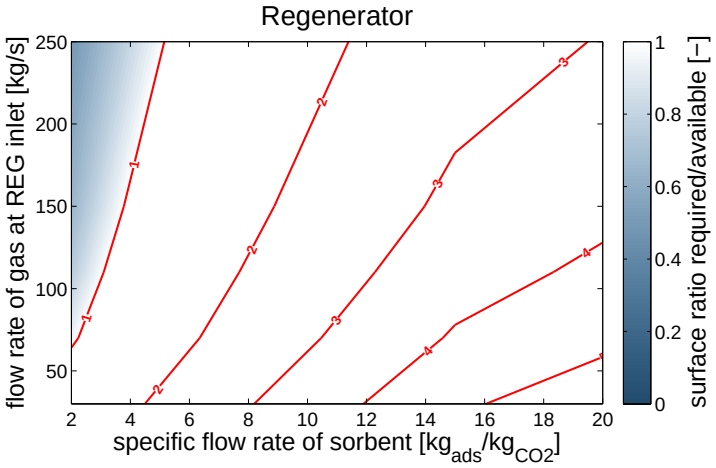

Figure 5.13: CFB, combined cycle: 'gas flow rate at regenerator–sorbent flow rate–available surface ratio' diagram for regeneration

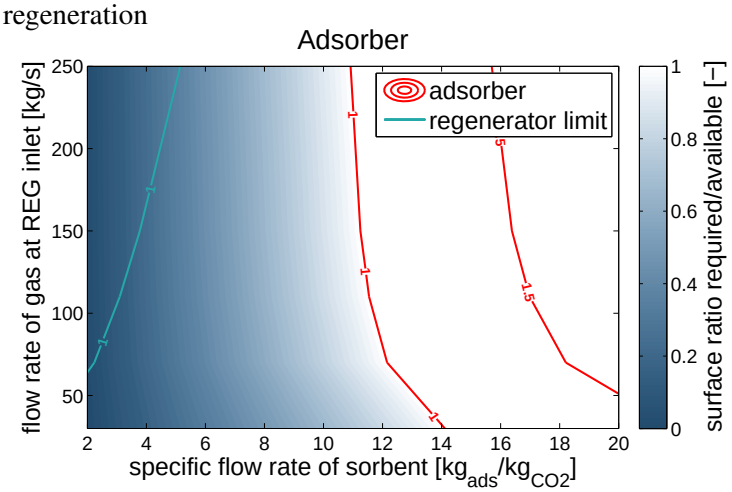

Figure 5.14: CFB, combined cycle: 'gas flow rate at regenerator–sorbent flow rate–available surface ratio' diagram for adsorption

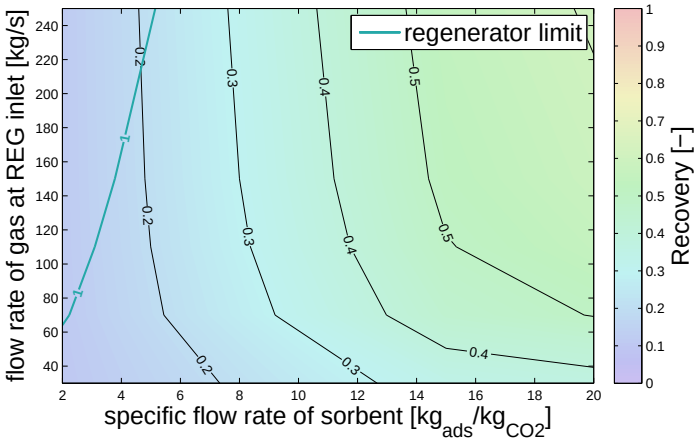

Figure 5.15: CFB, combined cycle: 'gas flow rate at regenerator–sorbent flow rate–recovery' diagram

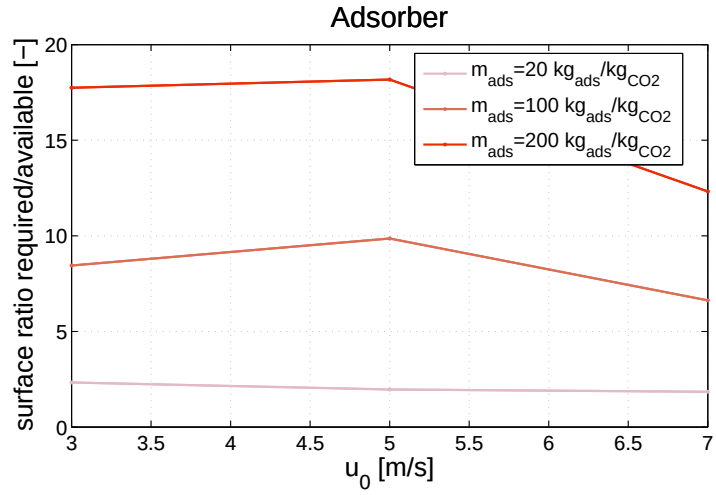

(a) Available surface ratio

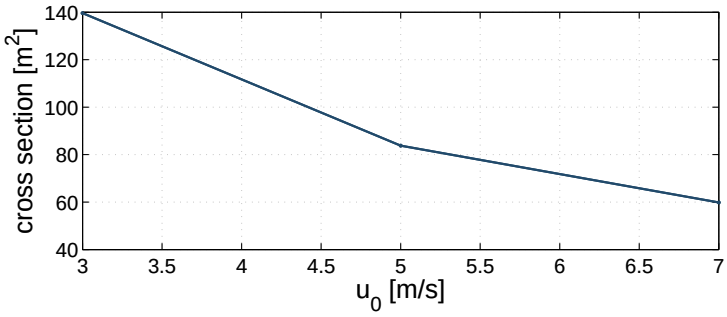

(b) Cross section

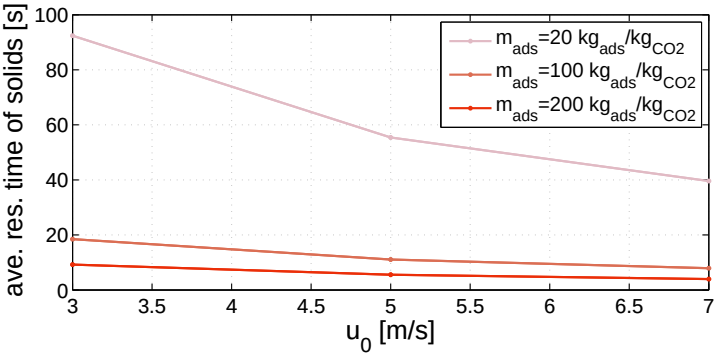

(c) Average residence time of particles

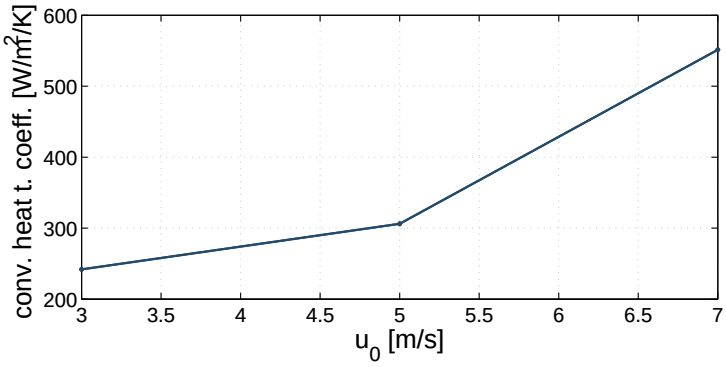

(d) Convective suspension–wall heat transfer coefficient

Figure 5.16: CFB, combined cycle: incidence of superficial velocity in the adsorber

Second issue: thermal power exchanged with the heating and cooling streams

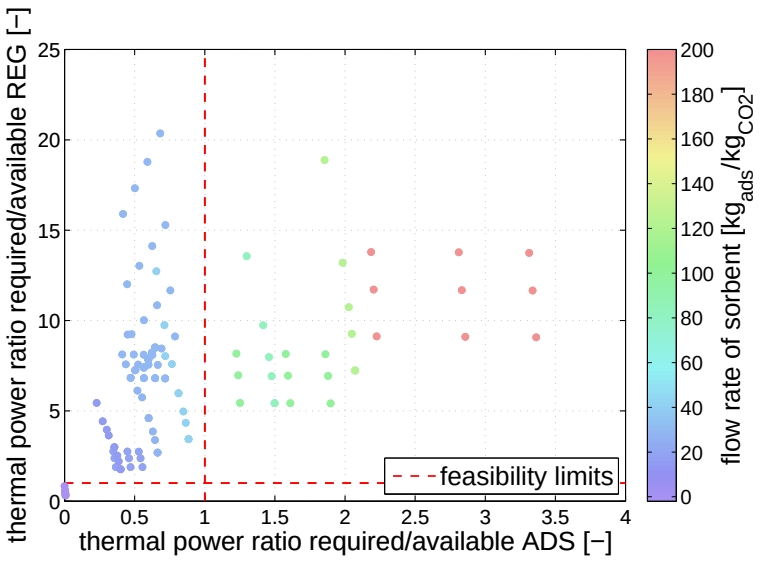

Figure 5.17: CFB, combined cycle: thermal power ratio for adsorption and regeneration

Once the number and the cross section of tubes which forms the water-walls is fixed, the flow rate of water or steam depends only from the speed they are flowing at inside the ducts. The enthalpy variation undergone by the stream depends on the ΔT and on the average temperature for the water and on the condensation temperature for the condensing steam. Once the flow rate and these temperatures are determined, the maximum amount of heat that the flow can exchange can be calculated. The model works as if all the $Q_{provided}$ or $Q_{removed}$ as established by the energy balances is transferred, but in reality the heating/cooling system might no be able to exchange that amount of heat (here defined as 'required'). As a matter of fact, in very few cases the heating/cooling systems appears to be adequate (Figure 5.17).

The flow rate of water cooling down the adsorber may struggle to remove as much heat as necessary, as shown in Figure **??**. In this case an increase in ΔT or in speed can help, but both might be rather difficult to extend over a certain value. For the example case here reported, where the adsorber operates at 40°C, the cooling system is characterized by an average water temperature of 19°C and a ΔT of 8°C, according to the data reported in Section 3.4.

For the heating of the regenerator the amount of heat that can be provided by the condensing steam stream appears to be even more scarce (Figure 5.18), when compared to the quantity required by the process. A higher temperature of the steam flow would help reducing the required/available ratio for the heat exchange surface (i.e. the first operational issue), but would also reduce the enthalpy difference Δh_{lv} between the saturated vapour and the saturated liquid, reducing the total amount of heat that the stream can release. Once again higher velocities help raising the flow rate, but likely the latent heat associated with the change in phase is almost never enough to provide the desired amount of energy; therefore the steam should be fed into the system when it is still supersaturated and cooled before the condensation; the subcooling of the condensed phase might be exploited as well.

Although this limitation is restricting the range of feasible operational conditions to a somewhat narrow interval, it has however to be remarked that for the adsorber this issue is less limiting than the one related to the heat exchange surfaces, while for the regenerator they are almost equally restrictive.

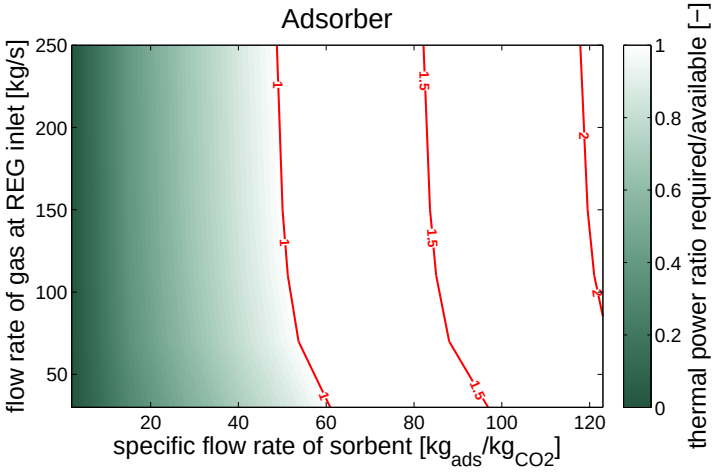

Figure 5.18: CFB, combined cycle: limited thermal capacity of the cooling fluid

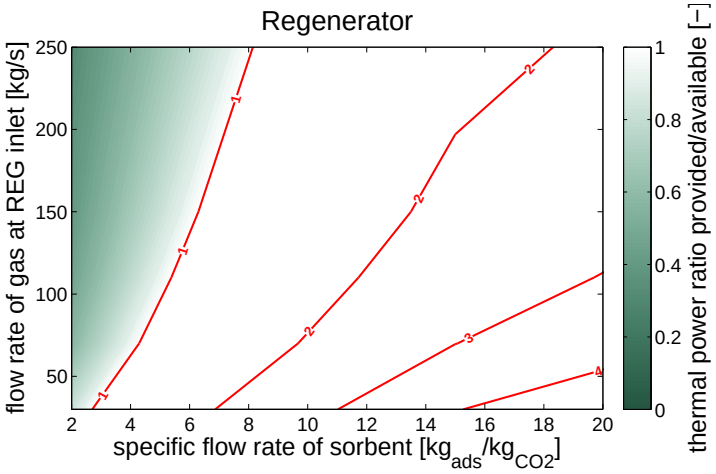

Figure 5.19: CFB, combined cycle: limited thermal capacity of the heating fluid

Third issue: amount of solid entrained by gasses at riser outlet

As previously observed, huge quantities of fresh sorbent must be fed to the adsorber to obtain good recovery rates. However, the circulation of solids is strictly bound to the amount of matter that gases are actually able to convey out of the risers. Low superficial velocities and, to a much smaller extent, small inventories participate in restrict-

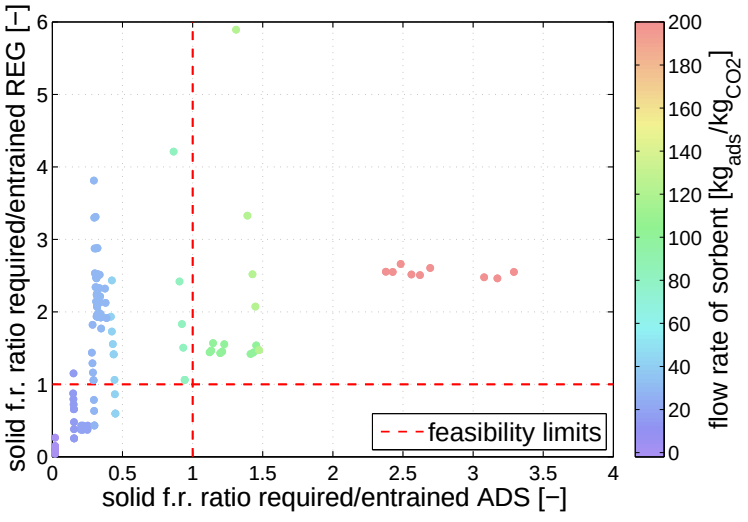

Figure 5.20: CFB, combined cycle: solid flow rate ratio for adsorption and regeneration

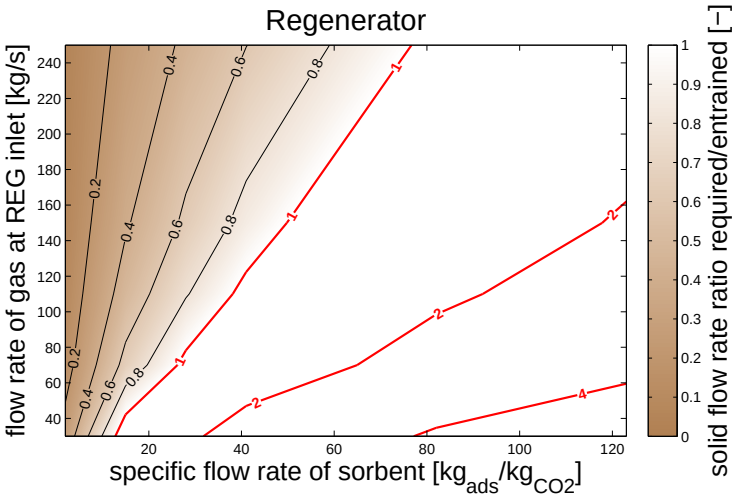

Figure 5.21: CFB, combined cycle: 'gas flow rate at regenerator–sorbent flow rate–solid flow rate ratio' diagram for regeneration

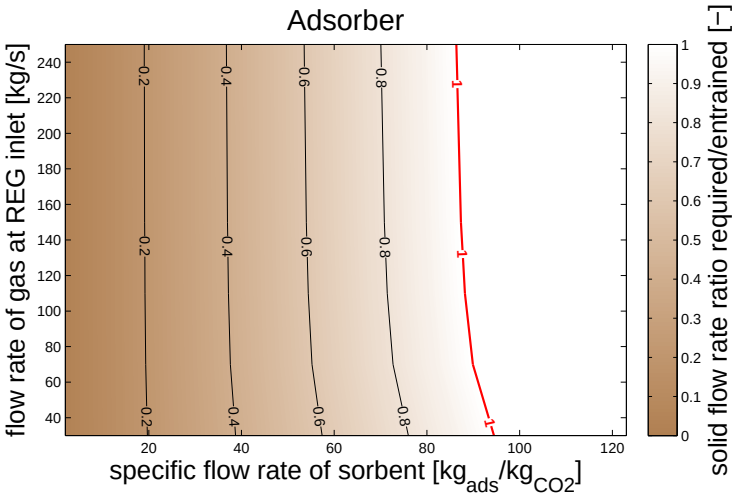

Figure 5.22: CFB, combined cycle: 'gas flow rate at regenerator–sorbent flow rate–solid flow rate ratio' diagram for adsorption

ing the maximum amount of solids entrained by the gases. If entrainment is to be assumed as the only mechanism for solid displacement, this could mean that the gas flow cannot carry out enough particles to match the desired flow rate of sorbent. During the simulation of the system, this limitation is neglected, and the 'required' flow rate of sorbent is always provided at riser inlet and assumed as entrained at riser outlet (otherwise the steady state hypothesis would not be verified, because the inventory would constantly increase).

Figure 5.20 shows how many cases are no strangers to this issue: although for the regeneration a solution could be found, since a higher gas flow rate can entrain a greater amount of solids (Figure 5.21, superficial velocity equal to 5 m/s) and that is a parameter which may arbitrarily set, the flue gas flow rate is fixed for the adsorber and it could be more difficult

to work out an expedient. It may be interesting to remark how the gas flow rate at regenerator also affect the recirculation rate in the adsorber: the higher the flow rate, the greater the inventory in the regenerator riser, the further regeneration process (and consequently adsorption) proceeds, the more moles of CO_2 are adsorbed, the smaller amount of gas flows out of the adsorber, entraining less solid matter (Figure 5.22, superficial velocity equal to 6 m/s).

As shown in the diagrams, this appears to be anyhow the less limiting and the easiest solvable out of the three issues here reported. The variation of the gas flow rate in the regenerator offers some improvement possibilities, without compromising other performances; moreover, in case of need some other solid displacement mechanisms might be taken into consideration in order to allow the desired amount of sorbent to circulate between the two reactors, extracting the solids from the lower part of the vessel.

Further discussion of the issues

As regards the three presented issues, the one related to the entrained flow rate of solids seems to be secondary compared to the ones which concern heat transfer at riser walls. The issues regarding the availability of surface for heat exchange and the thermal power handled by the heating and cooling fluids have many common causes: they are both mainly due to the limited extensions of the waterwalls, to the reduced temperature difference that work as driving force for heat transfer and to the huge sensible heat associated with the flows of solids (and of gases, to a minor degree).

Since the issue related to heat exchange surfaces appears to define the most restricting boundaries, it would be here considered as assessment parameter to evaluate how effective might be any modification of the process aiming at extending the range of feasible operational conditions.

In particular, it might be interesting to evaluate how the situation can improve by varying some boundary conditions under which the two risers are assumed to operate. Since major constraints limit the conditions under which heat is transferred in or out of the risers (in other words, it would be difficult either to provide higher surfaces, enhance the transfer coefficients or increase the temperature differences that work as driving forces), a reduction of the thermal power that has to be conveyed through the walls can be imagined, by means of:

- a lower temperature of the flue gas at the adsorber inlet might be considered, since the flue gas enters the process after a complete drying which would anyway cause temperature to be reduced to a certain level (even to 0°C, if drying is applied by means of mere cooling). This would reduce the thermal power that has to be removed from the adsorber;
- a higher fraction of heat could be assumed to be recovered from the hot solids directed to the and conveyed into the cold solid stream directed to the regenerator. As the efficiency of the heat exchange is already conjectured as equal to 1 in the standard case above discussed, this may only be done by hypothesizing a broadened temperature drop undergone by the hot stream. The consequences of such a modification would

positively affect both reactors;

- in a similar way, further heating or cooling of the solid streams would at least partially free the risers from the duty of canceling the temperature gap between the streams and the bed within the risers.

First of all, a reduction of the flue gas temperature is considered (Table 5.2).

Table 5.2: CFB, combined cycle: effect of a reduction in flue gas temperature

Temperature of flue gas at adsorber inlet	15°C
ΔT at cold side of the heat exchange between solid flows (minimum ΔT)	20°C
Heat exchange efficiency	1.0
Addiotional wingwalls	yes
Additional external cooling of hot solid stream	0°C

This modification is somewhat always almost ineffective, given the limited amount of sensible heat associated with the gas (compared to the huge one associated with the solids) and the fact that it can produce no positive effect for the regeneration reactor. As it can be estimated from Figure 5.23, the situation does not improve significantly by this means. For few cases, in which the surface was already allowing the desired heat exchange, this modification would produce the need of providing some thermal power to the adsorber; they however correspond to very low, almost ineffective solid flow rates.

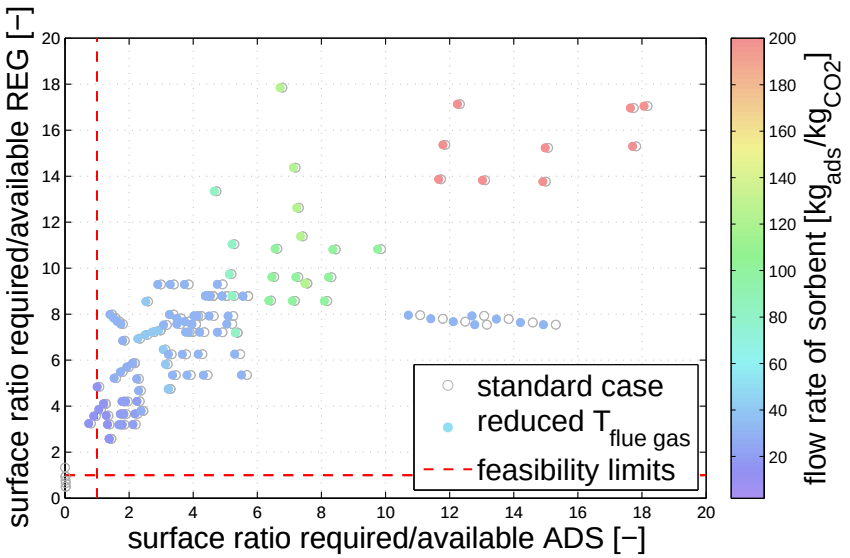

Figure 5.23: CFB, combined cycle: reduction in flue gas temperature

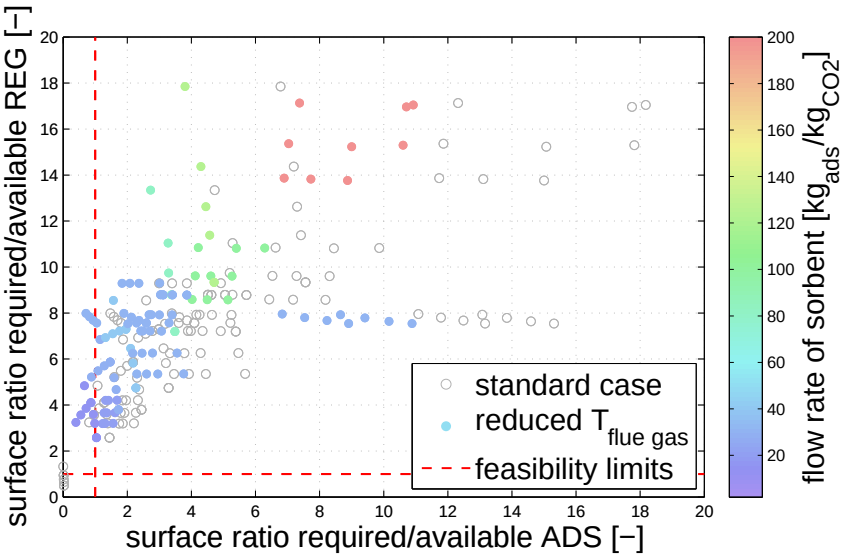

Figure 5.24: CFB, combined cycle: effect of reductions in flue gas temperature and regenerated solids temperature

Table 5.3: CFB, combined cycle: additional cooling of regenerated solids

Temperature of flue gas at adsorber inlet	15°C
ΔT at cold side of the heat exchange between solid flows (minimum ΔT)	20°C
Heat exchange efficiency	1.0
Addiotional wingwalls	yes
Additional external cooling of hot solid stream	10°C

On top of this expedient, if an additional decrease of 10°C in regenerated solids temperature via some external cooling stream were provided (Table 5.3), a significant additional improvement in the adsorber operating conditions would be achieved, as represented in Figure 5.24. The effectiveness of such a measure is to be justified once again with the considerable amount of sensible heat associated with solids, given their huge flow rate, rather than their anyway low temperature level. The extent to which the required surface is reduced is of course directly proportional to the flow rate of solid sorbent, as it can also be estimated from the graphics; it accounts for about the 30% of the total amount of power that has to be removed from the adsorber.

It could be otherwise imagined that this 10°C reduction at the cold end of the heat exchange between the two solid streams were operated by the heat exchange itself instead, so that a greater fraction of the sensible heat owned by the hot solids is conveyed into the cold stream (Table 5.4)

In this case also the regenerator would benefit from this condition, and like in the previous case the improvement would be significant, given what has already been said about the role

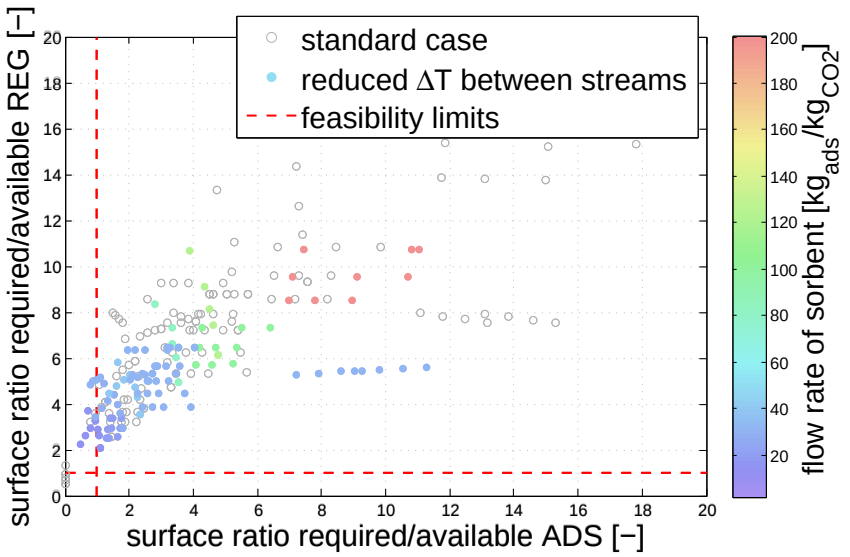

Figure 5.25: CFB, combined cycle: effect of a reduction in temperature difference between the two solid streams

Table 5.4: CFB, combined cycle: reduction of temperature difference between solid streams

Temperature of flue gas at adsorber inlet	20°C
ΔT at cold side of the heat exchange between solid streams (minimum ΔT)	10°C
Heat exchange efficiency	1.0
Additional wingwalls	yes
Additional external cooling of hot solid stream	0°C

of solids. Nevertheless, still the available surface would be insufficient both on the adsorber and on the regenerator side in the vast majority of cases (Figure 5.25).

Furthermore, in order to be thorough, it is important to briefly suggest a few other possible options which would allow to improve the heat transfer inside the bed, both outward to the cooling water and inward from the heating steam:

- first of all, adopting unusual values of the vessel aspect ratio (out of the range commonly suggested for circulating fluidized beds), a new riser design can be found to increase the total surface available for heat exchange;
- a second option is that of performing adsorption in a different fluidization regime, that of bubbling fluidized beds; thanks to the lower velocities of the suspension within the riser, in fact, bubbling fluidization allows installing additional heat exchange walls inside the dense zone of the bed, where most of the heat has to be transferred, with fewer corrosion issues.

These two possibilities are not discussed further in details, as they would require remarkable modifications to be implemented in the simulation code and are therefore not tested in this study.

Solids sensible heat recovery

In conclusion, a sizeable fraction of the total energy provided to the system is conveyed into the sensible heat of the during their path through the regenerator; this share becomes greater and greater as the flow rate of solid sorbent $\dot{m}_{ads}$ increases. As a matter of fact the cyclic capacity decreases if more sorbent flows in and out of the riser, because the average residence time of particles is reduced. Therefore to the same amount of captured CO_2 corresponds a larger amount of solids that has to be brought to the riser temperature and stores this energy as sensible heat, while the consumption terms related to the desorption reaction are only slightly affected by the lower adsorbed amount of CO_2. A certain value is though inevitably needed if suitable recovery rates are to be achieved.

The process itself would end up being too wasteful if this energy stored in the solid were not even partially recovered, as shown in Figure 5.26 and in the Sankey diagram (Figure 5.27, drawn to provide an example of the energy balance at the regenerator for a standard case cycle, whose data are reported in Table 5.5). In the figure, the best case scenario is represented as well: if the solid streams entered the riser already at the regeneration tem-

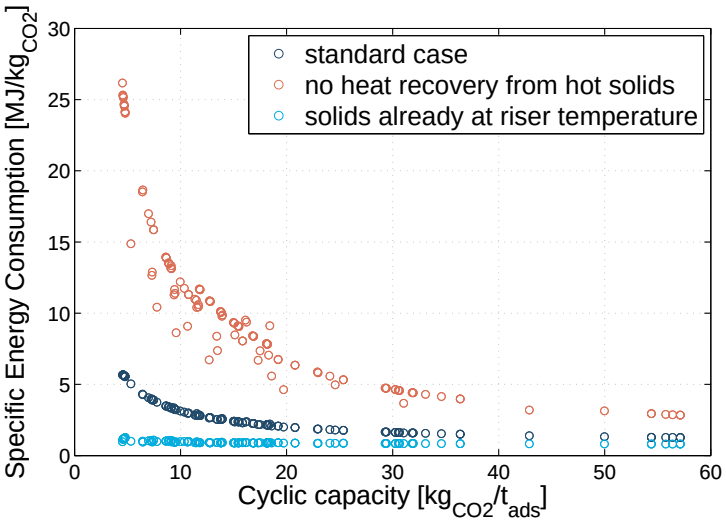

Figure 5.26: CFB, combined cycle: 'specific energy consumption–cyclic capacity' diagram

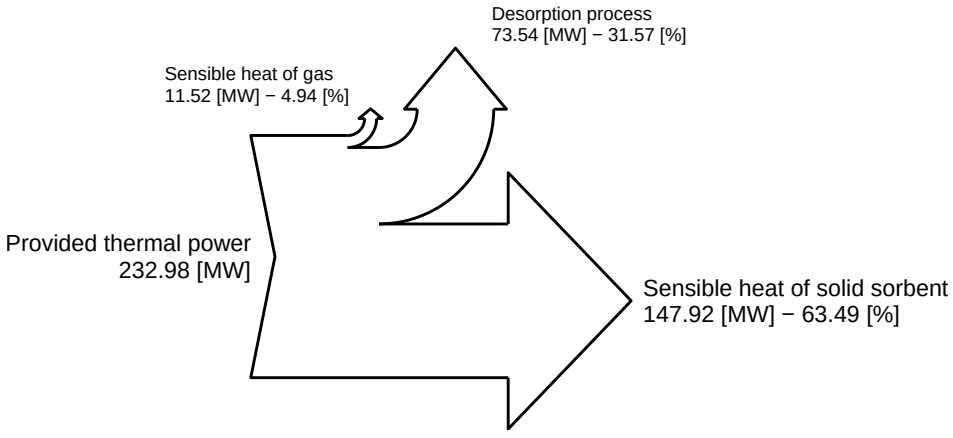

Figure 5.27: CFB, combined cycle: Sankey diagram of energy balance at regenerator

perature, the only heat required would be that required by the desorption process. This case represents the minimum possible energy consumption for a TSA process. As it can be estimated after these graphs, the total consumption rates of the system are strongly affected by the recovery of the sensible heat of solid (Figure 5.26). Depending of how effectively this can be operated, the total energy consumption of the process can become outstandingly low or unacceptably high. The standard configurations of the heat exchanging system that is adopted in these simulations derives from rather realistic assumptions; in particular, a minimum temperature difference of 20°C is a conservative value which compensate also for the efficiency parameter, which is here hypothized as being equal to one. Of course, the amount of sensible heat stored in the solid material is directly proportional to the amount of solids transferred between the reactors; at the same time productivity rates decrease as $\dot{m}_{ads}$ is raised. This causes the sorbent flow rate a strongly affecting parameter, as far as the energy consumption of the system is concerned. As already mentioned, the sorbent flow rate has also a very strong incidence over the final products of the process, so that very low values of $\dot{m}_{ads}$ correspond to unacceptably poor performances. In the end, it appears to be very difficult to find a balanced trade-off between the drawbacks of each extreme (Figures 5.28 and 5.29).

Table 5.5: CFB, energy balance at the regenerator for an example cycle

Flow rate of solid sorbent	100.0 kg/kg$_{CO_2}$
Regeneration temperature	150.0°C
Temperature of entering solid sorbent	128.9°C
Flow rate of gases at inlet	200.0 kg/s
Flow rate of gases at outlet	304.6 kg/s
Cycle recovery rate	91.2%
Cycle purity rate	55.7%

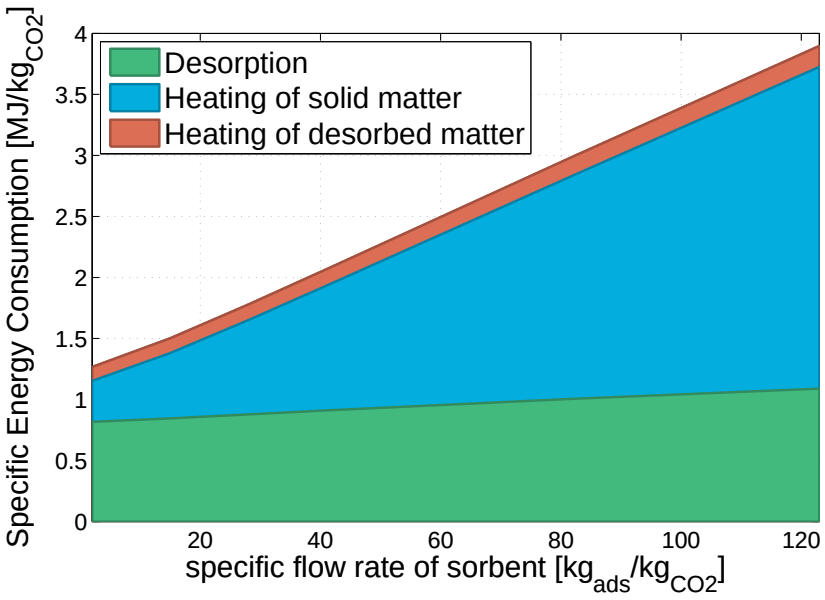

Figure 5.28: CFB, combined cycle: share of the sensible heat of solid depending on sorbent mass flow

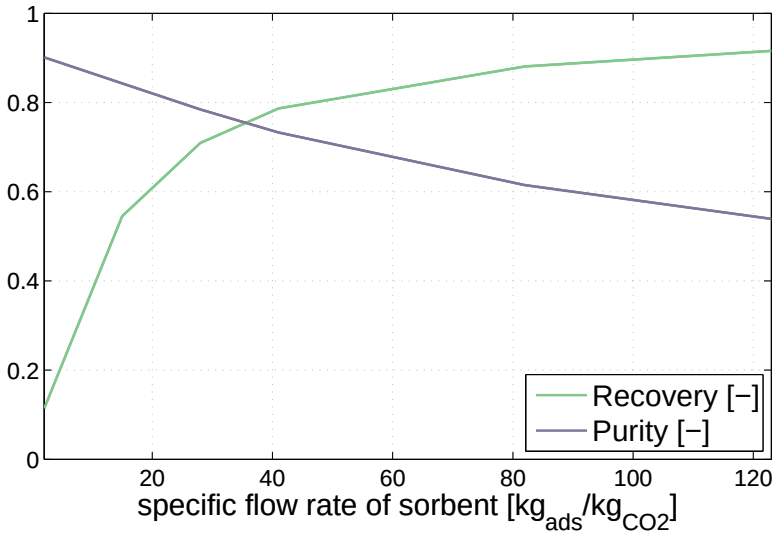

Figure 5.29: CFB, combined cycle: recovery and purity variation depending on sorbent flow rate

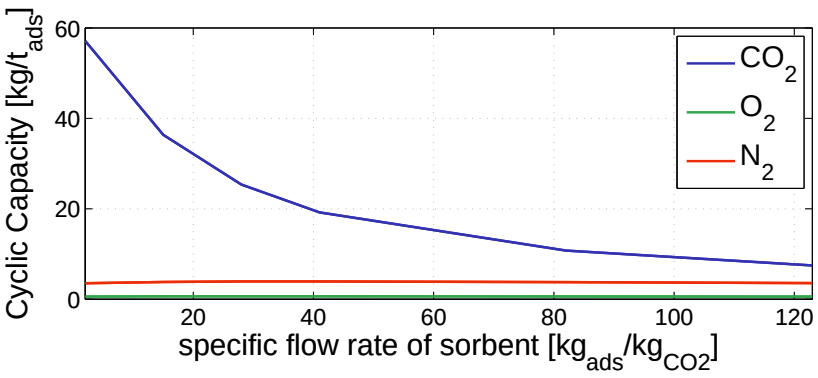

Figure 5.30: CFB, combined cycle: cyclic capacity variation depending on sorbent mass flow

5.1.3 Boiler case

Almost everything that has been so far stated for the combined cycle case, happens to be valid for the boiler scenario as well. Of course the final performances are to some extent different and the limitations defined by the discussed issues are come across at a different point; however, the trends that have already been identified for the first case are always found. Figures 5.31, 5.32 and 5.33 represent the results of the simulations of the boiler case, in the same way as the corresponding results for the combined cycle have been shown. The combined cycle results are also represented in order to provide a first comparison outlook, since most of the operational condition tested were the same for both scenarios.

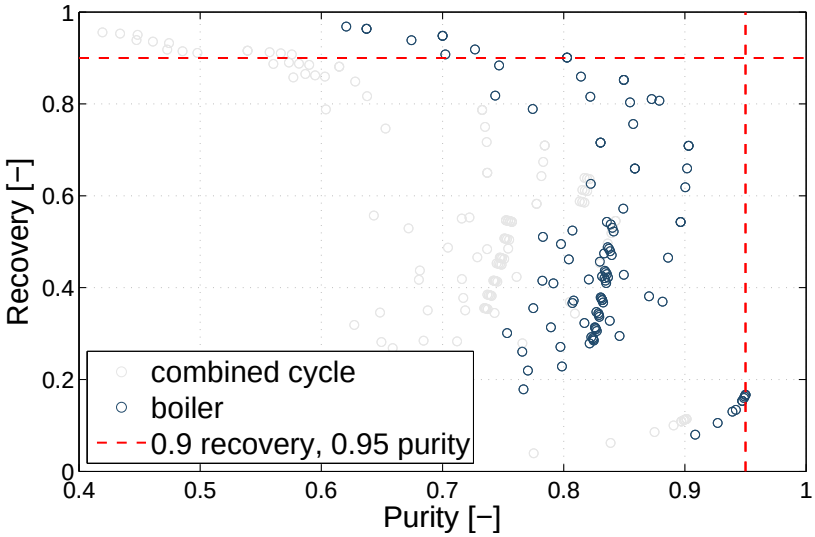

Figure 5.31: CFB, boiler: 'recovery–purity' diagram

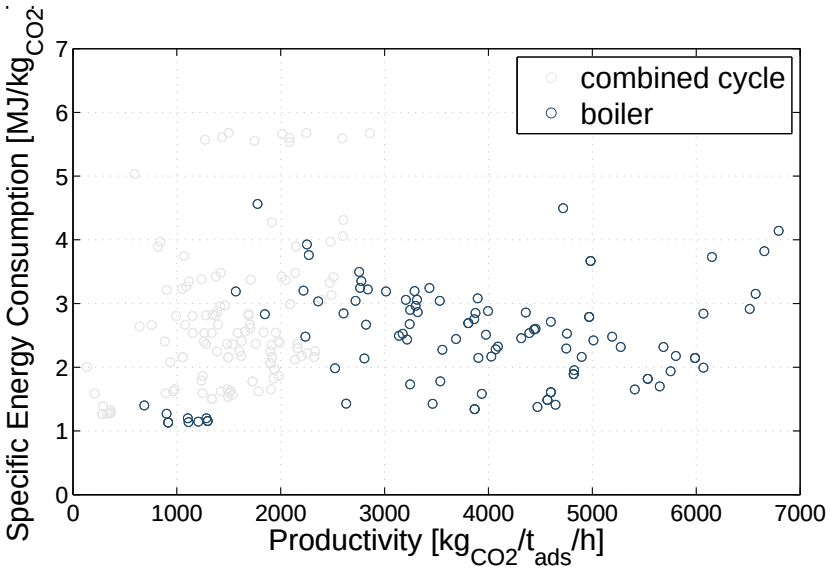

Figure 5.32: CFB, boiler: 'specific energy consumption–productivity' diagram

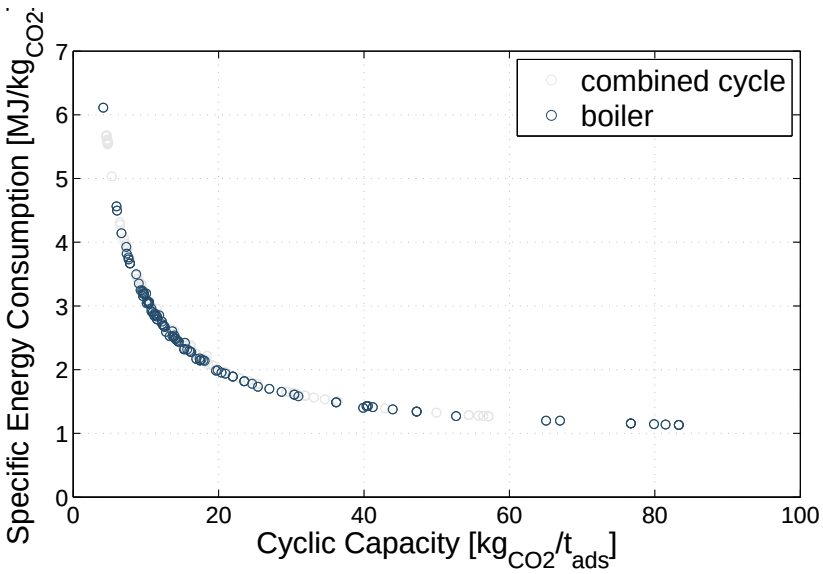

Figure 5.33: CFB, boiler: 'specific energy consumption–CO_2 cyclic capacity' diagram

All the difference may be explained looking at the composition of the flue gas flow gas for each case (in Table 5.6): The higher concentration of CO_2 of the boiler case causes purity rates to be generally superior, given the advantage in the competition for adsorption against the other species. If corresponding operational points are compared, it can also be observed that recovery rates reach higher peaks in the best cases, but results to be slightly more sensitive to those parameters that are related to the residence time of particles, i.e. inventories and superficial velocities. The almost vertical stripe of dense points that can be observed in the middle part of the diagram for both cases is in fact drawn by the variations of inventories and superficial velocities and shows an appreciably wider spread along the recovery axis.

	composition v. [%]		
case	CO2	O2	N2
combined cycle	10.36	10.87	78.77
boiler	28.41	0.77	70.82

Table 5.6: CFB: flue gas composition after drying

As far as specific energy consumption and cyclic capacities are concerned, the values trace perfectly in line with those of the combined cycle. Though, given the higher concentration of CO_2 in the feed, higher cyclic capacities peaks may be reached at very low values of the sorbent flow rate. This time the equilibrium adsorbed amount at adsorption conditions is higher –approximately equal to 190 kg of CO_2 per t of adsorbent (4.3 moles per kg)–, so that the upper limit for cyclic capacities is shifted up to around 110 kilograms per ton of sorbent (2.5 moles per kg), versus 75 kilograms for the combined cycle case.

Productivities are generally enhanced by the higher concentration of carbon dioxide in the flue gas not only because the cyclic capacities are higher (and the recovery rates accordingly), but also because the ratio between the mass of CO_2 entering the system and the total inventory stored in the reactor is higher. This means in the end that the amount of carbon cap-

tured using a ton of adsorbent is more than twice the best results obtained for the combined cycle case.

Operational issues

Given a certain fixed recovery rate, higher concentrations of CO_2 in the feed stream correspond to lower availability of surface per mass unit of CO_2. In this sense, it can be straightforwardly guessed that all the issues related to the heat exchange may only get worse in this boiler scenario. Unsurprisingly, this is exactly what can be observed. In particular, none of the simulations has been found under the feasibility limit, as far as the surface availability at the regenerator is concerned. The order in which the limitations are come across is the same of the previous case (surface availability and heat provision in the regenerator are the biggest issues), but they are all advanced to a more restricting degree (see Figures from 5.34, 5.35, 5.36, 5.37 and 5.38).

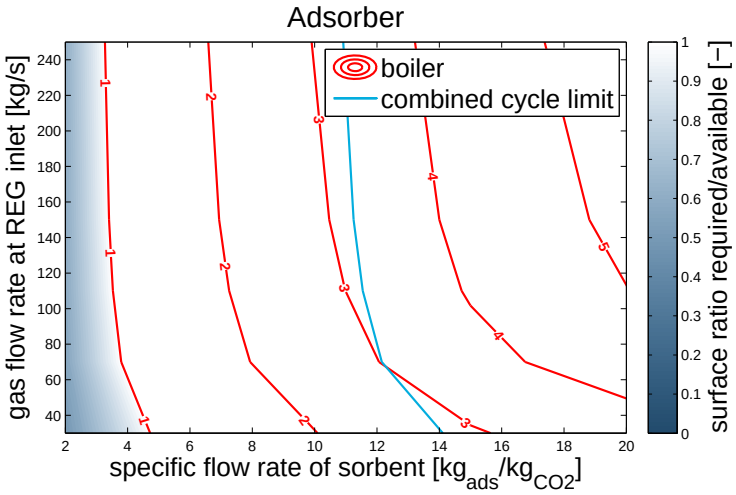

Figure 5.34: CFB, boiler: 'gas flow rate at regenerator–sorbent flow rate–available surface ratio' diagram for adsorption

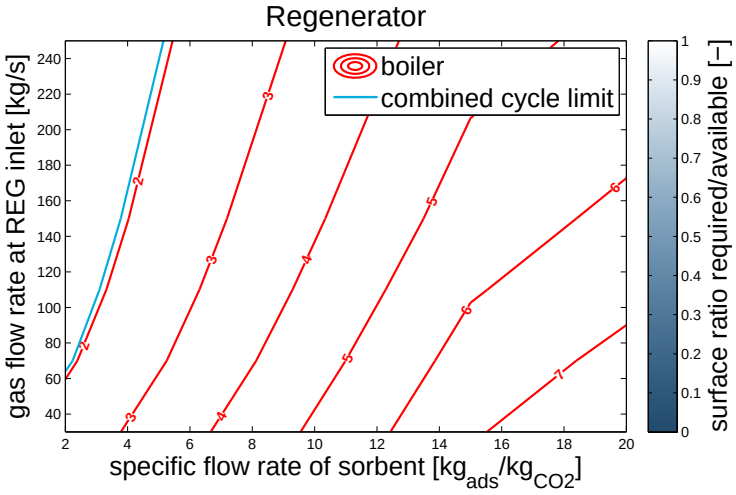

Figure 5.35: CFB, boiler: 'gas flow rate at regenerator–sorbent flow rate–available surface ratio' diagram for regeneration

As regards the ratio between the desired sorbent flow rate and the amount of solids entrained by the gas, once again the situation appears more critical, given that the high carbon dioxide concentration corresponds to a lower flow rate of flue gas per mass unit of CO_2. Figure 5.38 compares the results to the combined cycle case for the adsorption riser, which places the most restrictive limitation.

For the combined cycle case, some modifications of the assumptions under which the energy balances are computed have been taken into account. The same calculations are repeated for the boiler case as well; unsurprisingly, they pointed out exactly the same trends. Differences may be only noticed in the the term of the energy balance of the adsorber associated with the flue gas flow is more scarce than in the previous case, so that a reduction of the flue gas temperature ends up being even more ineffective.

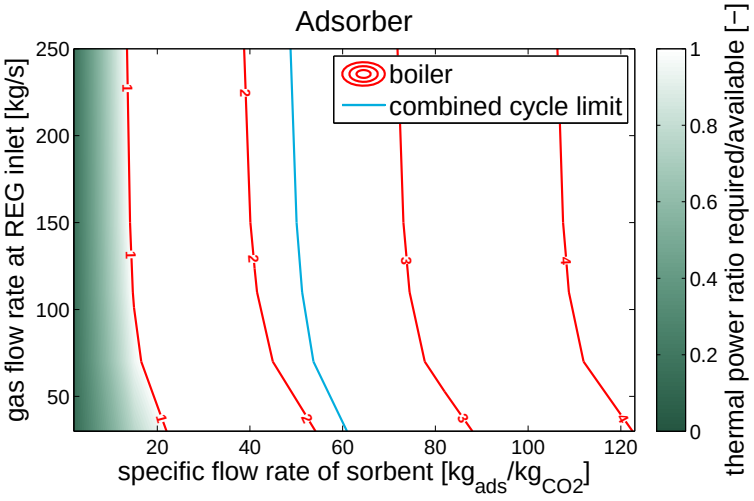

Figure 5.36: CFB, boiler: 'gas flow rate at regenerator–sorbent flow rate–available thermal capacity ratio' diagram for adsorption

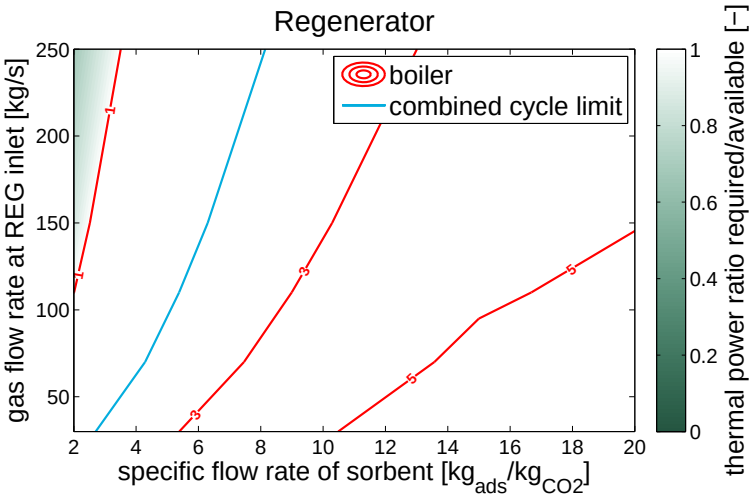

Figure 5.37: CFB, boiler: 'gas flow rate at regenerator–sorbent flow rate–available thermal capacity ratio' diagram for adsorption

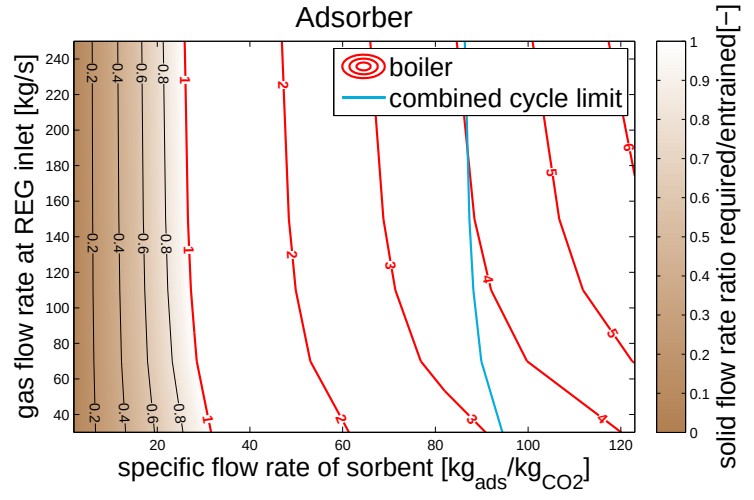

Figure 5.38: CFB, boiler: 'gas flow rate at regenerator–sorbent flow rate–solid recirculation rate' diagram for adsorption

5.1.4 Plant size

As one of the key features of the circulating fluidized beds is the compactness, a special remark is here dedicated to the total size of the plant as deriving from the simulations. The size of each reactor depends on both its cross section and its height, which are not completely unrelated though; in general an optimally designed CFB reactor is characterized by a height-to-diameter ratio comprised between 3 and 10.

The adsorbers simulated during this study have a rectangular cross section, as explained in Chapter 3, with an aspect ratio of 2. They are all featured with a height of 30 m, while their cross section depends mainly on the superficial velocity of the gas at inlet u_0 (and on the temperature and the composition of the gas, to a smaller extent).

As regards the regenerators, the shape of the reactor is the same, but a riser height of only 20 m has been considered, as the gas flow rates are usually lower than those of the adsorber one.

All in all, the size of the plant vary in the ranges summarized by Tables 5.7 and 5.8. As compactness is unequivocally to be considered a convenient quality, because allows reducing the capital costs related to plant construction, the biggest simulated plant is defined as 'worst case', while 'best case' identifies the most compact one, irrespective of the corresponding performances.

Table 5.7: CFB, combined cycle: plant size

worst case	
Superficial velocity at adsorber inlet	3 m/s
Superficial velocity at regenerator inlet	3 m/s
Gas flow rate ar regenerator inlet	200 kg/s
Cross section adsorber	139.6 m^2
Cross section regenerator	55.3 m^2
Total reactor footprint	194.9 m^2
Total reactor volume	5294 m^3
Total inventory	194.9 t_{ads}
best case	
Superficial velocity at adsorber inlet	7 m/s
Superficial velocity at regenerator inlet	7 m/s
Gas flow rate ar regenerator inlet	20 kg/s
Cross section adsorber	57.9 m^2
Cross section regenerator	3.0 m^2
Total reactor footprint	60.9 m^2
Total reactor volume	1797 m^3
Total inventory	60.9 t_{ads}

Table 5.8: CFB, boiler: plant size

worst case	
Superficial velocity at adsorber inlet	3 m/s
Superficial velocity at regenerator inlet	3 m/s
Gas flow rate ar regenerator inlet	200 kg/s
Cross section adsorber	83.9 m^2
Cross section regenerator	54.2 m^2
Total reactor footprint	138.1 m^2
Total reactor volume	3601 m^3
Total inventory	138.1 t_{ads}
best case	
Superficial velocity at adsorber inlet	7 m/s
Superficial velocity at regenerator inlet	7 m/s
Gas flow rate ar regenerator inlet	20 kg/s
Cross section adsorber	34.8 m^2
Cross section regenerator	2.9 m^2
Total reactor footprint	37.7 m^2
Total reactor volume	1102 m^3
Total inventory	37.7 t_{ads}

5.2 Fixed bed

After testing a wide range of cycle configurations, a five step cycle configuration is identified as the best promising one, for it could meet the minimal reference requirements of a CCS application, while its simplicity allows to limit consumption. The cycle layout has been presented in Chapter 4. The operational settings of the process have been varied to produce a sensitivity analysis over different values for four parameters, namely the time durations of all the steps, except for the pressurization step, whose length is anyway reduced compared to the other steps and is anyhow never affecting the performances of the process, as far as it is long enough to provide the small pressure increase required after the cooling step in a TSA cycle. A duration of 10 seconds is fixed for this pressurization step (unit 1) in all the simulations performed.

After the first few analyses, the observation of the results has indicated the existence of some Pareto fronts, which give effective information about the optimization of the cycle. The analyses have been therefore intensified in those parameter ranges which seemed to provide the best performances. This procedure has been firstly followed for the boiler scenario; it has been later repeated for the combined cycle case, exploiting the experience gained in the previous case in terms of acquaintance with the trends shown by the results.

5.2.1 Boiler case

Altogether approximately 850 different operational points have been tested for the boiler case. The results have been plotted in the diagrams already here adopted to represents process performances, that are the 'recovery-purity' diagram (Figure 5.39) and the 'specific energy consumption-productivity' diagram (Figure 5.40).

Moreover, as far as the 'recovery-purity' diagram is concerned, the existence of a Pareto front in the high recovery–high purity corner of the diagram is glaring. In Figure 5.41 a zoomed representation of the diagram is plotted.

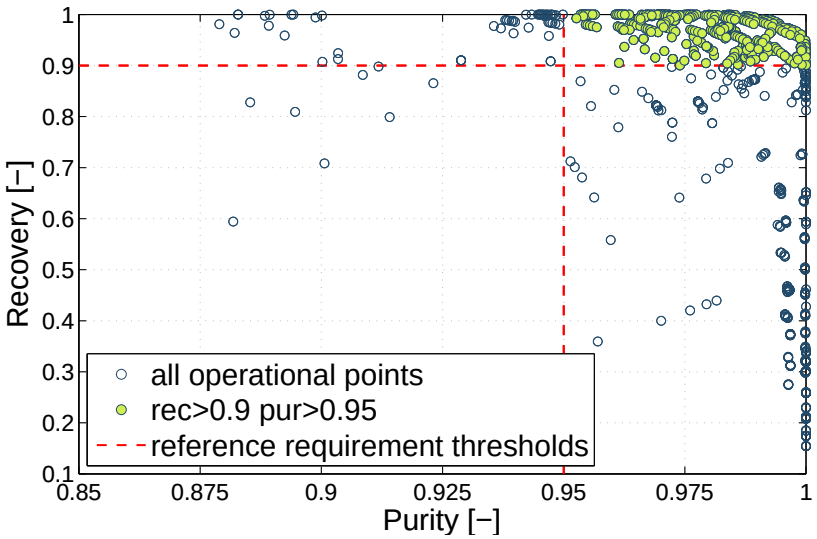

Figure 5.39: Fixed bed, boiler: 'recovery–purity' diagram

In the diagrams all the operational points that meet both the reference requirements for a CCS application –i.e. minimal recovery 0.9, minimal purity 0.95– have been highlighted. It can be immediately noticed how many of the results actually meet these requirements and how elevate are the purity rates for all the tested sets of input data, lying the lowest ones way beyond 85%. The peaks of both purity and recovery are placed very close to the absolute limit.

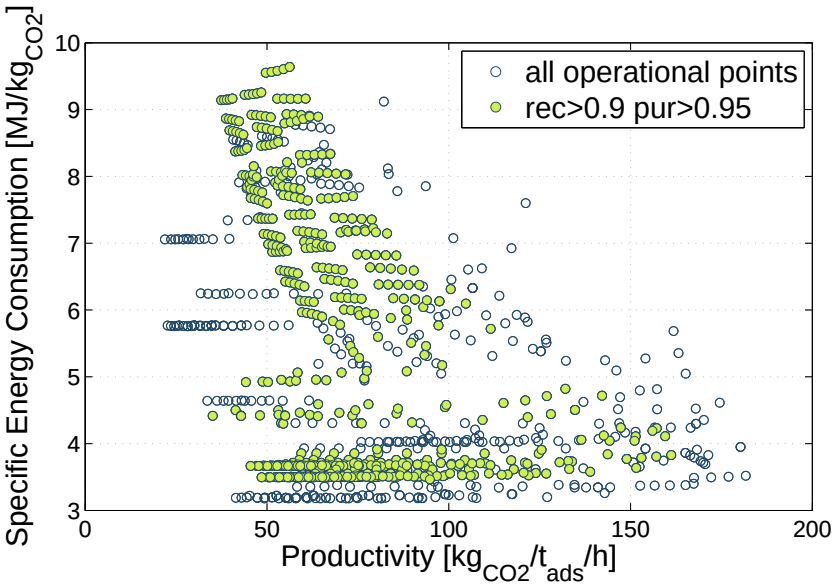

Figure 5.40: Fixed bed, boiler: 'specific energy consumption–productivity' diagram

As regards the 'specific energy consumption–productivity' diagram, a global Pareto front for low energy consumption and high productivity values can be observed. As a considerable quantity of points meet both reference requirements, it might be more interesting to outline a Pareto front among those operational points (Figure 5.42 and Table 5.9).

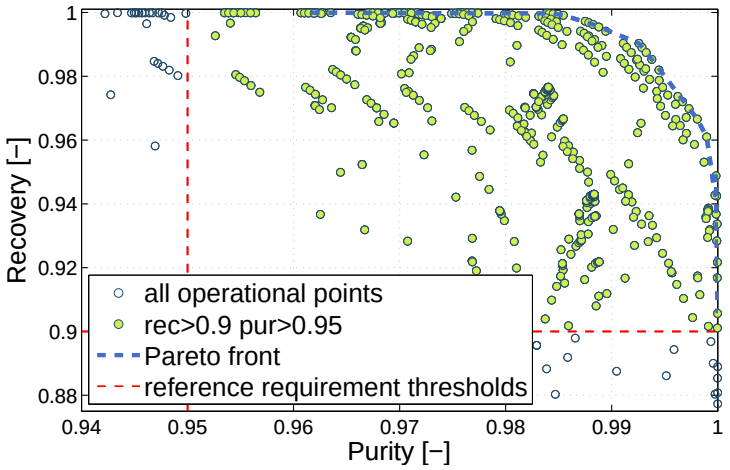

Figure 5.41: Fixed bed, boiler: Pareto front in 'recovery–purity' diagram

As far as a CCS application is concerned, once a desired minimum has been established for recovery and purity, the optimum configuration of the cycle will be the one which meets these requirements providing the highest possible productivity and causing the lowest possible specific energy consumption.

Table 5.9: Fixed bed, boiler: Pareto front points in 'specific energy consumption–productivity' diagram

Unit 2 [s]	Unit 3 [s]	Unit 4 [s]	Unit 5 [s]	Recovery [%]	Purity [%]	Spec. en. cons. [MJ/kg$_{CO_2}$]	Productivity [kg$_{CO_2}$/t$_{ads}$/h]
475	100	1000	1250	98.95	91.19	3.47	94.83
440	100	750	800	98.88	91.11	3.53	121.97
450	100	750	500	98.74	91.63	3.58	138.90
450	100	750	300	98.59	90.18	3.64	151.57
400	100	500	350	98.37	90.39	3.83	161.19

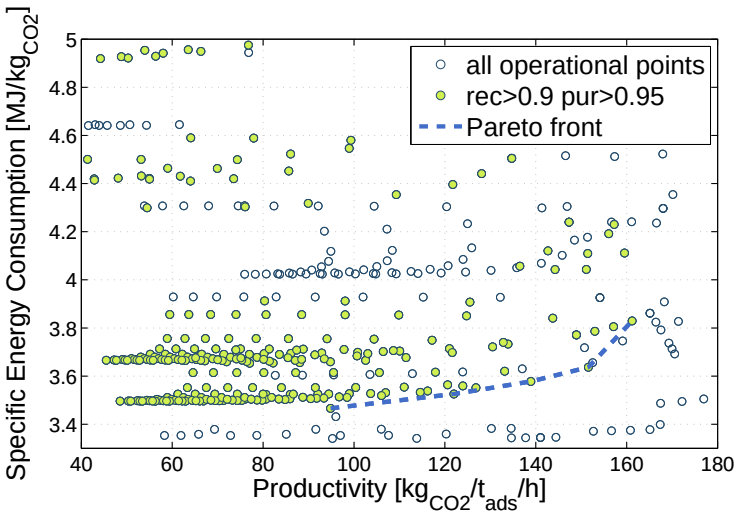

Figure 5.42: Fixed bed, boiler: Pareto front in 'specific energy consumption–productivity' diagram'

5.2.2 Combined cycle case

A little fewer simulations have been performed for this scenario (around 650), given the experience already made with the boiler case has allowed heading more directly to the Pareto front.

The results show trends analogous to those of the boiler case, but as it was the case for the circulating fluidized bed, the lower CO_2 concentration act as restriction, preventing from reaching performances as good as those of the boiler case. This can be found to be true not only for purity and recovery rates, but also for specific energy consumptions and especially for productivities (the maximals are halved compared to the boiler case). Figure 5.43 and 5.44 show these process performances.

However, since a remarkable amount of points meet both the reference requirements, the Pareto fronts can be outlined consistently, as it has been done for the previous case (Figures 5.45 and 5.46). Given the lower concentration of the species to be adsorbed from the flue

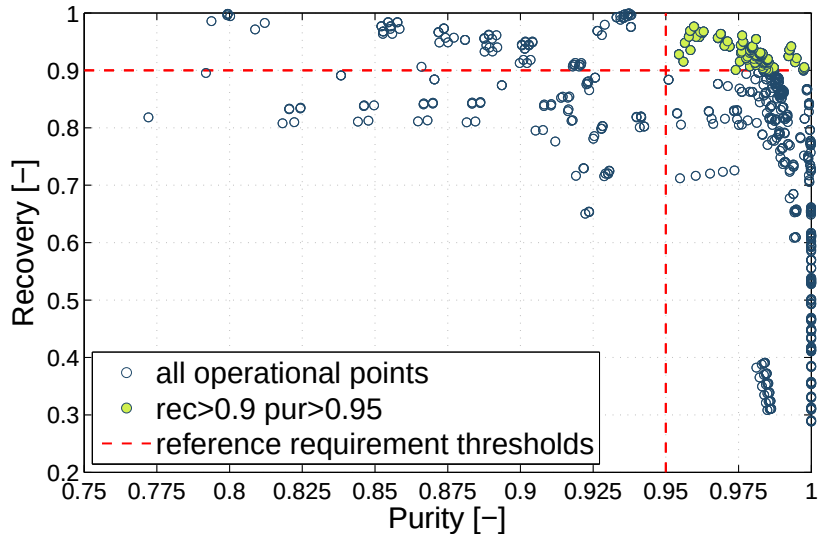

Figure 5.43: Fixed bed, combined cycle: 'recovery–purity' diagram

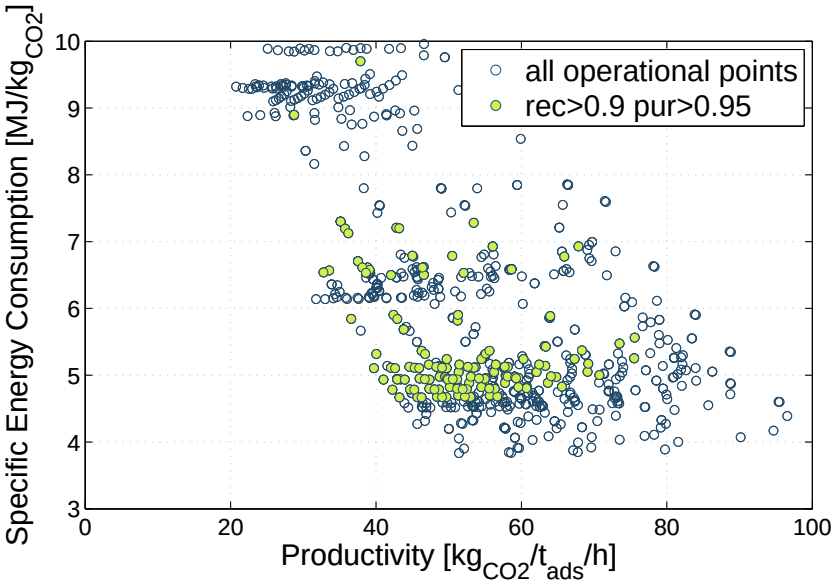

Figure 5.44: Fixed bed, combined cycle: 'specific energy consumption–productivity' diagram

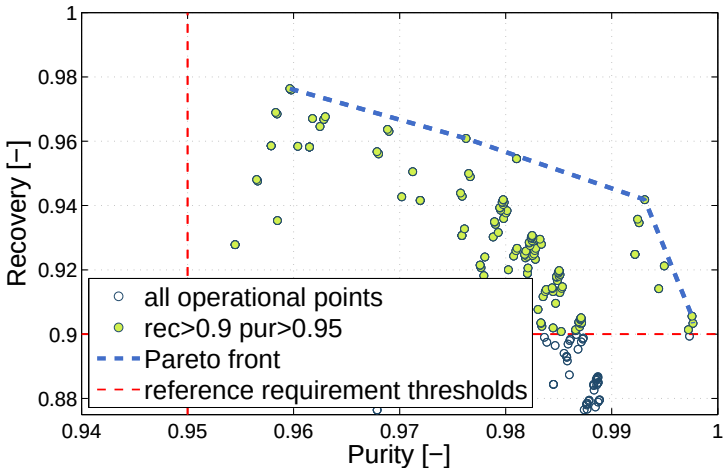

Figure 5.45: Fixed bed, combined cycle: Pareto front in 'recovery–purity' diagram

Table 5.10: Fixed bed, combined cycle: Pareto front points in 'specific energy consumption–productivity' diagram

Unit 2 [s]	Unit 3 [s]	Unit 4 [s]	Unit 5 [s]	Recovery [%]	Purity [%]	Spec. en. cons. [MJ/kg$_{CO_2}$]	Productivity [kg$_{CO_2}$/t$_{ads}$/h]
1000	150	1900	1500	98.71	90.51	4.67	43.23
1000	150	1600	1500	98.71	90.48	4.67	46.25
1000	150	1300	1500	98.72	90.35	4.67	49.69
1000	150	1300	1250	98.71	90.32	4.68	52.98
1000	150	1300	1000	98.70	90.23	4.68	56.68
950	150	1000	750	98.47	90.96	4.83	65.58
900	150	700	750	98.31	90.77	5.00	70.73
850	150	700	500	97.89	90.70	5.25	75.50

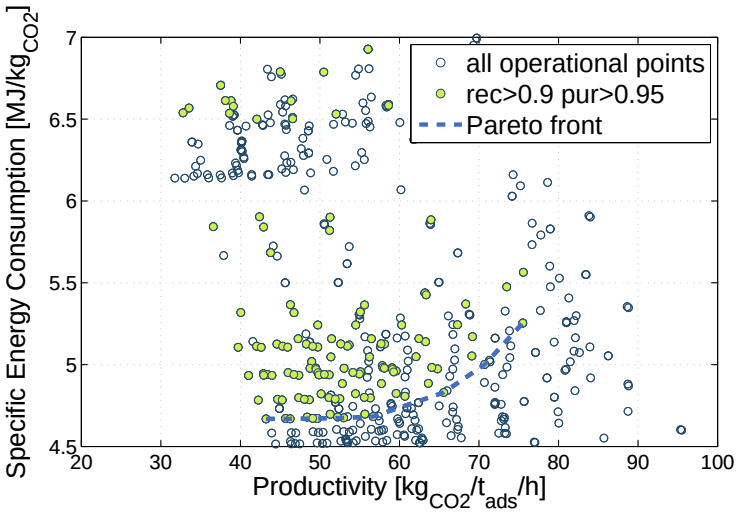

Figure 5.46: Fixed bed, combined cycle: Pareto front in 'specific energy consumption–productivity' diagram'

gas, the optimal adsorption times resulted to be more than doubled and the whole cycle has been stretched to a similar extent, as reported in Table 5.10.

Shape and position of the Pareto fronts

A few observation about the durations of the steps may help justifying the shape and the position of these Pareto fronts.

The adsorption time is one of the most affecting parameters as concerns recovery and the amount of CO_2 captured (see Figures 5.47). As this step time increases, the bed gets

loaded with more and more CO_2 up to a certain point, at which the adsorption front ideally breaks through the riser outlet; at this point the bed is fully loaded, no more CO_2 can be adsorbed and the gases flows through the reactor without undergoing any adsorption. Under less ideal assumptions, the adsorption front is actually a progressively declining curve rather than a perfectly defined step; as it proceeds along the riser length the bed gets loaded; when it comes close to the outlet, the CO_2 concentration of the exiting product starts increasing, as the bed is too full to remove the desired fraction of gas from the flow. This means the recovery is in the beginning almost constant; then it progressively goes asymptotically to zero as the adsorption front crosses the reactor outlet. Therefore a certain adsorption time allows the most CO_2 amount to be captured for any desired minimum recovery rate. When the recovery rate starts decreasing, the bed is not fully loaded yet: for this reason the Pareto front in the 'specific energy consumption–productivity' diagram does not overlie the lower edge of the cluster that represents all operational points. Since the adsorption is operated at low temperature, no additional energy consumption is needed for longer adsorption length, so that longer times cause the points to get shifted downwards as long as they provide a heavier loading of the bed (Figure 5.48).

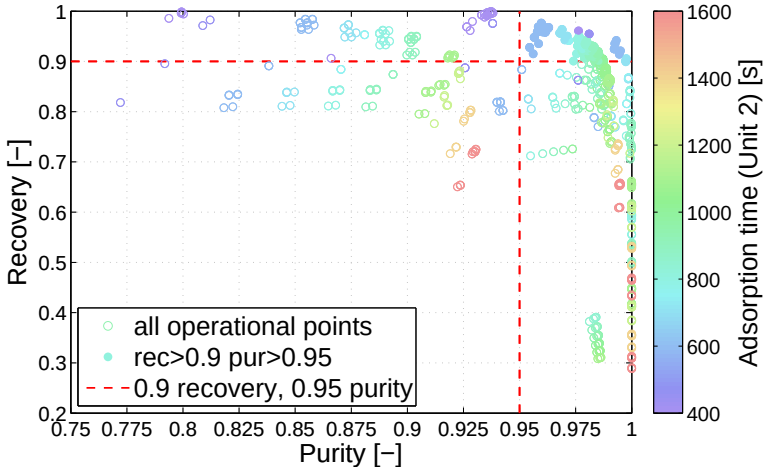

Figure 5.47: Fixed bed, combined cycle: 'recovery–purity–adsorption time' diagram

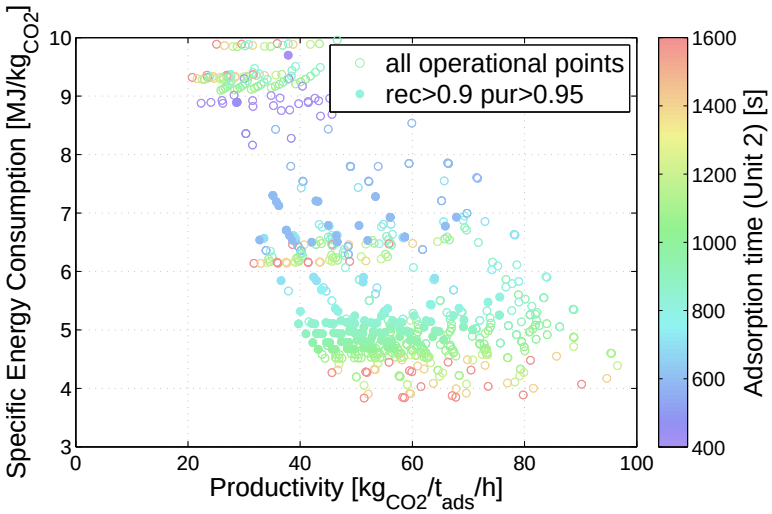

Figure 5.48: Fixed bed, combined cycle: 'specific energy consumption–productivity–adsorption time' diagram

For which time this optimum is to be reached, depends on the conversion degree of the bed at the beginning of the step. These conversion degree is determined by the heating and cooling sequence undergone by the solid in unit 3, 4 and 5. The two blowdown steps produce exactly the same effect on the bed (only the destination of the outflowing stream changes) and are to be considered together as the heating section of the cycle. Along the time axis,

the asymptotic conditions for the heating step are determined by the temperature of the heat source and the relative adsorption isotherm, which indicates the minimum reachable conversion degree. The longer the duration of the heating, the higher the temperature reached by the bed, which makes the regeneration proceed further unloading the bed from the adsorbed phase. Deeper regenerations yield higher cyclic capacities, but the need for longer timescales raises the total cycle duration: these two effects have counteracting incidences on the productivity value.

Conversely, the cooling time is responsible for defining the lower temperature level of the cycle: the longer the step, the lower the temperature, the higher the related adsorption isotherm, which means higher cyclic capacities, but the benefit might be not enough to improve the productivity, since the total cycle duration increases as well. It has to be remarked that during the cooling step the bed starts adsorbing small amounts of gas left inside the reactor at the end of the second blowdown step: This amount is anyway small compared to the total bed capacity, so that the most of the bed is actually loaded during the real adsorption step.

According to the way heating and cooling time affect productivities, when those time increase points move towards the left border of the diagram (example in Figure 5.49). At the same time, the bed starts the adsorption section with a lower content of adsorbed phase, so that the free space on the bed surface is ampler and adsorption can be conducted for longer times before completely filling it. This explains why the maximum limit for the adsorption time increases together with heating and cooling lengths.

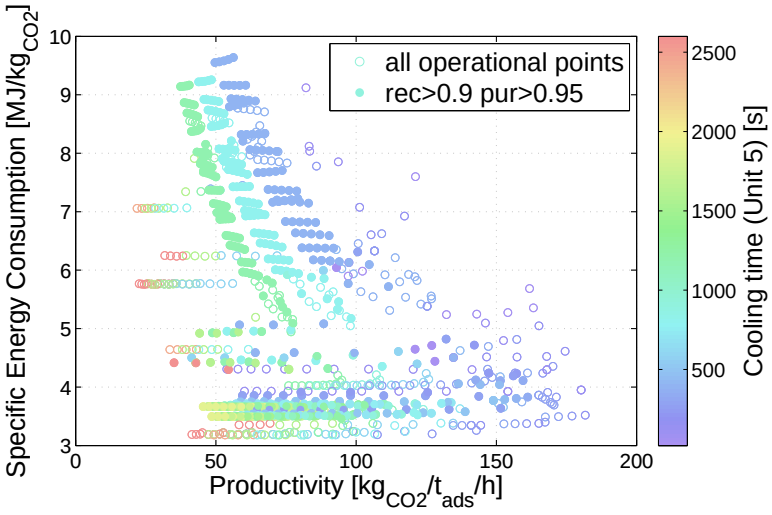

Figure 5.49: Fixed bed, boiler: 'specific energy consumption–productivity–second blowdown time'

Nothing has been said yet about the repartition of the heating section into unit 3 and unit 4. This setting has a direct incidence on the trade-off between recovery and purity; unit 2 is meant to avoid conveying the initial product of the blowdown (which has a lower CO_2 concentration, since it includes the gas phase left at the end of the adsorption phase) into the CO_2 flow led to storage.

Therefore increasing the first blowdown timescale, purity is improved, while recovery remains almost constant until a certain point, after which the CO_2 concentration in the flow recirculated to the adsorption is so high, that the bed is not able to adsorb enough to assure a sufficiently high recovery rate Figure 5.50. The shape of the Pareto front in the 'recovery–purity diagram' may be therefore explained as follows: to get very high purity, recovery must

be compromised, and vice versa. Longer heating and cooling times help pushing the results towards high values for both quantities, until raising them cannot provide any further benefit because the temperatures of the heat sources have been reached.

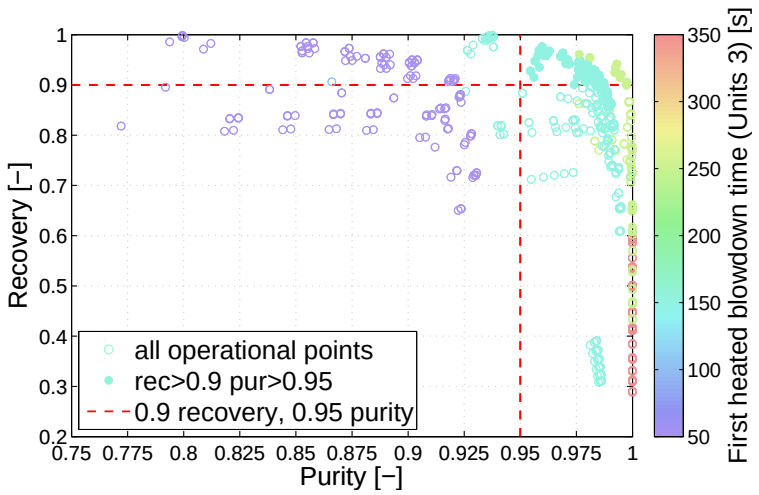

Figure 5.50: Fixed bed, boiler: 'recovery–purity–first blowdown time' diagram

5.2.3 Process scheduling and plant size

As extensively explained in Chapter 4, the number of vessel that form the whole plant can be determined only planning a time schedule for the whole process. As the scheduling computation procedure is quite time demanding, it is performed only for a selected set of points, those which form the Pareto front in the 'specific energy consumption–productivity' diagram. These points correspond to the cycle configurations which both satisfy the reference requirements of a CCS application (90% recovery, 95% purity) and at the same time allow operating carbon capture with the smaller resource expenditure, as they are the most efficient configurations.

The conditions N_{tr}=1 and N_{st}^{feed} correspond always to the minimization of the total number of vessels N_{st}, as it can be straightforwardly inferred from the equations used to determine this value. Usually it is more advisable to employ more trains simultaneously in a real plant, so that the other are still available in case a malfunction or a failure interrupts the functioning of one of them. Therefore here the optimization of the scheduling correspond to the value J>1 that provides the smaller number of vessels. Tables 5.11 and 5.12 report the data of the points of the Pareto fronts for the boiler and the combined cycle case.

As it can be observed looking at the tables, the total number of required vessels is always very high. Considering that a single vessel has a cross section of 7.30 m^2 and a height of 1.2 m:

- for the boiler case, the total footprint of the plant extends from around 6100 to 10700 m^2, being the related volumes 7300 and 12800 m^3 respectively;
- for the combined cycle case, the total footprint varies between 7800 m^2 (9400 m^3) and 13700 m^2 (16400 m^3).

Comparing this number with the one obtained for the CFB plants, it can be remarked that using this type of vessel a fixed bed system requires a footprint between 50 and 100 times larger than circulating fluidized bed. This is of course related to the lower velocity of the flue gas and to the very short length of the fixed bed columns, as modeled in the simulations.

As regards the velocity of the gases, for the simulations a flow rate $\dot{V}_{col}$ equal to 0.00015 m^3/s is established, which corresponds to a superficial velocity of 0.21 m/s. This means the gas flows about 30 times slower than in an average CFB reactor.

Table 5.11: Fixed bed, boiler: scheduling optimization

Sp. en. cons. [MJ/kg_{CO_2}]	Productivity [kg_{CO_2}/h/t_{ads}]	J [-]	N_{tr} [-]	K [-]	N_{st} [-]	N_{st}^{feed} [-]	t_{idle} [s]	New Productivity [kg_{CO_2}/h/t_{ads}]
3.47	94.83	125	2	731	1462	250	1.28	94.78
3.53	121.97	125	2	584	1168	250	2.40	121.83
3.58	138.90	125	2	492	984	250	0.56	138.86
3.64	151.57	2	125	7	875	250	0.00	151.57
3.83	161.19	25	10	83	830	250	1.20	161.05

Table 5.12: Fixed bed, combined cycle: scheduling optimization

Sp. en. cons. [MJ/kg_{CO_2}]	Productivity [kg_{CO_2}/h/t_{ads}]	J [-]	N_{tr} [-]	K [-]	N_{st} [-]	N_{st}^{feed} [-]	t_{idle} [s]	New Productivity [kg_{CO_2}/h/t_{ads}]
4.67	43.23	83	5	375	1875	415	0.82	43.22
4.67	46.25	32	13	135	1755	416	0.94	46.24
4.67	49.69	83	5	326	1630	415	6.99	49.60
4.68	52.98	83	5	305	1525	415	1.45	52.96
4.68	56.68	83	5	285	1425	415	8.07	56.54
4.83	65.58	52	8	155	1240	416	1.54	65.54
5.00	70.73	83	5	299	1145	415	0.72	70.70
5.25	75.50	83	5	214	1070	415	7.35	75.25

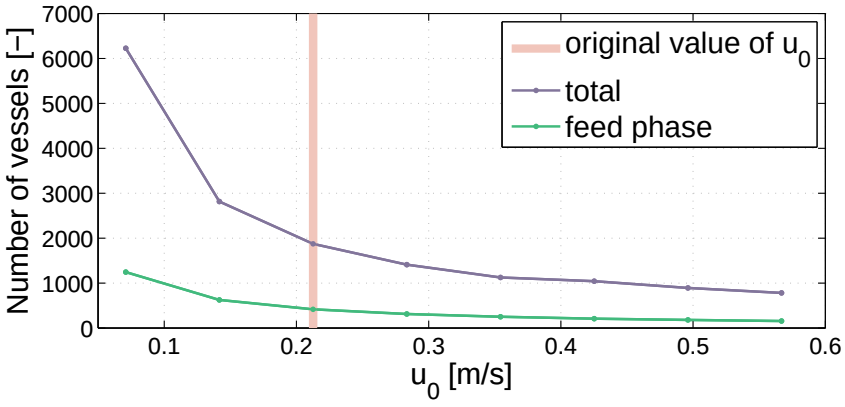

Figure 5.51: Fixed bed: plant size depending on gas velocity

A quick sensitivity analysis has been done on the points of the Pareto front for the combined cycle case to see which effect has a variation in the gas velocity on the performances of the system and on the footprint required by the plant. Figure 5.51 outlines the reduction of the number of vessels that can be obtained from an increase in gas velocity. Figures 5.52 and 5.53 show that as far as energy consumptions, producitivities and purity rates are concerned higher velocities could enhance the performances; nevertheless, without a new optimization of the cycle configurations, the recovery rate drop dramatically increasing the flow rate of gas. This should suggest that there is still little space for improvement of the performances varying the gas velocity, if no modification of the cycle or of the vessel geometry occurs.

In order to achieve the same recovery performances obtained at the velocity fixed for the purposes of this study (0.21 m/s) feeding higher flow rates of gas in the column a new vessel

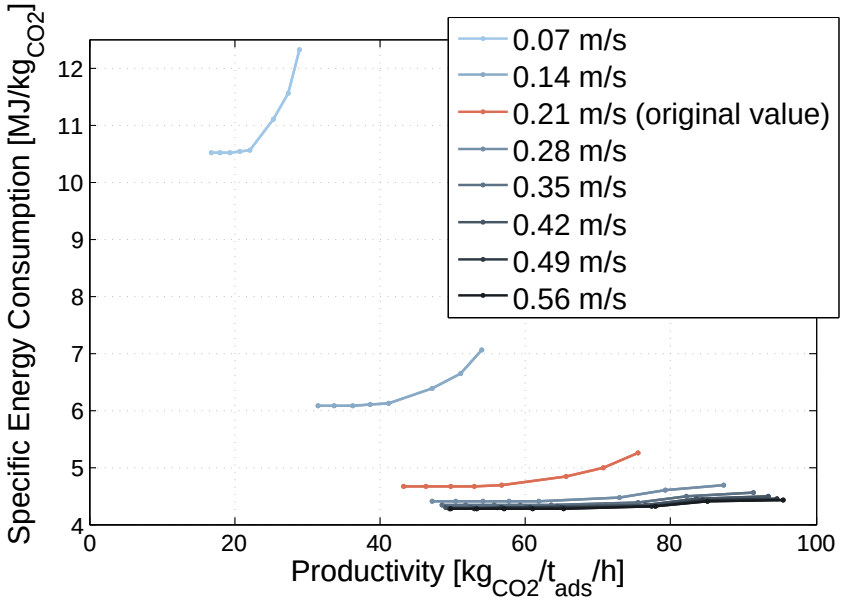

Figure 5.52: Fixed bed: effects of a variation of gas velocity in'Specific Energy Consumption–Productivity' diagram

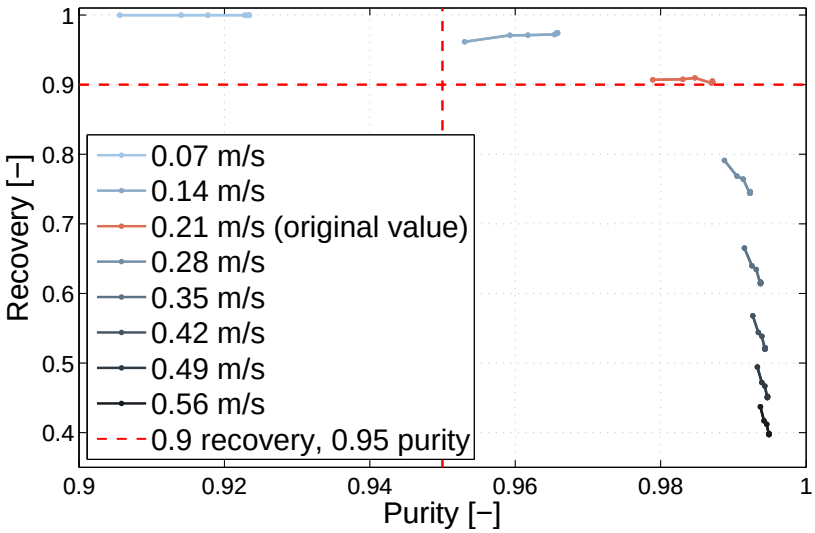

Figure 5.53: Fixed bed: effects of a variation of gas velocity in 'Recovey-Purity' diagram

design should be developed extending the height of the bed. Higher velocities and extended reactor length would though cause the pressure drop across the bed to increase dramatically: in this sense, a solution could be that of adopting particles with a larger diameter.

Conclusions

Although the specific case of steel mills is taken into account, the present work investigates many issues related to TSA cycles for CCS application in general. It can be undoubtedly stated that most indications given by the results here obtained may be reasonably extended to some similar cases, under proper assumptions. In the next few paragraphs a short review is provided of the main conclusions that can be drawn out of this study. The outlook that derives from them is briefly summarized immediately after.

As regards the adsorption process itself, the modeling adopted in this work (described in Chapter 2) has been already extensively used in literature and provides a sufficiently detailed explanation of the phenomenon. The experimental data provided by SPL are consistent with the results that can be found in literature for the same materials. In order to perform all the simulations consistently, a single solid sorbent is selected for the TSA process. Out of many possible options, two commercially available sorbents, namely activated carbon and zeolite 13X, whose data are available for the purpose of this work thanks to SPL, are compared to choose the most promising one. Out of these two, zeolite 13X results to be the most promising material.

As it has already been widely suggested in literature [11, 14, 27], zeolites show to have a good potential for CO_2 adsorption: As a matter of fact, zeolite 13X achieves satisfactory cyclic capacities within the range of pressures and temperatures that suits TSA cycles best and requires a relatively small amount of energy to be completely regenerated. Those materials can be artificially synthesized by means of a variety of industrial processes and are commercially available at a reasonable price, so that they are suitable for high scale applications like the ones considered in this work.

The software implemented at SPL and made available to perform simulations for the fixed bed systems has been already tested extensively by the researchers who developed it and are currently using it. As far as this work is concerned, it allows to simulate all the investigated configurations with a high level of detail. Although it is based on a experimental setup that is necessarily a scaled reproduction of the simulated one, the results it provides are undoubtedly realistic and are expected to provide reasonably small deviation from the experimental value that could be measured out of a true-scale operation. Among all the observation that can be derived from the results obtained for the fixed bed configurations, a few main ones can be summaried as follows:

- it should be recalled that, as it has been mentioned in the first chapters of this dissertation, the flue gas must undergo a drying process before entering the carbon capture

section; this would increase the total energy demand of the CCS system of approximately 1 MJ of thermal energy per kg of CO_2 using an adsorption-based process or around 0.5 MJ of electric energy adopting a cooling-based process instead;
- the optimized 5-step fixed bed TSA cycle configuration identified in this work appears really promising in terms of achievable recovery and purity performances for a CCS application in steel mills. Given the fact that all the assumptions made for the fixed bed modeling are rather conservative, a real implementation of the cycle should provide close results;
- the optimal design of the TSA cycle identified in this study promise to be an interesting solution for carbon capture also in other applications at different CO_2 concentrations, if high recovery and purities are seeked. Thanks to its flexibility, the cycle can be adapted to endorse one or the other rate more, depending on the specific requirements of the case;
- as regards productivities and energy consumptions, they drop to noteworthy values if the CO_2 content of the flue gas is rather high (as in the boiler case); in this case energy consumptions similar to those of the most-established post combustion CCS systems (around 3.5 MJ per kg of CO_2) are reached and the productivities are sufficiently high. Even better results may be reached optimizing the process design for slightly higher superficial velocities of gases, as suggested in Chapter 5;
- at the same time, though, performances are found to be highly sensitive towards the composition of the gas, so that specific energy consumption increase significantly if a CO_2-lean flue gas is handled (as in the combined cycle scenario);
- given the significant heat capacities of the bed, there should not be great margin to reduce the energy consumption of the system by means of a different design of the column or of the heating system, without compromising the separation performances of the cycle; in this sense the specific energy consumption is likely to be further reduced only by increasing its denominator (the amount of CO_2 captured) by means of a more effective cycle configuration, while no significant improvement can be expected from a more efficient handling of the heat fluxes;
- nevertheless it can be foreseen that enduring a slight deterioration of the purity and recovery rates more competitive energy consumption levels can be reached;
- on the one hand, low gas velocities are undoubtedly one key feature of fixed beds and represent a fundamental premise to the good recovery and purity rates they provide; on the other hand, they are to be identified as the main cause of the worst shortcoming of fixed bed system, which is the enormous number of vessel required by a real scale application, which appears thus to be totally unrealistic. Once again a slight improve of this velocity beyond the value assumed in this work could help achieving a smaller plant size without compromising the overall performances of the system.

In this sense, the compactness degree offered by circulating fluidized beds represent without doubts the greatest virtue owned by this type of reactor when huge flow rates are to be handled, as for CCS applications. However, the results presented in this work seem to show there that this technology has both a great potential and relevant limitations.

The modeling implemented to simulate the operation of CFBs offers a good overview of the performances that can be realistically obtained with these systems. The assumptions on which it is based are consistent with the work of other authors and would allow to represent the phenomena that occur in the reactor in a reasonably detailed fashion; nevertheless, under the specific conditions fixed by the TSA processes here considered, two assumptions result not to be always verified at the end of the computation procedure:

- the hypothesis that the reactor could isothermally operate at a given optimal temperature appears in most cases to be too restrictive both for the adsorption and the desorption stage, because the desired temperature levels hinder the capability of the system to exchange heat. Any set of conditions that cause this hypothesis not to be verified does not correspond to an unfeasible operational point, but rather to a case in which the thermal behavior of the system should be investigated under weaker assumptions; this could be done letting the temperature of the system be determined by the energy balances over the reactor, a solution which would though require the fluid dynamics and the thermodynamics of the process to be computed simultaneously;
- if only entraiment is responsible for the diplacement of particles from the adsorber to the regenerator and back, as it is assumed in the modeling, only a limited range of operational conditions can be realized. This is though a secondary issue, as it would not be difficult to implement an additional transport system to convey solids out of the reactor.

If a modification of the modeling were implemented to solve these two issues, results similar to the ones here presented would be obtained, even if the the reactor would be likely to operate under more unfavorable conditions if the desired process temperature could not be isothermally kept.

Various facts can be remarked out of the present results:

- as well as for the fixed bed, to the energy consumption directly caused by the operation of the system the amount required by the drying of the flue gas should be added;
- CFBs have a great potential in terms of limiting the total energy consumption of a TSA cycle for CCS as long as a major fraction of the heat stored in the hot solids is recovered; the capability of the system to operate this heat recovery is essential to determine the total energy demand of the system;
- the maximum performances yield by CFBs reactor are generally lower than those provided by fixed bed, the external conditions being equal. This is indeed consistent with the strong limitations previous studies have already highlighted for this technology [5]; the high CO_2 concentrations found in the desorption undoubtedly play a prominent role in among these constraints, as they can be identified as the most limiting factor for both recoveries and productivities;
- the heat exchange inside CFB is certainly enhanced by the fluid dynamics of the fluidization regimes –compared to other gas-solid contacting methods–, which allow obtaining very high values for the heat transfer coefficients. Nevertheless, as far as TSA cycle are concerned, the low temperature levels that best suit the process cause the need to exchange heat under limited temperature differences; this represents inevitably

a problematic issue of this application. In this sense, it must be observed that only a limited share of the total heat exchanged by the system is directly related to the adsorption and desorption processes merely intended as interaction between gas molecules and solid surface;

- the compactness of the system allows reducing the plant footprint down to very small size, compared to the fixed bed systems; this feature provides a solution to the their most hindering drawback, and could be found in some circumstances to fully compensate the worse performances yielded.

Outlook

For both technologies there is undoubtedly still room for improvement, but at different levels and in different directions.

As regards the fixed beds, more efforts might be advisably spent on the optimization of the reactor design. In this sense, since a margin seems to be available towards higher gas velocities, a new design might be developed optimizing the column length for higher velocities, so that the same notable recovery rates are obtained prolonging the path of the gas stream through the bed, i.e. elongating the interaction time between the gas an the solids. These measures would lead to smaller plant sizes, reasonably without compromising the overall efficiency performances, which might actually even slightly improve, as shown by the sensitivity analysis performed varying gas velocity on the Pareto front points. It could also be reasonably pondered if another type of vessel could fit the process operation better than the shell and tube design which is employed in this simulations.

Moreover, an appropriate complete optimization of the cycle would imply also the temperature of the external heating and cooling system to be varied: The range of possible temperatures would be anyway constrained by the integration of the system into the plant, if only available heat fluxes with a low exergetic content are to be exploited and a non-refrigerated fluid is employed for cooling.

With respect to circulating fluidized beds, first of all a more refined modeling, which consider the operational temperature inside the riser as a variable depending on the amount of heat involved in the adsorption and desorption processes and the energy actually transferred through vessel walls, might help assessing more accurately the performances within a wider range of operational conditions, determining the real limitations placed the cooling and heating systems.

It must be though stated that the most effort should be further spent on the design of the process itself. In particular, if the recovery of the sensible heat stored in hot solid streams were effectively operated, the premise would be posed in order to reach remarkably low energy consumption rates, even taking into account the additional consumption term associated with the drying of the gas. Hence an attempt is needed to identify an operable method to implement this heat recovery.

Furthermore, it would be possible to consider a completely new process design involving more than one reactor for the adsorption section. In fact the flue gas could flow through a

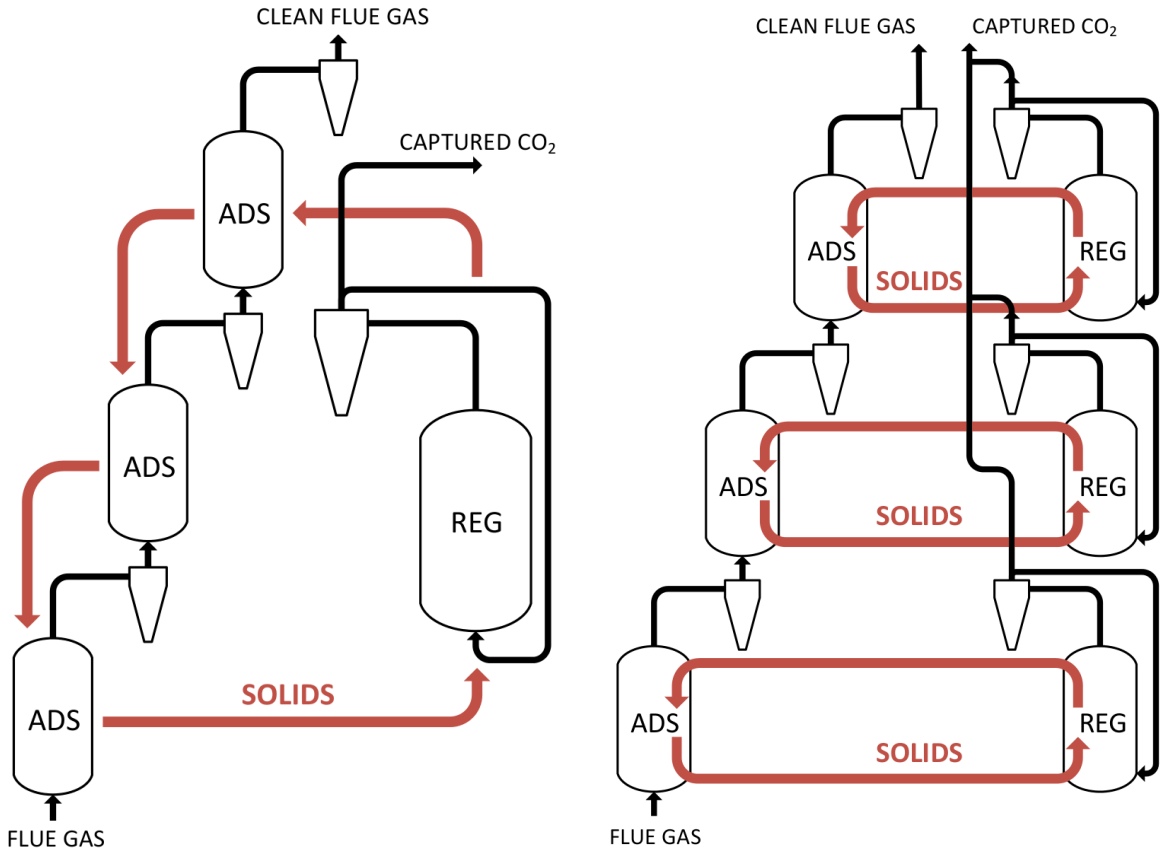

Figure 5.54: CFB: possible different process design

series of reactors in sequence; each vessel would be characterized by its own average degree of conversion of the solid. If the solid were initially fed in at the top reactor and sent to the lower risers one after the other, the gas would interact with the freshest sorbent as the most CO_2 has already been adsorbed, so that the adsorption process would be still hindered by the low partial pressure of the gas phase, but it would be at the same time promoted by the low conversion degree of the solid. The solid already loaded could instead be conveniently used in the lower reactors, where the high concentration of CO_2 would compensate the fact that the solid surface is already loaded with much adsorbate.

This design, which is schematically outlined in Figure 5.54a, does not necessarily require more than one regeneration reactor to be employed. Admitting that the desorption step could be split into more separated risers, it would be further possible to regenerate the solid coming from each adsorber into a different vessel (see Figure 5.54b). Thank to this measure, the desorption process could be performed at slightly different levels of CO_2 partial pressure (according to the composition of the adsorbed phase with which each solid stream is loaded), so that in some cases a little benefit deriving from a lower CO_2 concentration could be exploited.

Appendix A

Integrated steel mill plant layout

A.1 Boiler case

Power plant

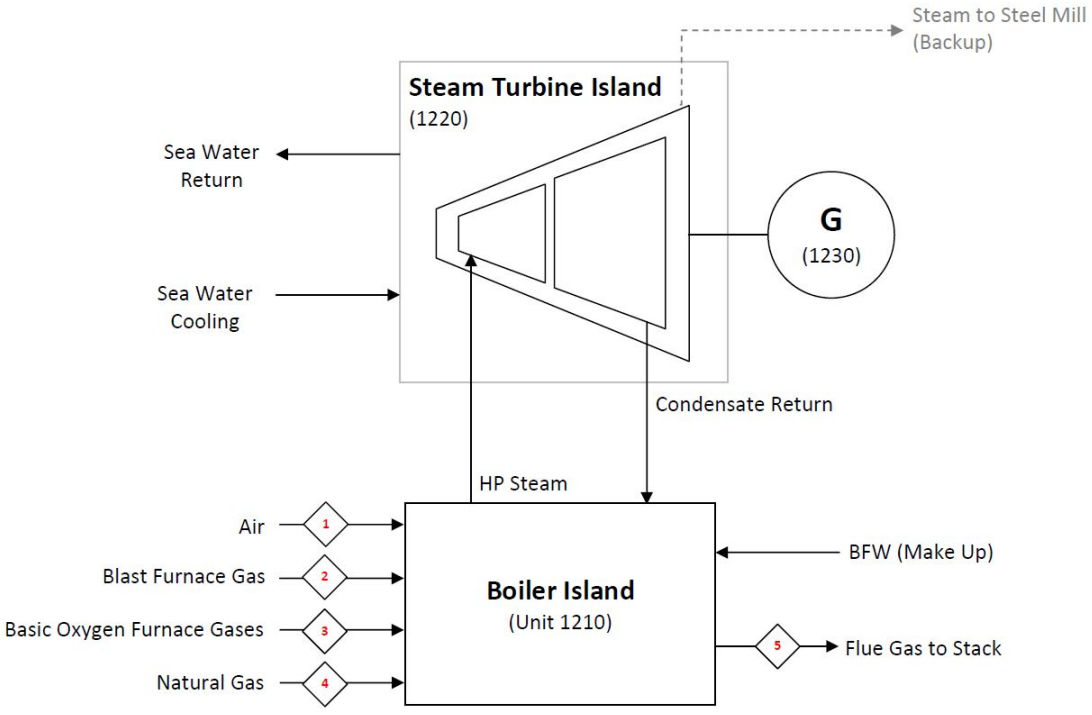

Figure A.1: Boiler case: powerl plant scheme [1]

Table A.1: Boiler case: power plant data

Cycle type	Sub-critical steam cycle without steam reheat
Boiler type	Gas fired boiler
Heating conditions	120 bar, 512°C
Nominal plant output	215 MW_e
Load factor	0.85
Average daily output	182.75 MW_e
Net efficiency	32.1%
CO_2 emission	1417 g/kWh

Table A.2: Boiler case: power plant fuel data

	source (v. fraction)
BFG	89.46%
BOFG	8.53%
Natural gas	2.01%
	CO content (v. fraction)
BFG	22.34%
BOFG	56.92%
Natural gas	0%
	CO_2 content (v. fraction)
BFG	22.10%
BOFG	14.44%
Natural gas	1.80%
	composition (v. fraction)
H_2	3.47%
CO	24.84%
CO_2	21.04%
N_2	44.82%
H_2O	3.86%
CH_4 and other hydrocarbons	1.97%
Air-to-fuel volumetric ratio	0.9653

Steel mill plant

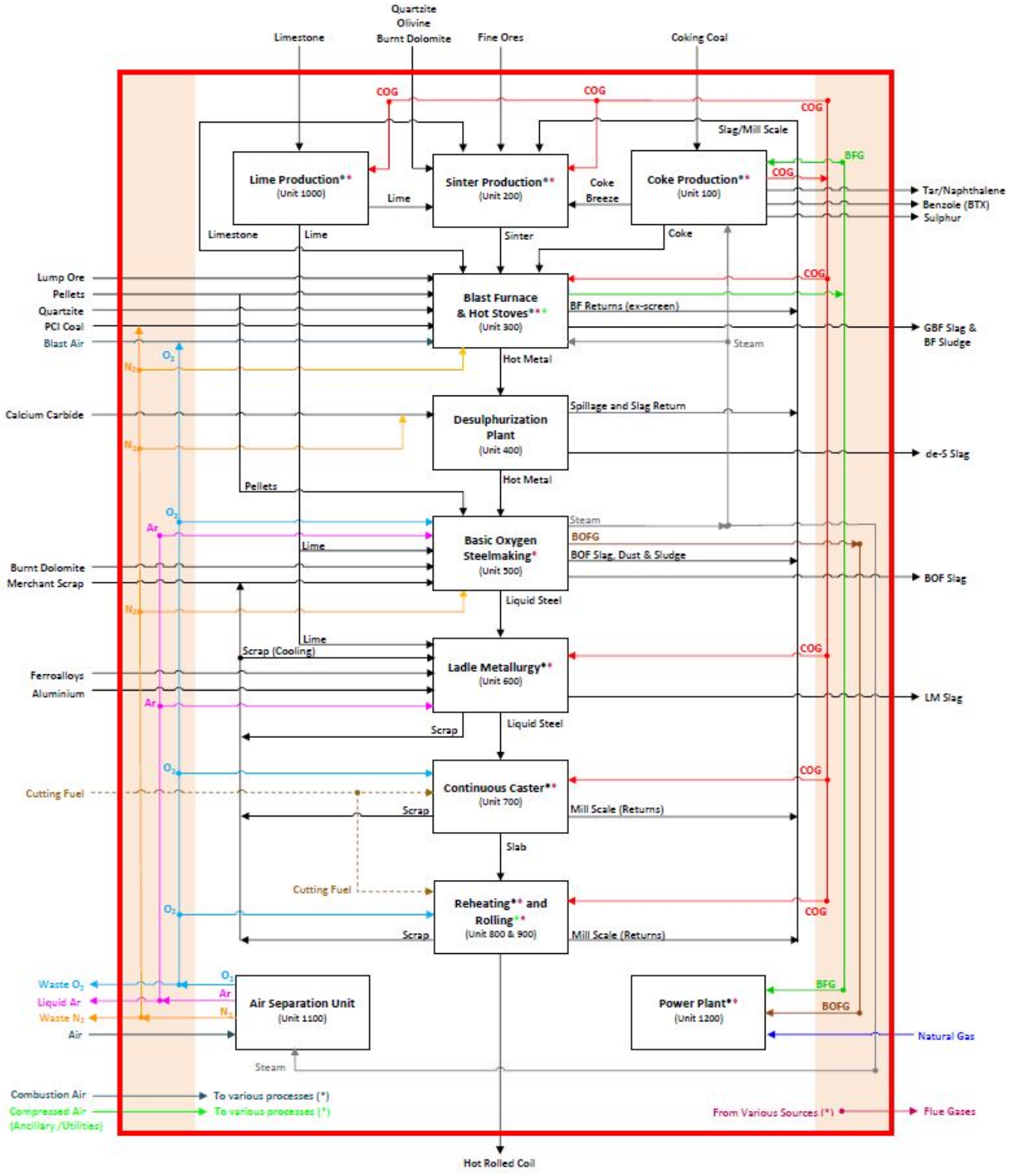

Figure A.2: Boiler case: steel mill plant scheme [1]

A.2 Combined cycle case

Power plant

Table A.3: Combined cycle case: power plant data

Gas turbine type	Generic F class
Turbine inlet temperature	1360°C
Pressure ratio	18.1
Steam cycle type	Sub-critical cycle with reheat, three pressure levels
Live steam parameters	130 bar, 565°C
Net output	319.2 MW_e
Net efficiency	52.8%
CO_2 emission	1338 g/kWh

Table A.4: Combined cycle case: power plant fuel data

	dry composition (v. fraction)
H_2	7.22%
CO	21.29%
CO_2	19.57%
N_2	49.53%
O_2	0.02%
CH_4 and other hydrocarbons	2.38%

Appendix B

Output of an example simulation employing the CFB computational code

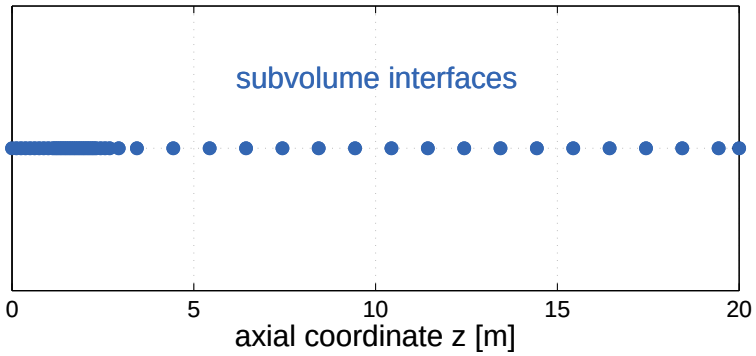

(a) spacial discretization along riser length

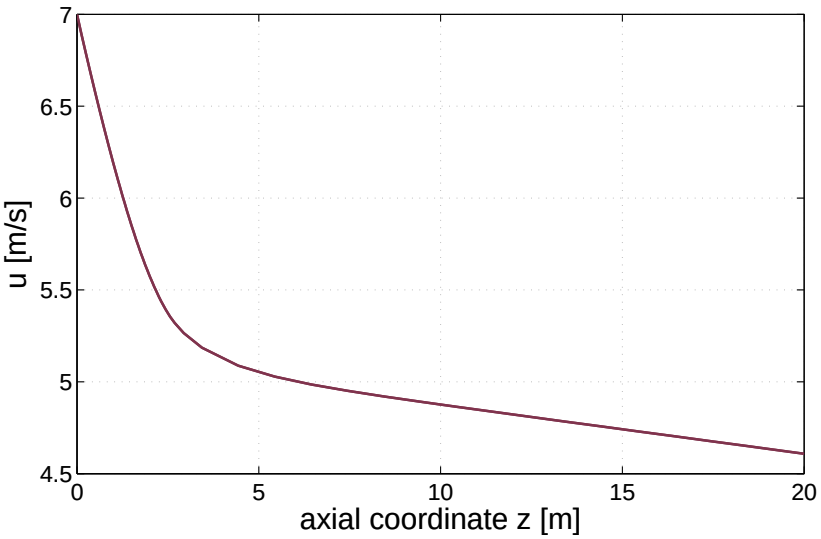

(b) superficial velocity along riser length

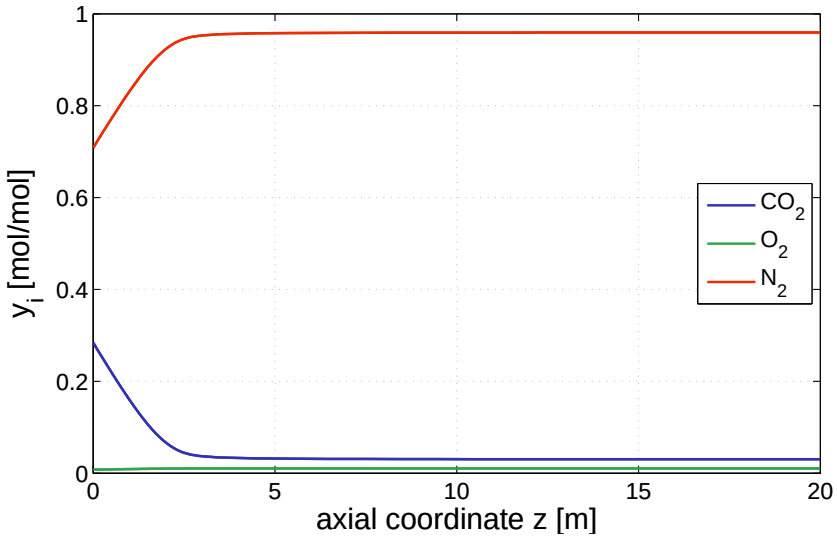

(c) molar fractions along riser length

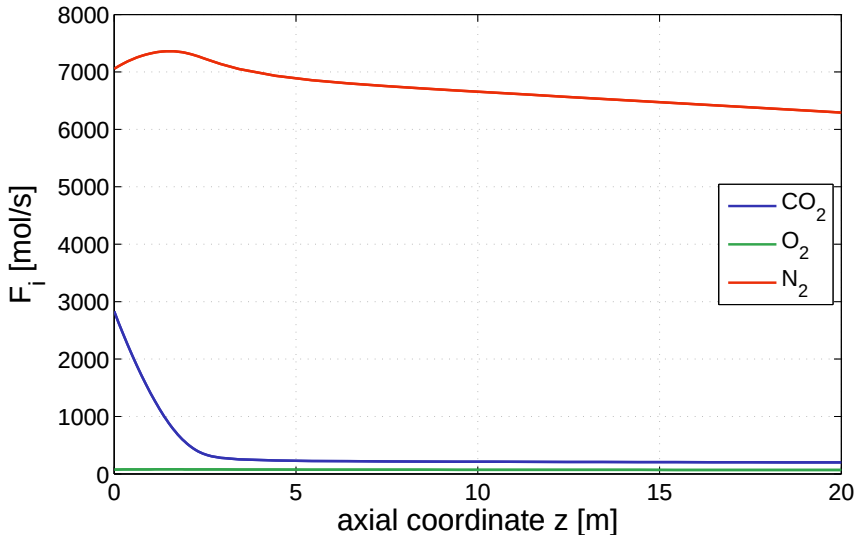

(d) molar flow rates along riser length

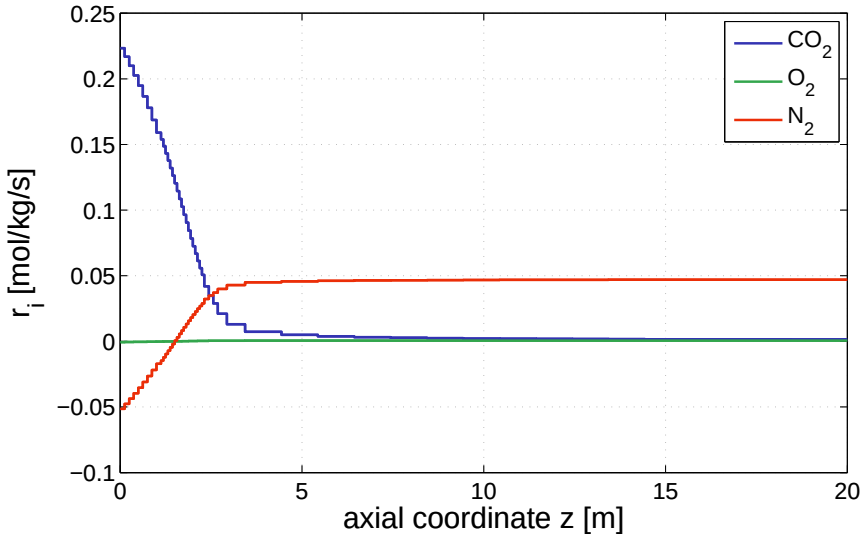

(e) average adsorption rates in each subvolume along riser length

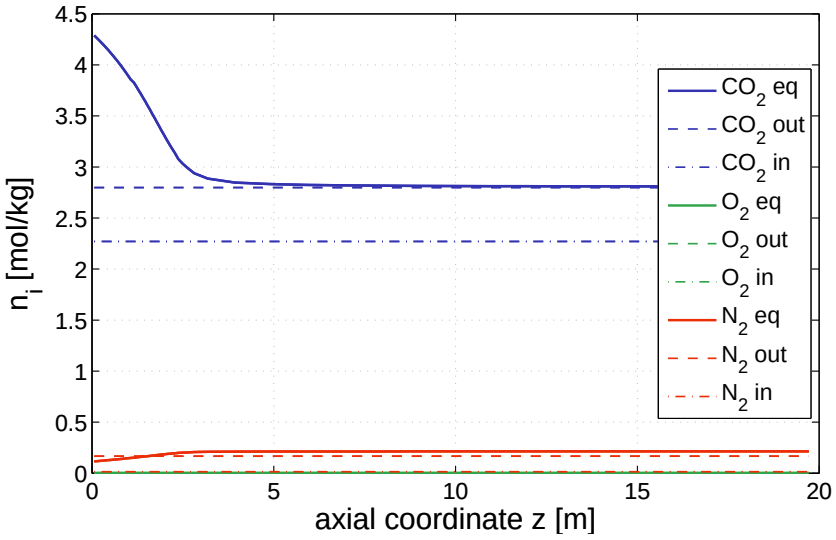

(f) equilibrium amount adsorbed along riser length

Figure B.1: CFB: example of result profiles as computed by the Matlab code

Appendix C

Fixed bed reactor design

Table C.1: Fixed bed: vessel and heat exchanging system data

Column length, L	1.2 m
Column internal diameter, d_i	0.029 m
Column external diameter, d_o	0.032 m
Minimum distance between columns, S_T	0.040 m
Arrangement pattern type	triangular
Number of tubes for each shell, N_{col}	5164
Shell internal diameter, D_{shell}	3.05 m
Total vessel cross section,	7.30 m^2
Total bed cross section, A	3.64 m^2
Heat exchange available surface	130 m^2/m^3
Metal volumetric fraction in the vessel	0.12 m^3/m^3
Particle size, d_p	0.002 m
Convective fluid-to-wall heat transfer coefficient ($u > 0$), h	80 W/m^2/K
Convective fluid-to-wall heat transfer coefficient ($u = 0$), h	50 W/m^2/K
Heat capacity of the column wall metal, c_{wall}	4 MJ/m^3/K

List of Figures

List of Tables

Acronyms

BFG blast furnace gas.

BOFG basic oxygen furnace gas.

CAP chilled ammonia process.

CCS carbon capture and storage.

CFB circulating fluidized bed.

COG coke oven gas.

COP coefficient of performance.

CSTR continuous flow stirred tank reactor.

LDF linear driving force.

MDEA methyl diethanolamine.

MEA monoethanolamine.

OBF oxy-blast furnace.

PSA pressure swing adsorption.

SPL Separation Processes Laboratory (ETH, Zurich).

TSA temperature swing adsorption.

WGS water-gas shift.

List of symbols

Greek letters

γ	surface inhomogeneity parameter for Sips equation	$[-]$
ε	void fraction	$[-]$
ε_s	volumetric fraction of solid	$[-]$
ε_s^{asym}	asymptotical value for $\varepsilon_s = f(x)$ function in the lean region in CFB riser	$[-]$
$\varepsilon_{s,d}$	volumetric fraction of solid in the dense region in CFB riser	$[-]$
η	efficiency of heat exchanger	$[-]$
κ	adsorption affinity coefficient	$\left[\frac{1}{Pa}\right]$
μ	dynamic viscosity	$\left[\frac{kg}{m\,s}\right]$
$\hat{\rho}_{mix}$	molar density of gas mixture	$\left[\frac{mol}{m^3}\right]$
ρ	density	$\left[\frac{kg}{m^3}\right]$
τ	average residence time of particles in CFB riser	$[s]$
ϕ_s	sphericity of solid particles	$[-]$
χ_s	conversion degree of solid	$[-]$
ω	lumped mass transfer coefficient	$\left[\frac{1}{s}\right]$

Latin letters

A	cross section area	$\left[\frac{m}{s}\right]$
a	constant for $au_{inlet} = const.$ expression	$\left[\frac{1}{m}\right]$

A_γ, B_γ	coefficients for γ	$[-]$, $[-]$
A_∞, B_∞	coefficients for n_∞	$\left[\frac{mol}{kg}\right]$, $\left[\frac{J}{mol}\right]$
A_κ, B_κ	coefficients for κ	$\left[\frac{1}{Pa}\right]$, $\left[\frac{J}{mol}\right]$
C	concentration	$\left[\frac{mol}{m^3}\right]$
c	specific heat capacity of liquid or solid	$\left[\frac{J}{kg\,K}\right]$
c_p	specific heat capacity of gas at constant p	$\left[\frac{J}{kg\,K}\right]$
C_R	solid-to-gas heat capacity ratio	$[-]$
D	diameter of a vessel	$[m]$
d_i	internal diameter of a fixed bed column	$[m]$
d_o	external diameter of a fixed bed column	$[m]$
d_p	average diameter of particles	$[m]$
$E(t)$	time probability distribution	$[-]$
F	molar flow rate	$\left[\frac{mol}{s}\right]$
g	acceleration of gravity	$\left[\frac{kg}{s^2}\right]$
g_c	gravitational conversion factor $g_c = 1\frac{kg\,m}{N\,s^2}$	$\left[\frac{kg\,m}{N\,s^2}\right]$
G_s	mass flow rate of solid entrained at CFB riser outlet (per cross section unit)	$\left[\frac{kg}{s\,m^2}\right]$
Δh^{ads}	heat of adsorption	$\frac{J}{mol}$
Δh_{lv}	heat of vaporization at given T	$\left[\frac{J}{kg}\right]$
h	convective heat transfer coefficient	$\left[\frac{W}{m^2\,K}\right]$
H_d	height of the dense region in CFB riser	$[m]$

H_t	height of reactor	$[m]$
J	number of fixed bed vessels in feed mode within a single train	$[-]$
K	number of fixed bed vessels within a single train	$[-]$
k	thermal conductivity	$\left[\frac{W}{m\,K}\right]$
L	length of fixed bed column	$[m]$
$\dot{m}$	mass flow rate	$\left[\frac{kg}{s}\right]$
$\dot{m}_{ads}$	mass flow rate of sorbent fed in CFB riser	$\left[\frac{m}{s}\right]$
M	molar mass	$\left[\frac{kg}{kmol}\right]$
m	mass	$[kg]$
M_R	loading ratio	$[-]$
$\bar{n}$	average specific amount adsorbed for solid mass unit	$\left[\frac{mol}{kg}\right]$
n	specific amount adsorbed per sorbent mass unit	$\left[\frac{mol}{kg}\right]$
n_∞	saturation capacity of sorbent material	$\left[\frac{mol}{kg}\right]$
N_{col}	number of columns inside a fixed bed shell and tube vessel	$[-]$
N_{sv}	minimum number of subvolumes in CFB riser	$[-]$
N_{tr}	number of trains of fixed bed vessels	$[-]$
N_{tubes}	number of tubes	$[-]$
Δp	pressure drop	$[Pa]$
p	pressure	$[Pa]$
$\dot{Q}$	thermal power	$[W]$
R_{rec}	recycle rate of solid particles in CFB riser	$[-]$
$\bar{r}$	average adsorption rate	$\left[\frac{mol}{kg\,s}\right]$

r	adsorption rate	$\left[\frac{mol}{kg\,s}\right]$
S_T	minimum distance between columns inside a fixed bed shell and tube vessel	$[m]$
T	temperature	$[K]$
t	time	$[s]$
t_{cyc}	total duration of a TSA operation cycle in a fixed bed system	$[s]$
t_{idle}	idle time	$[s]$
U	minimum scheduling time unit	$[s]$
u	superficial velocity of gases	$\left[\frac{m^2}{s}\right]$
u_t	terminal velocity of particles	$\left[\frac{m}{s}\right]$
$\dot{V}$	volumetric flow rate	$[m^2]$
N_{st}	number of fixed bed shell and tube vessels	$[-]$
v	speed of fluid	$\left[\frac{m}{s}\right]$
W_s	solid inventory	$[kg]$
x	mass fraction	$[-]$
x_v	vapour quality	$[-]$
X_{tt}	parameter for two-phase vapour-liquid turbolent flow	$[-]$
y	molar fraction	$[-]$
z	axial coordinate along reactor length	$[m]$

Other subscripts

$_0$	initial value
$_{col}$	column of fixed bed shell and tube vessel
$_{disp}$	dispersion
$_{eq}$	at equilibrium conditions
$_f$	fluid
$_{feed}$	feed steps (pressurization+adsorption) in fixed bed cycle

$_{fr}$ frictional

$_{g}$ gas mixture

$_{inlet}$ at riser inlet

$_{in}$ at CFB subvolume inlet

$_{i}$ i-th gas species involved in the adsorption process

$_{l}$ liquid

$_{mf}$ at minimum fluidization conditions

$_{og}$ as if only gas was flowing, instead of gas-solid suspension

$_{outlet}$ at riser outlet

$_{out}$ at CFB subvolume outlet

$_{ref}$ reference value

$_{s}$ solid

$_{st}$ fixed bed shell and tube vessel

$_{susp}$ suspension

$_{tubes}$ tubes forming heat exchange surfaces of CFB riser

$_{unit\,j}$ j-th unit in a fixed bed cycle (starting from pressurization)

$_{steam}$ steam flow of heating system

$_{water}$ water stream of cooling system

Other superscripts

* at first guess average concentration

$^{+}$ adimensional

^{ADS} adsorption riser of a CFB process

^{feed} feed steps (pressurization+adsorption) in fixed bed cycle

^{REG} regeneration riser of a CFB process

Adimensional numbers

Ar Arrhenius number

Nu	Nusselt number
Nu_D	Nusselt number as function of a Re_D number
Pr	Prandtl number
Re_D	Reynolds number referred to duct diameter
Re_p	Reynolds number referred to particle diameter
Re_{ls}	Reynolds number on the surface of a liquid stream

Bibliography

[1] International Energy Agency, Greenhouse Gas Protocol, *Iron and Steel CCS study (techno-economics integrated steel mill*, Report 2013/04, 2013

[2] M. Gazzani, M. Romano, G. Manzolini, *Application of sorption enhanced water gas shift for carbon capture in integrated steelworks*, Energy Procedia 37 7125-7133, 2013

[3] A. Arasto, E. Tsupari, J. Kärki, E. Pisilä, L. Sorsamäki, *Post-combustion capture of CO_2 an an integrated steel mill - Part I: Technical concept analysis*, International Journal of Greenhouse Gas Control 16 271-277, 2013

[4] W. Zhang, H. Liu, C. Sun, T. Drage, C. Snape, *Capturing CO_2 from ambient air using a polyethyleneimine-silica adsorbent in fluidized beds*, Chemical Engineering Science 116 306-314, 2014

[5] G. Pirngruber, F. Guillou, A. Gomez, M. Clausse, *A theoretical analysis of the energy consumption of post-combustion CO_2 capture processes by temperature swing adsorption using solid sorbents*, International Journal of Greenhouse Gas Control 14 74-83, 2013

[6] W. Yang, J. Hoffman, *Exploratory Design Study on Reactor Configurations for Carbon Dioxide Capture from Conventional Power Plants Employing Regenerable Solid Sorbents*, Industrial and Engineering Chemical Research 48 341-351, 2009

[7] G. Valenti, D. Bonalumi, E. Macchi, *A parametric investigation of the Chilled Ammonia Process from energy and economic perspectives*, Fuel 101 74-83, 2012

[8] J. Jee, M. Kim, C. Lee, *Adsorption Characteristics of Hydrogen Mixtures in a Layered Bed: Binary, Ternary, and Five-Component Mixtures*, Industrial & Engineering Chemistry Research 40 868-878, 2001

[9] J. Schell, N. Casas, R. Pini, M. Mazzotti, *Pure and binary adsorption of CO_2, H_2 and N_2 on activated carbon*, Adsorption 18 49-65, 2012

[10] J. McEwen, J. Hayman, A. Ozgur Yazaydin, *A comparative study of CO_2, CH_4 and N_2 adsorption in ZIF-8, Zeolite-13X and BPL activated carbon*, Chemical Physics 412 72-76, 2013

[11] C. Chen, D. Park, W. Ahn, *CO_2 capture using zeolite 13X prepared from bentonite*, Applied Surface Science 292 63-67, 2014

[12] R.P.P.L. Ribeiro, C.A. Grande, A.E. Rodrigues, *Activated carbon honeycomb monolith – Zeolite 13X hybrid system to capture CO_2 from flue gases employing Electric Swing Adsorption*, Chemical Engineering Science 104 304-318, 2013

[13] W. Won, S. Lee, K.S. Lee, *Modeling and parametere estimation for a fixedbed adsorption process for CO_2 capture using Zeolite 13X*, Separation and Purification Technology 85 120-129, 2012

[14] J.A.C. Silva, A.F. Cunha, K. Schumann, A.E. Rodrigues, *Binary adsorption of CO_2/CH_4 in binderless beads of 13X zeolite*, Microporous and Mesoporous Materials 187 100-107, 2014

[15] D. Kunii, O. Levenspiel, *Fluidization Engineering*, Second ed., Butterworth-Heinemann, 1991

[16] D. Geldart, *Types of gas fluidization*, Powder Technology 7 286-292, 1973

[17] M. Romano, *Modeling the carbonator of a Ca-looping process for CO_2 capture from power plant flue gas*, Chemical Engineering Science 69 257-269, 2012

[18] A Heider, O. Levenspiel, *Drag coefficient and terminal velocity of spherical and non-spherical particles*, Powder Technology 58 63-70, 1989

[19] M. Leva, *Fluidization*, McGraw-Hill, 1959.

[20] J. Lienhard IV, J. Lienhard V, *A Heat Transfer Textbook*, Fourth ed. v. 2.02, Phlogiston Press, 2012

[21] J. C. Chen, *Chapter 10: Heat Transfer* in *Handbook of Fluidization and Fluid-Particle Systems*, Marcel Dekker Inc., New York-Basel, 2003

[22] Y. Molodtsof, D. Muzyka, *Wall to suspension heat transfer in the similar profile regime*, Heat Mass Transfer 35 1665-1673, 1992

[23] H. Zhang, J. Baeyens, J. Degrève, A. Brems, R. Dewil, *The convection heat transfer coefficient in a Circulating Fluidized Bed (CFB)*, Advanced Powder Technology 25 710-715, 2014

[24] J. Goidich, S. Wu, Z. Fan, A. Bose, *Design Aspects of the Ultra-Supercritical CFB Boiler*, International Pittsburgh Coal Conference, Pittsburch, PA, September 2005

[25] J. Thome, *Engineering data book III*, Wieland-Werke AG, 2004

[26] S. Ergun, *Fluid Flow through Packed Columns*, Chemical Engineering Progress 48 89-94, 1952

[27] N. Tlili, G. Grévillot, C. Vallières, *Carbon dioxide capture and recovery by means of TSA and/or VSA*, International Journal of Greenhouse Gas Control 3 519-527, 2009

[28] A. Chiang, *Arithmetic of PSA process scheduling*, AlChE Journal 34 1910-1912, 1988

[29] A. Mehrotra, A. Ebner, J. Ritter, *Arithmetic approach for complex PSA scheduling*, Adsorption 16 113-126, 2010

[30] A. Mehrotra, A. Ebner, J. Ritter, *Simplified graphical approach for complex PSA cycle scheduling*, Adsorption 17 337-345, 2011

[31] Andreas Lauper's master thesis, Separation Process Laboratory, ETH Zurich